



FEDERAL UNIVERSITY OF SANTA CATARINA  
TECHNOLOGY CENTER  
AUTOMATION AND SYSTEMS DEPARTMENT  
UNDERGRADUATE COURSE IN CONTROL AND AUTOMATION ENGINEERING

Tiago Colvara Faria

**Evaluation of energy consumption of 5G devices for self-sustainable operation  
through multi-source energy harvesting**

Aachen, Germany  
2024

Tiago Colvara Faria

**Evaluation of energy consumption of 5G devices for self-sustainable operation  
through multi-source energy harvesting**

Final report of the subject DAS5511 (Course Final Project) as a Concluding Dissertation of the Undergraduate Course in Control and Automation Engineering of the Federal University of Santa Catarina. Supervisor: Prof. Rodolfo C. C. Flesch, Dr. Supervisorora Sarah Schmitt, Mst.

Aachen, Germany  
2024

Ficha catalográfica gerada por meio de sistema automatizado gerenciado pela BU/UFSC.  
Dados inseridos pelo próprio autor.

Faria, Tiago Colvara

Evaluation of energy consumption of 5G devices for self sustainable operation through multi-source energy harvesting / Tiago Colvara Faria ; orientador, Rodolfo César Costa Flesch, 2024.

109 p.

Trabalho de Conclusão de Curso (graduação) -  
Universidade Federal de Santa Catarina, Centro Tecnológico,  
Graduação em Engenharia de Controle e Automação,  
Florianópolis, 2024.

Inclui referências.

1. Engenharia de Controle e Automação. 2. NR5G. 3. Wireless Sensors. 4. Energy efficiency. 5. Energy harvesting. I. Flesch, Rodolfo César Costa. II. Universidade Federal de Santa Catarina. Graduação em Engenharia de Controle e Automação. III. Título.

Tiago Colvara Faria

**Evaluation of energy consumption of 5G devices for self-sustainable operation  
through multi-source energy harvesting**

This dissertation was evaluated in the context of the subject DAS5511 (Course Final Project) and approved in its final form by the Undergraduate Course in Control and Automation Engineering

Florianópolis, July 10, 2024.

Prof. Marcelo De Lellis Costa de Oliveira, Dr.  
Course Coordinator

**Examining Board:**

Prof. Rodolfo Cesar Costa Flesch, Dr.  
Advisor  
UFSC/CTC/DAS



Documento assinado digitalmente  
**Rodolfo Cesar Costa Flesch**  
Data: 22/07/2024 09:44:07-0300  
CPF: \*\*\*.466.879-\*\*  
Verifique as assinaturas em <https://v.ufsc.br>

Sarah Schmitt, Mst.  
Supervisor  
Company/Fraunhofer Institute for Production Technology IPT

**Sarah Schmitt**

Digital unterschrieben von  
Sarah Schmitt  
Datum: 2024.07.25 16:53:43  
+02'00'

Prof. João Paulo Zomer Machado, Dr.  
Evaluator  
UFSC/CTC/DAS

Prof. Hector Bessa silveira, Dr.  
Board President  
UFSC/CTC/DAS

This work is dedicated to my parents Neiva Regina Kohls Colvara And Luiz Paulo Cardoso Faria as well as all the teachers I have met in my life, as I was only able to become who I am and develop this project due to what you taught me.

## **ACKNOWLEDGEMENTS**

First I would like to thank my parents, Neiva Regina Kohls And Luiz Paulo Cardoso Faria for teaching me and supporting me on every step of my life and always believing in me.

To Milton Pereira, for incentivizing me to come to UFSC, for accepting me to work in his lab and lastly for appointing me for the BRAACHEN program, may I have shown I was worth of the opportunities you provided me.

To my uncle and Industrial Automation Engineer, João Vicente Cardoso Faria, for motivating me to join this course, I hope to be your colleague one day.

I am also grateful for the BRAACHEN program for providing me this invaluable opportunity of an internship at the Fraunhofer Institute. A special thanks to my supervisor, Sarah Schmitt, for her guidance and mentorship during the execution of this and other projects through the year I have at the institute. I would also like to thank Niklas Beckmann for supporting me and his insightful comments on the correction of this document.

To Rodolfo Costa Flesch, my academic advisor from UFSC, thank you for your contribution, valuable feedback on this work and answering my many emails.

To Joao Goulart Jr. for all you taught me during the technical course and the recommendation letter that helped me come to work at IPT.


To all the friends I made during this year in Germany, thank you for making this experience even more memorable. A special thanks to my friends from the 4th floor HiWi room, including Rafael, Davi, Fernanda, Juliana and David for their friendship, support and making work more enjoyable.

## DISCLAIMER

Aachen, Germany, June 28th, 2024.

As representative of the Fraunhofer institution for production technology in which the present work was carried out, I declare this document to be exempt from any confidential or sensitive content regarding intellectual property, that may keep it from being published by the Federal University of Santa Catarina (UFSC) to the general public, including its online availability in the Institutional Repository of the University Library (BU). Furthermore, I attest knowledge of the obligation by the author, as a student of UFSC, to deposit this document in the said Institutional Repository, for being it a Final Program Dissertation (*“Trabalho de Conclusão de Curso”*), in accordance with the *Resolução Normativa n° 126/2019/CUn*.

Sarah  
Schmitt

 Digital unterschrieben  
von Sarah Schmitt  
Datum: 2024.06.28  
10:50:54 +02'00'

---

Sarah Schmitt M. Sc.

Fraunhofer Institute for Production Technology IPT

## ABSTRACT

With the application of wireless sensors seeing widespread, increasing use in the industry as telecommunications technology advances. The introduction of New Radio 5th Generation (NR5G) technology designed to meet industrial needs makes it even more attractive by enabling high reliability and low latency transmission of large amounts of data. However, these increased capabilities come at a cost of an increase in energy usage, posing challenges for battery powered units. While there are efforts to reduce the power consumption of 5G and increase battery capacity, energy harvesting technologies may be one more possible solution. These technologies focus on collecting energy from the environment, often generated by the processes being monitored, and transforming it into electrical energy that can power the sensors and transceivers. With this local generation, batteries can be recharged and used as an aid, rather than being a limiting factor in operation. This document investigates the possibility of using energy harvesting to meet the demands of the 5G transceivers. Multiple power measurements were conducted using multiple 5G devices in order to map their energy usage and identify what factors are the most critical to energy consumption. This information not only provides a way to tailor the transmission to be more energy efficient, but also offers a basis for numerous possible applications. The data was then compared with the potential energy yield of different energy harvesting techniques in order to investigate the conditions required to partially or fully power the 5G devices. Finally, a theoretical application using milling operations as a basis was proposed in order to demonstrate that it may be possible to fully power a device by using multiple units of different types of energy harvesters, provided certain conditions are met.

**Keywords:** NR5G. Wireless Sensors. Energy consumption. Energy efficiency. Energy harvesting.



## RESUMO

Com a aplicação de sensores sem fio vindo um uso crescente e generalizado na indústria à medida que a tecnologia de telecomunicações avança, a introdução da tecnologia New Radio de 5ª Geração (NR5G), projetada para atender às necessidades industriais, torna-se ainda mais atraente, permitindo transmissão de grandes quantidades de dados com alta confiabilidade e baixa latência. No entanto, essas capacidades aumentadas vêm a custo de um aumento no consumo de energia, representando desafios para unidades alimentadas por bateria. Embora haja esforços para reduzir o consumo de energia do 5G e aumentar a capacidade das baterias, as tecnologias de coleta de energia podem ser uma solução adicional. Essas tecnologias focam em coletar energia do ambiente, muitas vezes gerada pelos processos que estão sendo monitorados, e transformá-la em energia elétrica que pode alimentar os sensores e transceptores. Com essa geração local, as baterias podem ser recarregadas e usadas apenas como um suporte, em vez de serem um fator limitante na operação. Este documento investiga a possibilidade de usar a coleta de energia para atender às demandas dos transceptores 5G. Várias medições de potência foram realizadas usando múltiplos dispositivos 5G para mapear seus usos de energia e identificar quais fatores são mais críticos para o consumo de energia. Esta informação não apenas fornece uma maneira de adaptar a transmissão para ser mais eficiente em termos de energia, mas também oferece uma base para inúmeras aplicações possíveis. Os dados foram então comparados com o rendimento potencial de diferentes técnicas de coleta de energia, a fim de investigar as condições necessárias para alimentar parcial ou totalmente os dispositivos 5G. Por fim, uma aplicação teórica usando operações de fresagem como base foi proposta para demonstrar que pode ser possível alimentar completamente um dispositivo usando múltiplas unidades de diferentes tipos de coletores de energia, desde que certas condições sejam atendidas.

**Palavras-chave:** NR5G. Consumo de energia. Eficiência energética. Coleta de energia.

## LIST OF FIGURES

Figure 1 – Fraunhofer society Logo. Source: Fraunhofer Institute database. . . . .	18
Figure 2 – Leading communication achievements for several generations (1G to 5G). Source:Solyman and Yahya (2022). . . . .	21
Figure 3 – Typical maximum power consumption of Telecom devices. Source:HUAWEI TECHNOLOGIES CO., LTD. (2023) . . . . .	22
Figure 4 – Structure of SA and NSA networks. Source:Rakuten Mobile (2021) . . . . .	24
Figure 5 – 4G spectrum versus 5G spectrum. Source: Barb and Ottesteanu (2020). . . . .	25
Figure 6 – Industrial automation use case requirements, as determined by 3GPP. Source : Gangakhedkar et al. (2018) . . . . .	29
Figure 7 – Quectel RM520-GL module. Source: Solutions (2024). . . . .	33
Figure 8 – Quectel RM520-GL in an Evaluation board. Source: Author. . . . .	34
Figure 9 – Quectel RM255-C in an Evaluation board. Source: Author. . . . .	36
Figure 10 – WNC 5G NR sub-6 i-Router router. Source: Author. . . . .	36
Figure 11 – RUTX50 router from Teltonika. Source: Author. . . . .	37
Figure 12 – Phoenix contact TC ROUTER 5004T-5G EU. Source: Author. . . . .	38
Figure 13 – Siemens Scalance M800 router. Source: Author. . . . .	39
Figure 14 – Command prompt running the ping tool. Source: Author. . . . .	43
Figure 15 – Ping and iPerf3 Power usage comparison Source: Author. . . . .	44
Figure 16 – Setup for testing the Siemens router with shielding Source: Author. . . . .	45
Figure 17 – Measurement setup for Quectel RM520-GL. Source: Author. . . . .	46
Figure 18 – QCOM interface during connection procedure with NSA network. Source: Author. . . . .	47
Figure 19 – Average Power measurements on Quectel RM520 on SA network. Source: Author. . . . .	48
Figure 20 – Average Power measurements on Quectel RM520 on NSA network. Source: Author. . . . .	49
Figure 21 – Redcap power consumption in SA network. Source: Author. . . . .	50
Figure 22 – Test setup for WNC. Source: Author. . . . .	51
Figure 23 – Average Power measurements on WNC 5G NR sub-6 router in SA network. Source: Author. . . . .	52
Figure 24 – Average Power measurements on WNC 5G NR sub-6 router in NSA network. Source: Author. . . . .	52
Figure 25 – Test setup for TC ROUTER 5004T-5G EU. Source: Author. . . . .	53
Figure 26 – First attempt at Average Power measurements on TC ROUTER 5004T-5G EU on SA network. Source: Author. . . . .	54
Figure 27 – Average Power measurements on TC ROUTER 5004T-5G EU on SA network. Source: Author. . . . .	55

Figure 28 – Test setup for RUTX50. Source: Author. . . . .	56
Figure 29 – Average Power measurements on Teltonika RUTX50 on SA network Source: Author. . . . .	56
Figure 30 – Test setup for Siemens Scalance M800. Source: Author. . . . .	57
Figure 31 – Siemens Scalance M800 information. Source: Author . . . . .	58
Figure 32 – Average Power measurements on Siemens Scalance M800 on SA network. Source: Author. . . . .	58
Figure 33 – Average Power measurements on Siemens Scalance M800 on NSA network. Source: Author. . . . .	60
Figure 34 – Comparison of average power measurements on SA and NSA net- works. Source: Author. . . . .	62
Figure 35 – Power Consumption values on some variations scenarios. Source: Author. . . . .	62
Figure 36 – Comparison of average power measurements on different 5G devices on SA network. Source: Author. . . . .	63
Figure 37 – Photovoltaic cell model “Seeded 313070003 monocrystalline”. Source:Marutsu (2024). . . . .	67
Figure 38 – Area required to supply the devices with the “Seeded 313070003 monocrystalline” solar harvester. Source: Author. . . . .	67
Figure 39 – Comparison of the area power density of the solar for LED lights. Source:Lauscher (2022) . . . . .	68
Figure 40 – Required area for “AM-5907CAR-DGK-E” harvester to supply 10% power to 5G devices under 1000 lx. Source: Author. . . . .	69
Figure 41 – Thermoelectric harvester model Laird 387005695 Source: PITCH Technologies (2024). . . . .	70
Figure 42 – Performance comparison of thermogenerators at increasing temper- ature. Source: Lauscher (2022). . . . .	71
Figure 43 – Required area for “Laird 387005695” thermoelectric harvester under a gradient of 115 °C to supply full power to 5G devices. Source: Made by the author. . . . .	71
Figure 44 – Required area for “Laird 387005695” thermoelectric harvester under a gradient of 115 °C to supply 10% power to 5G devices. Source: Author. . . . .	72
Figure 45 – Required area for “ReVibe 00204” Kinetic electromagnetic harvester to supply power to 5G devices under vibrations of 27.27 N. Source: Author. . . . .	74
Figure 46 – Required area for “ReVibe 00204” Kinetic electromagnetic harvester to supply power to under different intensities of vibration at 51 Hz. Source: Author. . . . .	76

Figure 47 – Enter Caption . . . . .	77
Figure 48 – Required area for “S452-J1FR-1808XB” Kinetic piezoelectric harvester to supply power to 5G devices under vibrations of 27.27 N. Source: Author. . . . .	78
Figure 49 – Current use by the STM32L051RBt6 Microcontroller during normal operation Source:STMicroelectronics (2019) . . . . .	81
Figure 50 – Circuit diagram for Multi source energy harvesting test case. Source: Kongara (2023). . . . .	83
Figure 51 – ADP5091-1-EVALZ board. Source: Devices (2022a) . . . . .	84
Figure 52 – Diagram for the theoretical use case circuit. Source: Author. . . . .	87

## LIST OF TABLES

Table 1 – Maximum Data Rates of Quectel RM520-GL . . . . .	33
Table 2 – Power Consumption values on RSRP scenarios. . . . .	61
Table 3 – Power Consumption values on some variations scenarios . . . . .	63
Table 4 – Area measurements and required number of units to guarantee power to the 5G devices. . . . .	75
Table 5 – Use Case Table with Viability Considerations . . . . .	79

## CONTENTS

<b>1</b>	<b>INTRODUCTION</b>	<b>15</b>
1.1	MOTIVATION AND CONTEXT	15
1.2	OBJECTIVES OF THE THESIS	16
<b>1.2.1</b>	<b>General objective</b>	<b>16</b>
<b>1.2.2</b>	<b>Specific objectives</b>	<b>16</b>
1.3	DOCUMENT OUTLINE	17
<b>2</b>	<b>THE FRAUNHOFER SOCIETY</b>	<b>18</b>
<b>3</b>	<b>THEORETICAL BACKGROUND</b>	<b>20</b>
3.1	NEW RADIO 5G	20
<b>3.1.1</b>	<b>NR5G capabilities</b>	<b>21</b>
<b>3.1.2</b>	<b>Technology types</b>	<b>23</b>
<b>3.1.3</b>	<b>Technical aspects</b>	<b>24</b>
3.2	ENERGY HARVESTING	25
<b>3.2.1</b>	<b>Multi-source energy harvesting</b>	<b>26</b>
<b>4</b>	<b>METHODOLOGY</b>	<b>27</b>
4.1	FACTORS TO CONSIDER	27
<b>4.1.1</b>	<b>Network technology</b>	<b>27</b>
<b>4.1.2</b>	<b>Packet size</b>	<b>28</b>
<b>4.1.3</b>	<b>Sending frequency</b>	<b>28</b>
<b>4.1.4</b>	<b>Signal quality</b>	<b>30</b>
<b>4.1.5</b>	<b>Transmission power and distance</b>	<b>32</b>
4.2	5G END DEVICES	32
<b>4.2.1</b>	<b>QUECTEL RM520-GL</b>	<b>32</b>
<b>4.2.2</b>	<b>Quectel RG255C (RedCap)</b>	<b>35</b>
<b>4.2.3</b>	<b>WNC 5G NR sub-6 i-Router</b>	<b>35</b>
<b>4.2.4</b>	<b>Teltonika: RUTX50</b>	<b>37</b>
<b>4.2.5</b>	<b>Phoenix contact: TC ROUTER 5004T-5G EU</b>	<b>38</b>
<b>4.2.6</b>	<b>Siemens Scalance M800</b>	<b>39</b>
4.3	POWER MEASUREMENT SYSTEMS	39
<b>4.3.1</b>	<b>For devices powered via USB</b>	<b>40</b>
<b>4.3.2</b>	<b>For devices with proprietary power sources</b>	<b>41</b>
4.4	TEST PLAN AND SETUP	42
<b>4.4.1</b>	<b>Software tools used</b>	<b>42</b>
<b>4.4.2</b>	<b>Test plan</b>	<b>44</b>
<b>5</b>	<b>DATA ACQUISITION AND ANALYSIS</b>	<b>46</b>
5.1	TESTING	46
<b>5.1.1</b>	<b>Quectel RM520-GL</b>	<b>46</b>

5.1.2	<b>Quectel RG255C</b> . . . . .	<b>49</b>
5.1.3	<b>WNC 5G NR sub-6 i- Router</b> . . . . .	<b>51</b>
5.1.4	<b>Phoenix contact: TC ROUTER 5004T-5G EU</b> . . . . .	<b>53</b>
5.1.5	<b>Teltonika RUTX50</b> . . . . .	<b>55</b>
5.1.6	<b>Siemens Scalance M800</b> . . . . .	<b>57</b>
5.2	<b>RESULTS DISCUSSION</b> . . . . .	<b>60</b>
6	<b>ENERGY AUTONOMY VIA ENERGY HARVESTING</b> . . . . .	<b>65</b>
6.1	<b>SINGLE SOURCE ENERGY BALANCE FOR 5G DEVICES</b> . . . . .	<b>66</b>
6.1.1	<b>Photovoltaic powering comparison</b> . . . . .	<b>66</b>
6.1.2	<b>Thermoelectric powering comparison</b> . . . . .	<b>69</b>
6.1.3	<b>Kinetic powering comparison</b> . . . . .	<b>72</b>
6.2	<b>EXAMPLE FOR MULTI-SOURCE CONFIGURATION</b> . . . . .	<b>78</b>
6.2.1	<b>Use case: Process monitoring</b> . . . . .	<b>80</b>
7	<b>CONCLUSION</b> . . . . .	<b>88</b>
7.1	<b>FUTURE WORKS</b> . . . . .	<b>90</b>
	<b>References</b> . . . . .	<b>91</b>
	<b>APPENDIX A – PYTHON SCRIPT: FAST PING ON WINDOWS PLUS PUTTY SINCRONIZATION</b> . . . . .	<b>99</b>
	<b>APPENDIX B – PYTHON SCRIPT: COMMUNICATION WITH UM34C MEASUREMENT DEVICE</b> . . . . .	<b>101</b>
	<b>APPENDIX C – PYTHON SCRIPT: RAW TEXT OUTPUT FROM UM34C TO EXCEL FORMATTER</b> . . . . .	<b>102</b>
	<b>APPENDIX D – PYTHON SCRIPT: RSRP EXTRACTOR FROM QCOM LOGS OF SA MEASUREMENTS</b> . . . . .	<b>103</b>
	<b>APPENDIX E – PYTHON SCRIPT: RSRP EXTRACTOR FROM QCOM LOGS OF NSA MEASUREMENTS</b> . . . . .	<b>105</b>
	<b>APPENDIX F – PYTHON SCRIPT: INA219 LOG TO EXCEL FILE CONVERTER</b> . . . . .	<b>107</b>

## 1 INTRODUCTION

Wireless sensors have already been widely adopted in industry and, as telecommunications advance, their use has been increasingly growing over the last few years (BELFKIH; DUVALLET; SADEG, 2019). With the advent of New Radio 5th Generation (NR5G) and parts of its design specifically aimed to serve industrial networks and their needs, they have become even more attractive to industries. With 5th generation mobile network (5G) technology, hundreds of megabits of data collected by sensors can be transmitted with latencies as low as 1 ms (ATTARAN, 2023).

However, this increased capacity for data transmission comes with a cost in energy consumption (HUAWEI TECHNOLOGIES CO., LTD., 2023). While efforts are being made both in reducing this consumption and offering more powerful batteries to supply them, another solution may be in order. One possible answer to the energy requirements of the devices may be to use the ambient energy already being generated by the very same processes being monitored (YOON; PARK; YU, 2018). This is called energy harvesting and may come in many forms, but basically consist of converting different forms of energy from the environment into electrical energy. With these harvesting techniques, batteries can be recharged on site, greatly reducing the need to constantly stop the processes in order to exchange them. In ideal scenarios, the sensors and transmitter may even be fully powered by the harvester, with the battery acting as only a backup or aid.

In order to verify the viability of this solution, a study of how much power is consumed by different 5G transceivers in various scenarios is necessary. This would allow for a comparison with the current power generation capabilities of various energy harvesting technologies.

This initial chapter outlines the context and motivation for this work. This will be followed by a description of the objectives and scope of this work, concluding with a description of the structure of the rest of this Bachelor's thesis.

### 1.1 MOTIVATION AND CONTEXT

The main ideas brought by Industry 4.0 include connectivity, decentralization, interoperability, remote data availability, and real-time data analysis (RAO; PRASAD, 2018). For these aspects to be implemented, high speed connectivity with minimal latency is needed. However, while the demands for this type of data increase, the physical restrictions on transferring said data from where it must be collected remain constant. The transmission aspect itself has been solved with technologies such as the LTE 4G and NR5G networks. The challenge now is to support these technologies, especially NR5G, due to its higher capacity and lower latency (BARB; OTESTEANU, 2020). The aspect of remote data collection systems which requires the most attention



is the power source, since the battery or capacitor used for that purpose dictates the maximum operating time of the process (FAN et al., 2020). Due to the many limitations batteries have, a renewable energy source would be ideal. Since energy harvesting already had many applications in the past for powering sensor nodes and other Internet of Things (IoT) applications of the previous generations (SUDEVALAYAM; KULKARNI, 2011), it is one of the ideal candidates for this role. So this project came to fruition, aiming to verify if it would be possible for the current energy harvesting techniques to supply the current 5G transceivers.

In order to verify if energy harvesting techniques would be a viable candidate, a study on the power consumption of multiple 5G transceivers was conceived. The various elements that constitute the communication were studied to determine what influences the power usage of these devices. This helped verify which aspects are the most critical in order to reduce the power consumption and provide a comprehensive overview of potential variations in power consumption a device may have.

In this way, there is concrete data on the power requirements of multiple devices and what can influence them, allowing for informed decisions on the device and details needed for projects. This needed to be done as usually the analysis of the devices is restricted to one specific setup and application. This study would allow the design of an energy harvesting system that could supply the sensor units. This data would also allow for the reverse approach, where, based on information on the amount of energy available for the harvesters, a study of viability and design of a sensor unit can be made.

## 1.2 OBJECTIVES OF THE THESIS

### 1.2.1 General objective

The main goal is to analyze the energy requirements of different 5G routers to offer references for future projects and compare how close energy harvesting techniques are of supplying them. With this research, energy critical systems will have a basis of the energy costs of the data they transmit. In addition, projects aiming to use energy harvesters will have a basis to estimate the amount of area and conditions required in order to fulfill this energy need.

### 1.2.2 Specific objectives

From the main objectives, specific tasks were drawn to achieve the intended results:

- Determine the factors that can influence the energy consumption in 5G devices during communication.
- Develop a methodology to test the devices based on those findings.

- Develop ways to measure said energy consumption.
- Take the measurements and compare the data with the energy generation from energy harvesting methods.
- Create a theoretical use case where a 5G sensor unit is powered by multiple energy harvesters in order to evaluate its viability.

### 1.3 DOCUMENT OUTLINE

This document is divided into seven chapters presenting the development of the project.

**Chapter 1** introduces important information about the project, including its motivation and context. It also outlines the objectives and scope of the author's work.

**Chapter 2** presents the institute and department where the project was conducted.

**Chapter 3** provides the theoretical background of the thesis. It outlines concepts about NR5G, use case requirements, and an introduction to energy harvesting technologies. The information presented is intended to situate the reader, allowing them to understand what is presented in the remaining chapters.

**Chapter 4** presents the development of the testing methodology that would be applied in chapter 5. It also introduces the devices to be tested with said methodology and the instruments to be used.

**Chapter 5** is where the testing procedure and the results obtained from it are shown and analyzed.

**Chapter 6** is where the results generated previously are cross compared with energy harvesting techniques to check how viable it would be for different energy harvesting techniques to power each device. This comparison would consider both each technique separately, as well as a study of multi-source energy harvesting.

**Chapter 7** concludes this thesis discussing the obtained results, comparing them to the initial objectives, while also discussing possible future works that can use the collected data and results.

## 2 THE FRAUNHOFER SOCIETY



Figure 1 – Fraunhofer society Logo. Source: Fraunhofer Institute database.

The Fraunhofer society, known as *Fraunhofer Gesellschaft* in German, is one of the world's leaders in applied research. The society's logo can be seen in Figure 1. Founded in 1949 and named after Joseph von Fraunhofer (1787–1826), an inventor and researcher hailing from Munich. Mr. Fraunhofer is considered one of the fathers of modern optics, due to his contributions to lens manufacturing and research about the spectral composition of light (FRAUNHOFER, 2022).

Headquartered in Germany, this group forms a non-profit organization with the mission to pioneer technology and strengthen the German and European economies while committed to ethical values. As of 2023, it is composed of more than 80 research facilities, including 76 institutes and research units employing more than 30 thousand workers, primarily scientists and engineers. Engaging in both privately and publicly funded research projects, approximately one third of its funding comes from industry contracts. Another third comes from public backed projects, and the remaining third originates from the German government at Federal and state levels as base funding (FRAUNHOFER, 2023).

As research facilities, the Fraunhofer institutes aim to create the technology and scientists of the future. Their mission is to strengthen companies' performance and efficiency with their research while simultaneously training the next generation of engineers needed for economic and technological advancement.

One of the many facilities of the Fraunhofer Society is the Fraunhofer Institute for Production Technology (IPT), located at the Rheinisch-Westfälische Technische Hochschule (RWTH) campus in Aachen. This institute specializes in crafting systems solutions geared towards fostering sustainable, resilient, and digitally-driven production methods for resource-efficient products (IPT, 2023a).

The Fraunhofer IPT is vast, contemplating many areas, from production technology, to bio-adaptive production. While all departments in the institute are worthy of note, for the case of this project one must be focused on. The Production Metrology department focuses on non-invasive optical measurement technology, digital infrastructures for production and automation in the life sciences. It uses and develops advanced equipment to provide measuring services and continuously improve their methods. One of the achievements of this department is the management of the 5G industry Campus Europe, which is one of the largest 5G test beds in Europe, with 1 km<sup>2</sup> of outdoor networks

and 7000 m<sup>2</sup> on indoor machine halls. These test beds have multiple configurations and technologies, such as non-standalone, standalone, and even millimeter wave networks, all of which have projects or studies being executed with them. The department is also helping to push the boundaries of technology in areas such as automation of industrial processes, biomedical imaging, digitalization of industrial processes, optics testing, lithography, in-line laser process control, and fiber optic sensors for structural integrity monitoring (IPT, 2023b).

### 3 THEORETICAL BACKGROUND

This chapter provides a theoretical overview of key subjects present on this thesis. The first section offers a summary of NR5G technology. In the second section, Industry 4.0 and the importance of 5G in its existence is discussed. Lastly, an introduction to multi-source energy harvesting is presented. All sections together aim to provide the fundamentals to comprehend the remaining chapters of this document.

#### 3.1 NEW RADIO 5G

Telecommunications technology has evolved significantly over time. At its inception in 1980, the technologies that would come to be called the first generation only allowed 2.4 kbps of voice data to be transmitted. Today with massive data services and IoT applications becoming a reality (SHARMA, 2013). A cursory glance at the capabilities of each generation can be observed in Figure 2.

In the pursuit to improve this technology, in 1998, the seven big players in the telecommunication field at the time came together in order to organize the development of technical specifications of 3G networks. This partnership, known as 3rd Generation Partnership Project (3GPP), initially aimed to generate technical specifications and reports for the 3rd generation of telecommunications. However, the benefits of such a group proved invaluable, resulting in the scope of the association to be amended to address the development of the future generations (3GPP, 2024). As a result, the 3GPP is the main organization defining the characteristics and other elements of the generations through what are called releases. These releases present the agreement of the partner companies on what should be the characteristics and standards of the technology at that time.

With the release 15 by 3GPP, published in 2018, NR5G standards were defined. These standards as well as the capabilities of this technology were developed further in release 16, that also had the name 5G phase 2 (3RD GENERATION PARTNERSHIP PROJECT, 2022). This second phase introduced time sensitive communication (TSC), industrial IoT, Ultra Reliable Low Latency Communication (URLLC), improved localization services, improved energy efficiency, among other aspects, demonstrating the continuous improvement of this technology. This energy efficiency improvement came in many forms. From simply having more efficient components to build the core and transceivers, to having an extra configuration for the stations named the Radio Resource Control (RRC) inactive mode. While this mode is exclusive to SA networks, it allows for power saving while not disconnecting from the network, saving the power and time required for this action (ETSI, 2018). Alongside with the updates, there was also the creation of 25 new use cases that required lower latencies and higher data transmission rates to make their realization possible. Some of the use cases were

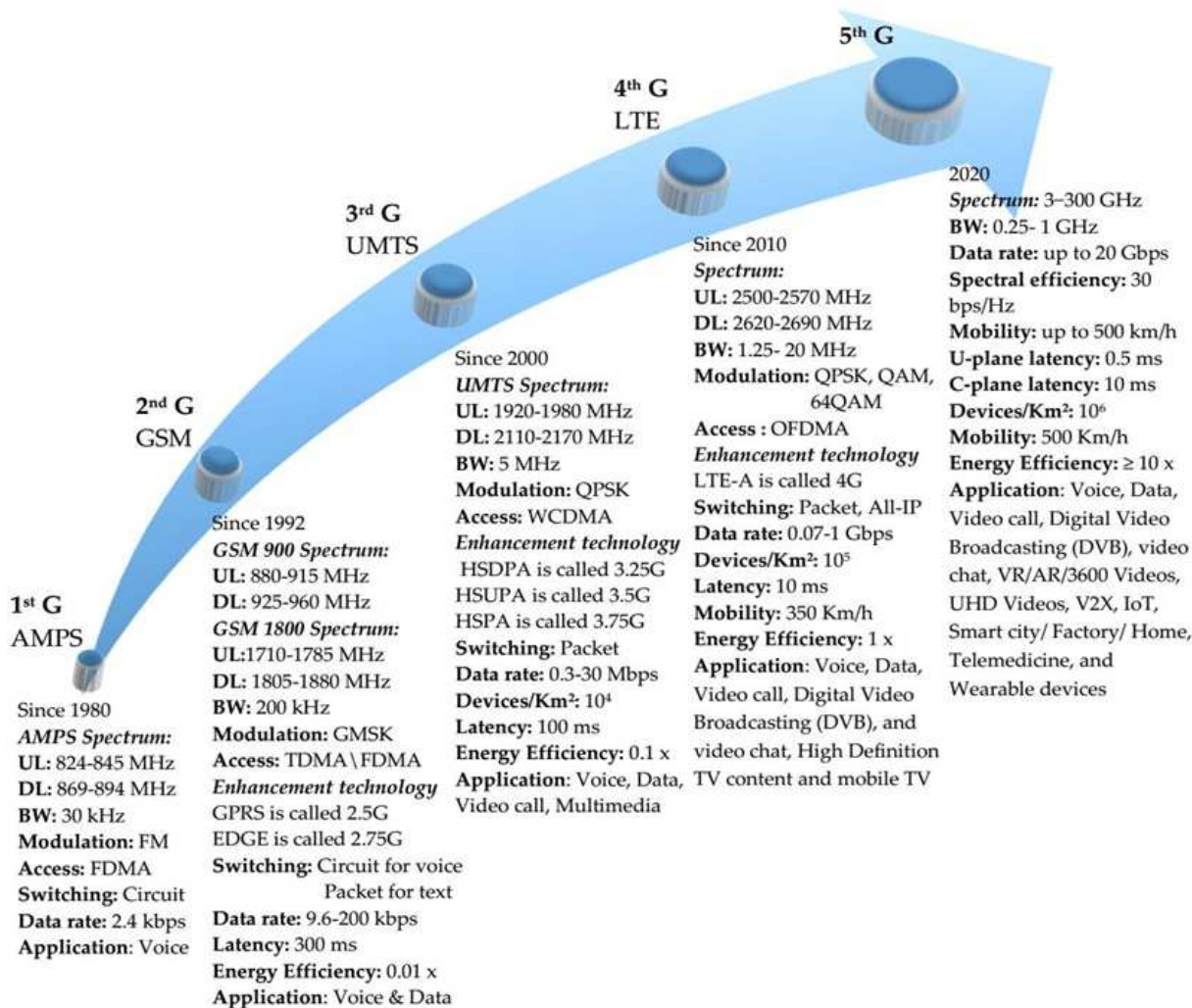


Figure 2 – Leading communication achievements for several generations (1G to 5G).  
Source: Solyman and Yahya (2022).

related to assisted or autonomous driving, where milliseconds can be the difference between an accident happening or not due to a missing instruction to break or turn (KIM, Younsun et al., 2019). Other use cases were used for augmented reality, where delays in the visuals could induce nausea in users. The remaining aimed to cater to real-time processes or large amounts of data transfer that were required for industry 4.0.

### 3.1.1 NR5G capabilities

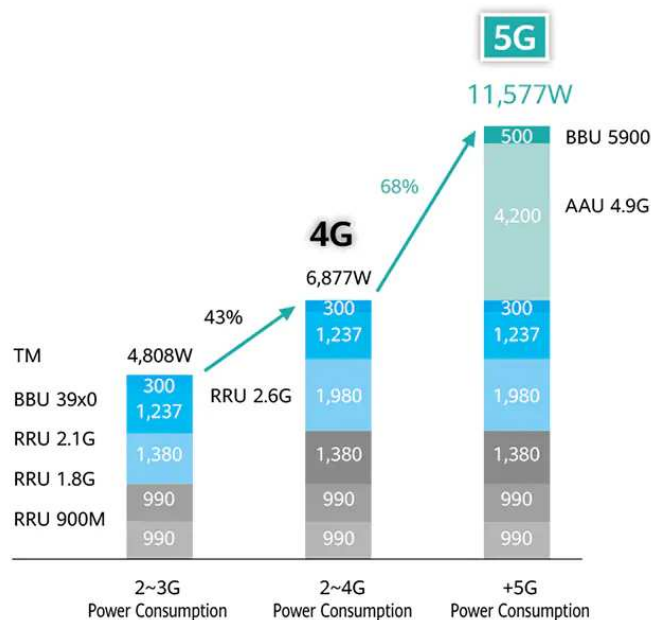
This new generation of 5G standards was created to improve upon its predecessors and solve the challenges that plagued them. The very first improvement of NR5G when compared to Long Term evolution (LTE) 4G is the maximum amount of data it can transmit. This improvement is not isolated to lab conditions and other ideal scenarios, but also to what is commonly referred to as average user experienced rate. This term is a metric to measure the average performance of the network in common day-to-day

scenarios. For example, a connection with a mobile device outside on a windy day or without line of sight.

In 4G, the peak data rate was of 1 Gpbs, with this peak considering ideal circumstances. If the same conditions are applied to 5G, a peak data rate of 20 Gpbs can be achieved. In more realistic scenarios, 5G in its original setup can provide an average user data rate of 100 Mbits to mobile units, 10 times higher than LTE 4G networks (BARB; OTESTEANU, 2020).

Regarding latency, LTE is limited to a theoretical minimum of 10 ms, which is too high for many time sensitive applications. NR5G can, in theory, bring it down to less than a millisecond. Outside ideal conditions, this reduction still brings the latency close to or even below 10 ms. This opens many paths, particularly for real time control scenarios, such as autonomous driving. Since in 10 ms a car at 100 km/h can move 28 cm before it even gets the signal to slowdown, this delay can be a matter of life or death in an accident. This reduction in delay coupled with the higher throughput also allows for automated cars to drive closer to have better communication between each other while not risking crashing, making the lanes safer and more efficient (BAGHERI et al., 2021).

Even though its performance opens the way for multiple new technologies, it does not come without costs. NR5G is also the more energy hungry than its predecessors, as can be seen in Figure 3.



Typical maximum power consumption of a single 5G base station

Figure 3 – Typical maximum power consumption of Telecom devices. Source: HUAWEI TECHNOLOGIES CO., LTD. (2023)

Although at a first glance this appears to be a major problem, it is remedied to an extent. The faster communication means less time actively transmitting, considering the amount of data remains constant. This time reduction translates to a reduction in the amount of required energy. This fact, coupled with sleep and energy saving modes that take advantage of these idle times can make 5G networks more energy efficient than their counterparts (FRENGER; TANO, 2019). This increase in efficiency is only possible if the network is not being used to its full capability, allowing for idle time. In these extreme cases, 5G technology is required because such traffic would overload the base stations of the older generations.

Another new feature of NR5G that was not present in its predecessors are the Reduced Capacity devices, often Shortened to RedCap devices. Originating from release 17 onwards, this technology aims to mitigate the high energy requirements of NR5G by sacrificing performance in order to be even more energy and cost-efficient (VEEDU et al., 2022). At a first glance, harming performance of the device seems counterproductive, but it is well within reason. Those devices are designed for specific applications where the data amounts to be transmitted are relatively low, while the battery life is a higher priority. This means that the standards set the minimum throughput for RedCap devices at 50 Mbit/s, a reduction of 80% from the normal capabilities of the original devices. On the other hand, the expected battery life for a mobile device using a RedCap device is expected to last multiple years (RAHMAN et al., 2021).

### 3.1.2 Technology types

NR5G networks can be divided into different categories depending on their deployment and architecture. The two main divisions are its accessibility and its usage of 4G resources. The use of the 4G resources creates the division between non-standalone (NSA) networks and standalone (SA) networks.

This classification between NSA and SA comes from the network use of 4G technologies. When 5G was designed in 3GPP 15, released in 2018, it was created with two architectures in mind, standalone and non-standalone (3RD GENERATION PARTNERSHIP PROJECT, 2019).

This double deployment strategy was done aiming to ease the implementation of NR5G, since Non-standalone systems would use the existing LTE 4G infrastructure and core. Because of the shared resources, the implementation of NSA networks was far more cost-effective than deploying a network from the ground up (RAKUTEN MOBILE, 2021). Since part of the transmission was made using 5G there are many improvements in the speed and latency of communication. However, this technology it still limited by the 4G core, hindering the capabilities of the 5G portion. The solution to this was the SA architecture that used pure 5G, allowing for faster processing and communication at the cost of needing a new core and associated hardware to operate. An illustration



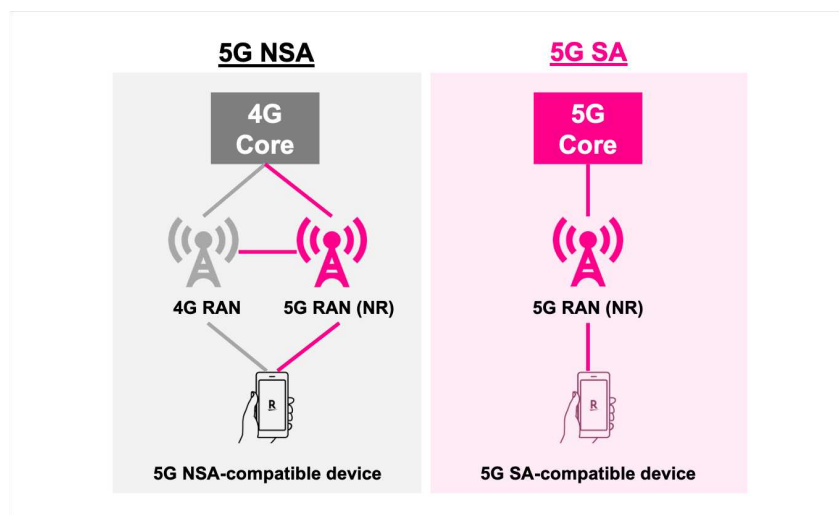


Figure 4 – Structure of SA and NSA networks. Source: Rakuten Mobile (2021)

of the structure of each architecture can be seen in Figure 4. Both technologies have been strenuously tested. For example, a test comparing their performance in an indoor application proved a better uplink data rate for the SA network compared to the NSA (MOHAMED; ZEMOURI; VERIKOUKIS, 2021).

The accessibility factor originates from the differing requirements 5G networks may have depending on the intended application. Public networks are usually considered the standard application, since they offer telecommunication service to the public, which was the original reason for the development of this technology. In order to meet this demand, public networks are tailored for supporting massive amounts of users, sacrificing latency and performance if needed. On the other hand, private networks are tailored for specific applications, having far fewer users and coverage, focusing on meeting specific needs of the company that deploys it. While both networks provide the additional benefits of 5G technology, such as low latency and high reliability, private networks have the benefits of doing so in a controlled and secure environment. This helps companies to keep their information secret and free of disturbances which may affect performance (AIJAZ, 2020).

### 3.1.3 Technical aspects

NR5G uses frequencies from 450 MHz to 43.5 GHz in licensed bands, with the higher frequencies being specific for 5G communication (KIM, Younsun et al., 2019) and (ZHAO et al., 2023). The actual division can be better understood in the diagram shown in Figure 5.

The frequencies can actually be divided in two groups, the ones below 6 GHz and the C-Bands, that are above this threshold. The communication in the C-bands is often referred as in millimeter waves, or mmWave, because of the frequency wavelength being in the scale of millimeters. Despite this configuration having incredibly high

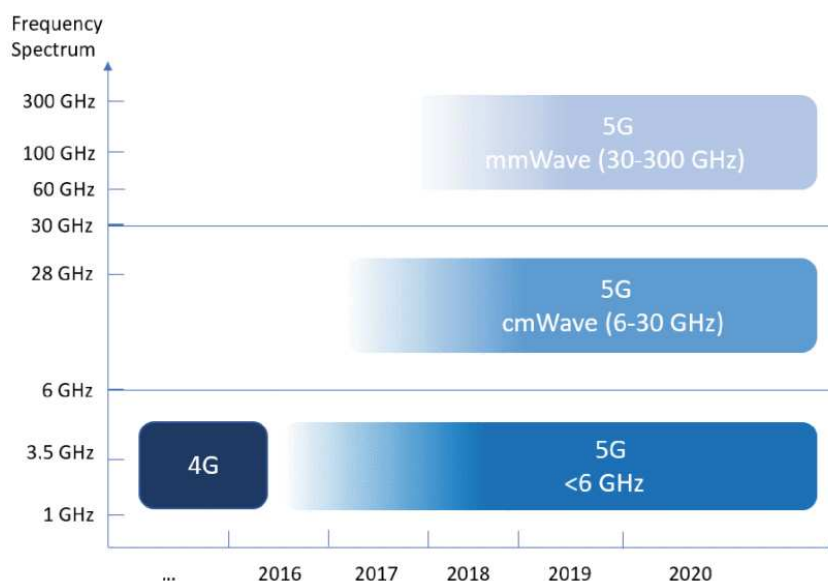


Figure 5 – 4G spectrum versus 5G spectrum. Source: Barb and Ottesteanu (2020).

speeds, it suffers greatly from obstructions due to using such a high frequency. So, in this study, the focus is on the technologies using sub 6 GHz bands.

To clarify, the frequencies are usually defined in bands, although their exact composition varies depending on the region of the world. Since this project is being conducted in Germany, the European Union standards will be the ones used. This signifies that 5G uses the spectrum between 3.7 GHz and 3.8 GHz (3RD GENERATION PARTNERSHIP PROJECT, 2019).

### 3.2 ENERGY HARVESTING

Energy Harvesting refers to a collection of technologies which aim to extract, or in other words harvest, the energy available from the environment in small amounts. This energy is used to power microsystems, including wireless sensors, biomedical implants, military monitoring devices, structure-embedded instrumentation, remote weather station, and various others (HARB, 2011).

In any process, energy losses occur, resulting in the energy employed being converted into other less desirable types of energy that are dissipated into the environment. Be it as kinetic as vibrations, heat, light, electromagnetic, etc., regardless of form, this energy byproducts are usually addressed under the umbrella term of ambient energy. This term comes from the energy being lost in the environment itself. Just as there are many ways for processes to saturate the environment with different types of energy, there are also many forms of energy harvesting to collect them. For instance, piezoelectric and triboelectric methods generate electrical current from mechanical stresses, while thermoelectric and pyroelectric technologies use temperature gradients for that purpose. Additionally, photovoltaic systems convert light into electricity. These

examples represent just a few of the many approaches to energy harvesting (LEE et al., 2016).

### **3.2.1 Multi-source energy harvesting**

One challenge with energy harvesting technologies is their conditional or intermittent power generation. A possible solution to this problem is the combination of different energy harvesters (WEDDELL et al., 2013). This approach enables that one or more harvesters compensate the idle time of the others, increasing the stability and adaptability of the system. With increased generation, the system can also support more energy intensive applications to a certain extent (DENG et al., 2019).

## 4 METHODOLOGY

To develop a methodology for testing the devices, several points must be considered. Five factors were identified as having a possible influence on the power consumption of the devices, and are discussed in the subsections of Section 4.1. Next, the end devices to be tested were decided upon and are briefly presented on Section 4.2. This was accompanied by explanations of their characteristics and limitations. This is followed by the presentation of the measuring instruments to be used in Section 4.3. Lastly, the tools used to control the data being sent and the test plan are elaborated upon, considering the elements discussed previously in this chapter.

### 4.1 FACTORS TO CONSIDER

For energy consumption to be studied, the multiple factors that can influence it must be acknowledged. Factors such as packet size, sending frequency, network technology and signal quality impact the power usage need to be considered to properly estimate the device energy usage. Since each of these factors will influence power consumption in different ways, they must be considered in order to design the test plan. In the following subsections, all of these influencing factors will be discussed in detail.

#### 4.1.1 Network technology

One factor that influences the energy consumption is the connection itself, as it dictates how information will be transmitted and received on many levels. Looking at a NSA network, in order to establish connection, the device will need to communicate with the 5G network and with its 4G anchor band. Therefore, from the moment of connection, there are differences in the energy consumption between an SA and a NSA connected device. Upon research, this line of thought was confirmed as even without considering the addition of the Radio Resource Control inactive mode exclusive to SA, NSA showed a higher power consumption (LIU et al., 2020). Said mode is a more efficient option to idle mode, created with the intention to reduce power usage along other things. Overall, the study of the impact of different mobile networking structures have in energy consumption is not something new. Although it has been studied since the first mobile base stations were conceptualized, 5G brought a renewed focus to this topic. In fact, it has been directly or indirectly the subject of many studies, such as Shurdi et al. (2021) cited previously.

The conclusion from this is that all test scenarios conducted for this project need to be measured twice: once in an SA network and once in a NSA network. Although, one exception would be needed for the RedCap devices. This type of device sacrifices performance in order to be more energy efficient, resulting in lower energy usage. This

sacrifice is possible by having the network do more of the processing required for a successful communication, requiring a special version of the SA network to be running in the 5G core. Since this special version is exclusive to the SA network, it is not possible to connect this type of device in NSA networks, rendering testing within it impossible.

#### 4.1.2 Packet size

One of the common metrics to measure energy efficiency in single links (one device to one antenna) is given by:

$$E_E = R/P, \quad (1)$$

where  $E_E$  is energy efficiency,  $R$  signifies the system throughput, and  $P$  is the power used in the transmission. The unit for energy efficiency is bit per joule.

From this relationship, it is clear that there is a link between the amount of data being sent and the power consumed by the device. This is somewhat logical, because the device must spend energy broadcasting the data or interpreting it. Therefore, the payload size must be considered in this study, as it directly influences the device throughput.

Since the amount of data can vary significantly between use cases, the paper presented in Gangakhedkar et al. (2018) was used as a reference. It contains a list of various use cases for industrial automation determined by 3GPP. A summary of the requirements of each use case is illustrated in Figure 6. Although some of these use cases do not align with the ones being currently worked on by the author's department, they serve as a baseline. It also follows the main idea of this project to both future-proof and provide data for ongoing projects.

With those parameters in mind, it was decided that the starting payload would be of 0 bits, or idle, to have as a baseline. The second test would have 128 bytes, and each following one would double the payload. This would continue until the payload reaches 1024 bytes. Those values were chosen because they are close to the maximum transfer unit (MTU) of the network. Any payload that surpasses this value would be fragmented into smaller chunks in order to be transmitted. Because the objective is to evaluate how much one transmission impacts the power consumption, fragmenting it into many smaller transmissions is counterproductive, and its impact will be addressed in the next section.

#### 4.1.3 Sending frequency

A second aspect to be impacted by the energy cost-per-bit transmitted is the interval between transmissions, also known as sending frequency. The sending frequency must not be confused with frequency bands used to transmit the signal, as these are different concepts. Research upon the topic returned the paper (CHEN et al., 2015)

Communication Requirements Use case		Link Requirements						System requirements		
		Time-critical or cyclic			Non-critical					
		Cycle time	Payload	Jitter	E2E Latency	Data rate	Jitter	Service area	Number of nodes	Node mobility
Motion Control	Printing machine	<2 ms	20 B	< 1 $\mu$ s	-	> 1 Mbps	-	100 m x 100 m x 30 m	> 100	<20 m/s
	Machine Tool	<0.5 ms	50 B	< 1 $\mu$ s	-	> 1 Mbps	-	15 m x 15 m x 3 m	~ 20	<20 m/s
	Packaging machine	<1 ms	40 B	< 1 $\mu$ s	-	> 1 Mbps	-	10 m x 5 m x 3 m	~ 50	<20 m/s
Control-to-control communication	Communication between different industrial controllers	4-10 ms	< 1 KB	< 1 $\mu$ s	< 10 ms	> 5-10 Mbps	-	5-10 times the service areas for Motion Control	5-10	-
Process Automation	Closed-loop control	10-100 ms	Few Bytes	< 1-10 ms	-	-	-	Hundreds of m <sup>2</sup>	10-1000	Low
	Process Monitoring	50 ms	-	-	-	-	-	Several km <sup>2</sup>	< 10000	Low
	Plant Asset Management	50 ms	-	-	-	-	-	Several km <sup>2</sup>	< 10000	Low
Mobile Robots	Precise cooperative robotic machine control	1 ms	40-250 B	< 50% of Cycle time	-	> 10 Mbps	-	< 1km <sup>2</sup>	100	< 50 kmph
	Machine Control	1-10 ms								
	Cooperative Driving	10-50 ms								
	Video-operated remote control	10-100 ms								
	Standard robot operation & Traffic management	40-500 ms								
Human-centered Monitoring	Safety Control Panels	4-8 ms	40-250 B	< 2-4 ms	< 30 ms	> 5 Mbits/s	< 15 ms	10 m x 10 m up to 200 m x 300 m	2-4	Medium
	Augmented Reality	< 10 ms	20-50 Mbits/s	-	-	-	-	Typical factory floor size	≤ Number of workers	Low

Figure 6 – Industrial automation use case requirements, as determined by 3GPP.  
Source : Gangakhedkar et al. (2018)

which studies this relation. As highlighted in the paper, the more data are transmitted, the more energy must be consumed to broadcast it. In the same way, the more data is received, the greater the energy spent on interpreting it.

With confirmation that this aspect was worthy of study, how this would be done was to be considered. Once again, the use cases in industry present great variations in their frequency of updates. Dynamic processes may require updates every couple of milliseconds, while slower or the less time sensitive ones may require them only every minute or have even longer windows of time. There are even systems that reduce their update rate in order to hibernate between transmissions, which is another point to be considered.

Once again, referencing the table in Figure 6, the fastest cycle time is that of

machine tools, being smaller than half a millisecond. However, considering most other use cases had intervals of or superior to 1 ms and due problems with generating the messages in the correct intervals while also recording the results, 1 ms was chosen as the smallest value. Also from the table, the intervals of 10 ms, 100 ms, and 500 ms were extracted as the highest. Still, keeping in mind that other applications may have lower sending frequencies, values in the order of seconds must be considered. This is particularly important because allowing systems to hibernate for extended periods in order to save power is a well-known strategy. After verifying other use cases from past projects at IPT and partners, a spread of intervals was decided. So it was chosen to test the following intervals of time between each packet: 1 ms, 10 ms, 100 ms, 0.5 s, 1 s, 10 s, and 30 s.

The last variable to be determined for this test is the amount of data to be transmitted. Considering there will already be tests verifying the impact of this aspect, the payload must be constant for the sending frequency scenarios. In order to still have a significant payload for the tests, the value of 256 bytes was chosen. This value was chosen because it is in the middle of the scale set for the payload tests.

#### 4.1.4 Signal quality

The fourth element to consider is the quality of the signal received by the devices. Considering Frii's Equation (SHAW, 2013), presented below:

$$\frac{P_r}{P_t} = G_t G_r \left( \frac{\lambda}{4\pi d} \right)^2, \quad (1)$$

where  $P_r$  is the power received,  $P_t$  is the power transmitted by the original device or antenna,  $G_t$  is the gain or amplification of the transmitter,  $G_r$  is the gain of the receiver,  $\lambda$  is the wavelength, and  $d$  is the distance between the transmitter and receiver.

From this equation, we can assert that the larger the portion of transmitted power is received by the device, the less energy is needed to boost the signal for transmission or upon reception. Therefore, a stronger and more reliable link between the antenna and the device results in greater energy efficiency during communication (ZAPPONE et al., 2016).

One of the main metrics to evaluate the quality of a connection is the Reference Signal Received Power (RSRP). This metric evaluates the current signal power received by an end-device (AFROZ et al., 2015). The result is in decibels per milliwatt (dBm), starting at 0 which can be converted to 1 mW of received power. The minimum value for this metric is tied to the receiver sensitivity, which is the minimum power required for a device to be able to discern the signal from noise. The actual minimum value depends heavily on the device, as the regulation dictating it is that the device is able to transmit 95% of the maximum throughput defined for fixed reference channels (PERALTA et al., 2018), (3RD GENERATION PARTNERSHIP PROJECT, 2019).

Another compelling reason to choose RSRP as the reference for this study is its widespread use in end devices for handover decisions. This metric is, between others, used to select to which cell should a device connect for optimal performance. Because of this, the RSRP value is readily available from the perspective of all the measured devices, eliminating the need for extra equipment and ensuring the data collected represents the studied devices' points of view.

However, two problems appear when studying the quality of the connection. The first and lesser of the two is that due to their differing construction, any two devices when exposed to the same signal may obtain different RSRP values. Trying to move or shield them so all have the same average value would overly complicate the tests while bringing no real benefit to the research. The solution proposed is that all devices are to be measured in the same place, so they, in theory, are exposed to the same signal. This place would be the 5G showroom at IPT since it presents great signal quality. The second and more concerning problem is that the routers only evaluate the signal strength of the link every few seconds. Since this is a metric to be studied, this would imply in either a small sample size or impossibly long tests. Thankfully, doing preliminary tests with all devices has shown that as long as there are no interferences with the signal, its strength is remarkably stable.

Taking this into account, and considering that the measurements could take up to five minutes, it was decided that RSRP would be monitored alongside the power measurements and assigned to each of them, but the average RSRP would be calculated from all the values added together. The importance to pair each power measurement with an RSRP measurement is that in case something affected the network and had an impact in the power measurement, there would be a register to possibly explain the result and indicate that the measurement needed to be retaken.

Another reason to measure the signal strength during all other tests is to obtain the average signal power received by the device. With an average value to act as a reference, it was possible to test to other scenarios, one with a degraded signal strength, and another with the signal quality as high as possible. Due to the excellent coverage in the institute, the average power received by the devices is around or above  $-80$  dBm, which is considered good or even excellent in industry standards (PRAMONO et al., 2020). While this does not leave much room for improvement, there is ample opportunity for degrading the signal. This degradation can be obtained by either distancing the transceiver from the antennas or by adding shielding between. The actual process used will be discussed further in Section 4.4.2.

Lastly, since both frequency and payload size have tests dedicated to them, both values can be static in these tests. For the two RSRP tests, an interval of one second and a packet size of 256 bytes will be used, as those are the default values for these metrics when not being evaluated in the previous tests.



### 4.1.5 Transmission power and distance

From Frii's equation, it can also be inferred that the more energy is emitted, the higher the chance that the signal will be received with sufficient strength. The same logic also applies to distance, as the two devices being closer reduces the losses to the environment. However, both of these aspects are already represented in RSRP variation scenarios, so no special test is required for them. In reality, the reduction of distance is the planned course of action for improving the RSRP value for its respective test.

Regarding the power used in the transmission, while if the device is capable of modulating it, it will use RSRP or a similar metric as a basis for the modulation. Many devices are not even capable of doing so, especially those expected to operate without a connection to the power grid. Since they operate with a battery, it depends on the main antenna which has more power available to power to amplify the signals transmitted and received. Because of this, by evaluating the RSRP value and its link with the power consumption, those two metrics are also considered.

## 4.2 5G END DEVICES

For this project, six devices were chosen to be tested after deliberation with the other team members. The main reason for the choices were the fact that all six devices are already in use, or will be used in future projects that would benefit from this data. One of this projects in special involves multi-source energy harvesting and would require the data that are generated in this project are to determine which devices are the best matches for the proposed use cases. In addition to the main purpose, there are some other reasons for testing some transceivers. For example, one WNC 5G NR sub-6 i- Router is being used in a mobile automatically guided vehicle (AGV). Since the vehicle is battery powered and expected to work for long periods, the data about its power consumption can be of value for the project.

Each of the following subsections is dedicated to one of the six used 5G transceivers, starting with the USB powered devices.

### 4.2.1 QUECTEL RM520-GL

The Quectel RM520-GL is a small chipset optimized for IoT and enhanced Mobile Broadband (eMBB) applications. It supports a wide range of networks types, including Long-Term Evolution Frequency Division Duplex (LTE-FDD), Long-Term Evolution Time Division Duplex (LTE-TDD), Wideband Code Division Multiple Access (WCDMA), Global Navigation Satellite System (GNSS), NR5G SA, and NSA. This module was designed with energy efficiency in mind, having cutting-edge technologies such as carrier aggregation and MIMO to enhance data throughput while minimizing power con-



Figure 7 – Quectel RM520-GL module. Source: Solutions (2024).

sumption. It also has sleep and power down configurations in order to save power in applications with intermittent communication. In Table 1, it is possible to read its maximum data rates for different network technologies (QUECTEL WIRELESS SOLUTIONS CO., LTD, 2022).

Table 1 – Maximum Data Rates of Quectel RM520-GL

<b>Technology</b>	<b>Downlink</b>	<b>Uplink</b>
5G SA Sub-6	2.4 Gbps	900 Mbps
5G NSA Sub-6	3.4 Gbps	550 Mbps
LTE	1.6 Gbps	200 Mbps
WCDMA	42 Mbps	5.76 Mbps

Source: Author.

Because of its connectors and lack of in-built antennas or heat sink, the Quectel module must be connected to an evaluation kit or a custom printed board circuit. The evaluation board used in this work, the 5G RMU500 EVB Kit, is shown in Figure 8 with the Quectel module connected under the heat sink. As illustrated, the board provides the features required for the Quectel module to operate. It has four antennas for communication, a SIM card socket for network registration, and a USB-C plug for communication and to provide power to the module. Additionally, it presents two LEDs to provide info to the users: a red one to indicate power and a blue one to indicate the SIM-card recognition.

In order to communicate with the module to configure it or inquire aspects of the network, the Hayes AT commands set must be used. AT commands are a short text command language created in 1981 for use in modems and have been used in



Figure 8 – Quectel RM520-GL in an Evaluation board. Source: Author.

telecommunication since 1990. Using these commands, configurations such as the technology to use, bands to connect, and any other settings can be established. This also allows querying information collected by the board, such as networks it can detect, the RSRP measure from the cell it is connected, and other information.

In order to set up the board, the program QCOM, also from Quectel Ltd. is used to communicate with the board using the aforementioned AT commands. During the tests, this same program was used to obtain the current RSRP values from the board and log them for further study. The command used to do so was `AT+QENG="servingcell"`, as it returns information about the radio cell the device is currently connected to and provides details about the link, including the RSRP metric. An example response can be seen below:

```
[2024-04-25_16:30:04:509]at+qeng="servingcell"
```

```
[2024-04-25_16:30:04:509]+QENG: "servingcell", "NOCONN", "NR5G-SA", "TDD",  
999,99,00002C001,20,230A,650016,78,3,-72,-11,25,1,-
```

In this response, it can be extracted that the device was connected to a private SA network, as indicated by the "NR5G SA" and "999,99" indicators. The value of interest, RSRP, is the fourth starting from the end, in this case, -72 dBm. The data from these logs was extracted using the script in appendix D for the tests in the SA network and the script in appendix E for the NSA.

#### 4.2.2 Quectel RG255C (RedCap)

As the name suggests, this is a reduced capacity version of the Quectel module, like the RM520-GL discussed in Section 4.2.1. Due to this, the device shares the same physical chip connectors, possible evaluation boards that can be used, and configuration via AT commands.

Due to being a reduced capacity device, its performance and other features were diminished or made to be handled by the core network. The result is a cheaper and less energy hungry chipset. One thing to highlight is that despite the reduction in capabilities, it is still able to have 50 Mbit/s throughput in both upload and download, making it fit for all use cases presented in Section 4.1.2. One aspect that must be considered about the RedCap device is that it is a very recent technology, still in its engineering sample phase. Said sample was also damaged during its first test, so it only has one of the two antenna connectors for 5G communication.

Similarly to Quectel RM520-GL, this module also uses an evaluation board to provide it with the necessary ports and connectors. In this case, the evaluation board is the model 5G RedCap EVB Kit, which has been designed for this module. The one used in the tests with the module and antennas connected can be seen in Figure 9.

Also because it is so recent, this device requires features from the NR5G release 17 to be active on the network in order to work properly. This is expected, since the concept of RedCap devices was also outlined in this release. However, these requirements make it incompatible with the current IPT network that runs a configuration from release 16 for the SA network. The solution to this is to temporarily update the SA network to release 17 in order to perform tests with the RedCap device. Since there cannot be an update of this type to the NSA network, testing of this module were exclusive to the SA 5G network.

#### 4.2.3 WNC 5G NR sub-6 i-Router

The WNC 5G NR sub-6 i-router, presented in figure 10, has a very descriptive name. It is a router made by the Wistron NeWeb Corporation (WNC), designed to connect to NR5G networks using bands under 6 GHz. This device is one of the most used

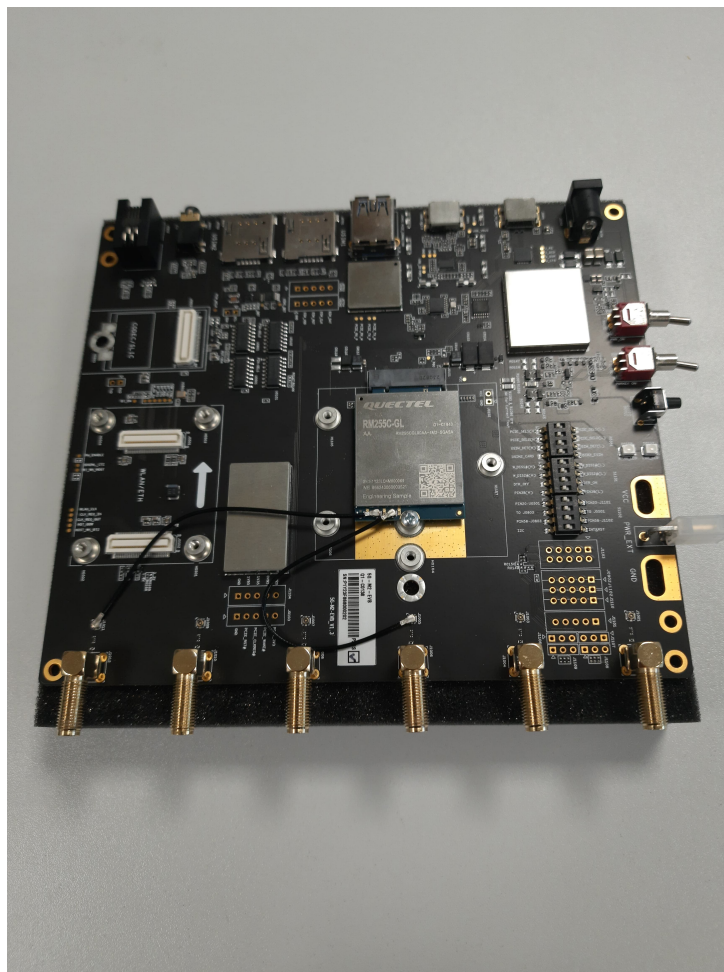


Figure 9 – Quectel RM255-C in an Evaluation board. Source: Author.



Figure 10 – WNC 5G NR sub-6 i-Router router. Source: Author.

devices in 5G projects at IPT due to its ease of use, small size, and great capabilities. In order to configure it, there is only the need to set the access point name (APN) and technology to be used, since the device is compatible with both 4G and 5G. Often, if

the technology matches, it will connect automatically without the APN being needed. Another factor that contributes to its widespread use is having six antennas, which can guarantee good signal reception even when the device is moving. Lastly, the device is able to provide connection via both USB-C and Ethernet cable, making it viable for multiple projects.

#### 4.2.4 Teltonika: RUTX50



Figure 11 – RUTX50 router from Teltonika. Source: Author.

The Teltonika RUTX50 is a dual-SIM multinet network industrial router designed for fast and reliable connection using 5G technologies, while being backwards compatible with LTE 4G and 3G technologies. This router excels in demanding environments, having multiple Ethernet ports and wireless interfaces to connect multiple devices to the network. The communication is secure due to features such as firewall, multiple concur-

rent Virtual Private Networks (VPN), authentication, and attack protection (TELTONIKA NETWORKS, 2022).

Considering this router even has GPS capabilities and inbuilt IoT platform functionality, it can be the ideal device for many future projects. Thus, measuring its energy consumption will generate data of great usefulness.

Despite the router being able to connect to multiple devices, the tests discussed in section 4.1 were only conducted with one device connected. This decision was made since the number and characteristics of the attached devices would influence the test results. Since this project aims to study 5G transceivers for use with 5G sensor units, the connection of multiple devices to the same transceiver exceeds the scope of the study.

#### 4.2.5 Phoenix contact: TC ROUTER 5004T-5G EU

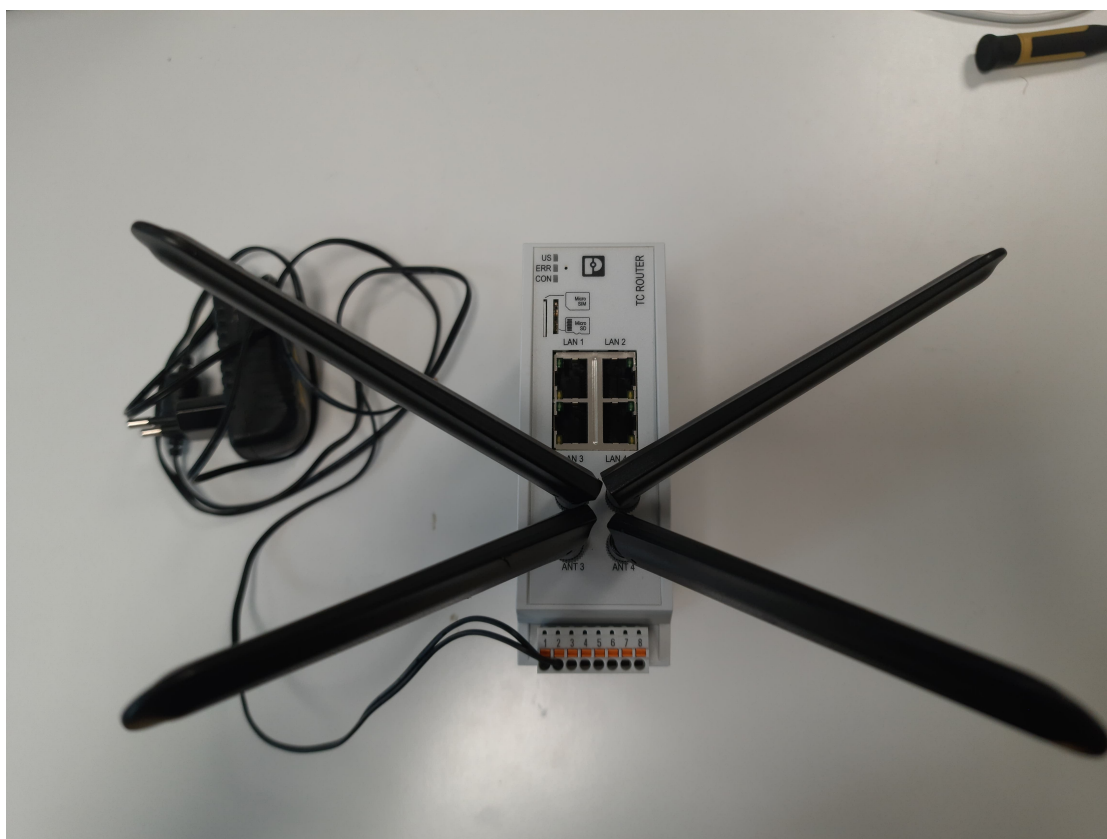


Figure 12 – Phoenix contact TC ROUTER 5004T-5G EU. Source: Author.

The TC ROUTER 5004T-5G EU is a recently launched ultra modern router made by Phoenix contact, bringing new solutions to industrial connectivity with great support of both private and public NR5G networks. This device is equipped with security features such as firewalls and VPN support, as well as a switchable power saving mode while not sacrificing performance. Physically, it is compact yet capable to supply up to 4 devices with connection and has a high grade of protection against magnetic interference and

power surges. This device also has inbuilt connectors to be assembled on top-hat rails, facilitating its installation and use.

This router also can take full benefits of the network, with maximum 2.1 Gbps Downlink speed and 900 Mbps Uplink in SA mode. While on a NSA network, it can reach 2.5 Gbps Downlink and 650 Mbps Uplink.

Because the goal of this project is to provide data for projects with energy limited applications, all tests were done with the energy saving mode of this device active.

#### 4.2.6 Siemens Scalance M800



Figure 13 – Siemens Scalance M800 router. Source: Author.

The Siemens Scalance M800 router is an industrial router designed to ensure secure and stable communication across factory settings. Being the most robust of the devices in this study, its performance matches its sturdiness. It is compatible with multiple broadband cellular network technologies, including NR5G, allowing for fast and reliable data transfer in demanding environments. Additionally, it includes VPN and firewall functionalities to boost the security of communication if required. This router is engineered for easy integration into existing infrastructures, with special focus on condition monitoring and connection of industrial equipment (SIEMENS AG, 2023).

### 4.3 POWER MEASUREMENT SYSTEMS

The power measurements are meant to show how much energy is required in each configuration in each of the devices mentioned in section 4.2. With this data, it will be possible to determine which factor has the biggest influence in the energy



consumption of each device. This information will then be used to verify how viable it would be for energy harvesting techniques to make those devices energy autonomous.

In order to minimize random aspects that could influence the results, each test would consist of five hundred measurements or more. The average and max values of these measurements are then verified in order to provide a more accurate picture of the true energy values. However, a factor that became clear with the start of the tests was that the current value oscillated greatly through the measurement. Upon investigation of why there were such oscillations regardless of the instrument used to measure the current, it was discovered the reason was in the process of communication itself. In order to transmit the data, the device draws more power to send to its antennas. From the current point of view, the current drawn is continuously oscillating in the same frequency as the messages are being sent.

This, when compounded with factors such as an unstable connection and large periods of idleness, increases the uncertainty of the current measurement. The result is that the uncertainty from the standard deviation overshadows the forms of uncertainty from digits or precision of the instruments. In order to attenuate this behavior, the number of measurements was doubled to one thousand.

Since the Quectel modules are powered via USB and the other four devices have specific power sources, each type of power source requires a different measurement device. In Section 4.3.1, the instrument and techniques used to measure the USB powered devices are presented. In Section 4.3.2, the system used for the remaining devices is discussed.

### 4.3.1 For devices powered via USB

Since the Quectel modules are powered and configured via USB cable, a USB power monitor was deemed more adequate for the experiment. The monitor, model UM34C, made by the company Ruideng, has an accuracy of ( $\pm 0.8\%$ ) +3 digits for voltage and ( $\pm 0.2\%$ ) for current in its measurements.

Although power is also advertised as measured, in reality it is calculated based on these two values. Because of this, Gaussian propagation of uncertainty was used to determine the relative and absolute uncertainty portions of each power measurement. This was done using equation (2) (MIT, 2024).

$$\frac{\delta z}{z} = \sqrt{\left(\frac{\delta x}{x}\right)^2 + \left(\frac{\delta y}{y}\right)^2} \quad (2)$$

In this case,  $\delta z$  would be the absolute error in power and  $z$  would be the calculated power value.  $\delta x$  is the absolute error in voltage and  $x$  the average voltage value. Similarly,  $\delta y$  is the absolute error in current and  $y$  the average current value.

Despite being connected to a USB port, the measuring unit sends the data it collects using the Bluetooth protocol. Originally, it was supposed to interface with a smartphone app also made by the same company. However, said app has become incompatible with the devices owned by any member of the team. The solution to this was to use a Python language library that mimics the app, requesting the measured data and allowing it to be logged using a python program. The link to the page containing the library is presented on (JARVISMS, 2023). With this library it was possible to create the python script presented in Appendix B. This program was used to read and log the measured values into text files to speed up the measurement process.

Since the data was saved as raw text, another python script was needed in order to treat the generated file. The answer to this is the script presented in appendix C that reads the raw data and generates a comma separate values (csv) file that can be used with Excel and other software for easier analysis.

#### **4.3.2 For devices with proprietary power sources**

The remaining routers have proprietary power sources, each using a different connector. In order to measure the energy usage of these devices, an energy monitoring system was developed using a INA219 module. The INA219 is a high-side current shunt and power monitor with an I2C-compatible interface. This device offers precise current measurement capabilities across a wide voltage range, from 0 V to 26 V (TEXAS INSTRUMENTS, 2020).

In order to read and register the values measured by the INA219, the module was connected to an Arduino Portenta H7. This circuit was connected to the power source of the device on one end, having the power signal go through the INA219 and the neutral connected to both the Arduino and the router. How this connection was done for each device is addressed in the sections pertaining to the testing of that device.

The data measured by the Arduino was read via serial communication using the software putty. The raw data text result was then passed through a python program in order to format it to be added to Excel. The python code can be found on the appendix F.

Regarding the precision of the measurements, the INA 219 has a resolution of 4 mV and 0.1 mA with an associated percentage accuracy of ( $\pm 0.2\%$ ) for both of the values. Again, due to the expected large variations in the current value and fast speed of this sensor, a minimum of 5000 measurements were to be done in each test with this device. Because of difficulties synchronizing the Arduino with the computer doing the ping, the actual number of measurements done per test oscillated between 5000 and 7000. While these extra values are not considered when calculating the average, they were analyzed in case of anomalies in the measurements.

## 4.4 TEST PLAN AND SETUP

As discussed in the Section 4.3, it was decided to have tests consisting of one thousand power measurements. These tests would require specific network traffic for each scenario, which necessitated the tools discussed in Section 4.4.1. Using all elements discussed in chapter 4, a test plan was created and is discussed in Section 4.4.2.

### 4.4.1 Software tools used

To test any element of a network, whether the endpoints or the router themselves, one must use the proper tools. Many protocols and tools exist for this purpose, from simply sending small packages of data to completely mimicking the communication of other devices. From the many existing tools and protocols, two were narrowed down for having the flexibility to be configured with the parameters discussed in the previous sections, namely Ping and iPerf3.

Ping test is a tool that uses the internet control message protocol (ICMP) to send and receive packets. As a network diagnosis tool, it allows for the configuration of sender and targets IP, the size of the packet, and whether it can or not be fragmented. Once executed, it sends an echo packet with the set characteristics to the target. The echo packet is a type of packet in this protocol that requests an answer in its header, commonly used to detect if the target port is available. Using the ping tool, this answer also contains the round-trip time statistics. In Figure 14, a command prompt running the ping protocol sending packets of 1024 bytes can be observed. One thing that must be considered is that while characteristics such as the latency and others may vary depending on the server that is being targeted, the power measurement only analyzes the power used to send the message and then to interpret the answer. In other words, when measuring power, the only part being investigated is the wireless transmission from the transceiver to the main antenna. Since the processing times in the server are negligible, and the target address is the one with the least possible number of hops, they do not influence the results.

One thing to keep in mind with the ping tool is that the actual amount of bytes is always 28 bytes higher than what is specified in the tool. This is due to the 8-byte header from the ICMP protocol and another 20-byte header from the ping tool itself. Since this comes naturally from using the ping tool, it was decided to name the test scenarios and other uses of the ping tool without counting these header bytes.

The other tool was the third iteration of iPerf, or iPerf3, an open-source tool for measuring the maximum throughput a network can provide using TCP and UDP protocols. Being highly customizable and able to measure packet loss and jitter, this tool can create traffic between two devices in order to assess network performance.

```
ca: Prompt de Comando
Resposta de 8.8.8.8: bytes=68 (enviado 1024) tempo=11ms TTL=118
Estatísticas do Ping para 8.8.8.8:
  Pacotes: Enviados = 4, Recebidos = 4, Perdidos = 0 (0% de
perda),
Aproximar um número redondo de vezes em milissegundos:
  Mínimo = 11ms, Máximo = 12ms, Média = 11ms
C:\Users\tiago>ping 8.8.8.8 -f -l 1024 -t
Disparando 8.8.8.8 com 1024 bytes de dados:
Resposta de 8.8.8.8: bytes=68 (enviado 1024) tempo=11ms TTL=118
Resposta de 8.8.8.8: bytes=68 (enviado 1024) tempo=11ms TTL=118
Resposta de 8.8.8.8: bytes=68 (enviado 1024) tempo=11ms TTL=118
Resposta de 8.8.8.8: bytes=68 (enviado 1024) tempo=12ms TTL=118
Resposta de 8.8.8.8: bytes=68 (enviado 1024) tempo=11ms TTL=118
Resposta de 8.8.8.8: bytes=68 (enviado 1024) tempo=11ms TTL=118
Resposta de 8.8.8.8: bytes=68 (enviado 1024) tempo=11ms TTL=118
Resposta de 8.8.8.8: bytes=68 (enviado 1024) tempo=11ms TTL=118
Resposta de 8.8.8.8: bytes=68 (enviado 1024) tempo=12ms TTL=118
Resposta de 8.8.8.8: bytes=68 (enviado 1024) tempo=11ms TTL=118
Estatísticas do Ping para 8.8.8.8:
  Pacotes: Enviados = 10, Recebidos = 10, Perdidos = 0 (0% de
perda),
Aproximar um número redondo de vezes em milissegundos:
  Mínimo = 11ms, Máximo = 12ms, Média = 11ms
Control-C
^C
C:\Users\tiago>
```

Figure 14 – Command prompt running the ping tool. Source: Author.

The way the tool works is by having the target device running iPerf3 in server mode and a sender device running in client mode that would then send a request to initiate communication. This procedure was done to set if TCP or UDP would be used, if the server should listen or send data and other aspects. Once the request is accepted, communication would begin.

iPerf3 also has a header of 40 bytes that is not considered in the packet size. Once again, since this header is inherent to the tool, it was not added to the count of bytes being sent in any tests using the iPerf3 tool.

However, this tool was not made with single packet communication or varying frequencies in mind, it was made to simulate constant traffic. While it is possible to configure it to send a single message by manipulating the buffer size, and control the frequency by sending this instruction repeatedly, this generated conflicts with the server. These conflicts were due to the ports used by the server being already occupied, causing communications to fail. The use of multiple servers was attempted, but the number required would surpass the number of ports normally available in the 5G core, which would require consultation with the provider to solve. It is also suspected that since each communication in iPerf3 is prefaced with a request to start the server, this extra communication would also interfere with the amount of data and frequency of communication planned, thus affecting the results. Because of this, it was decided to first verify if the different tools would have any impact on tests involving packet size before continuing to pursue a solution for the use of iPerf3 in the tests involving the

interval between transmissions.

The comparison test was conducted using the Quectel module RM520 and packets of 128, 512, and 1024 bytes. Energy measurements were done using both protocols.

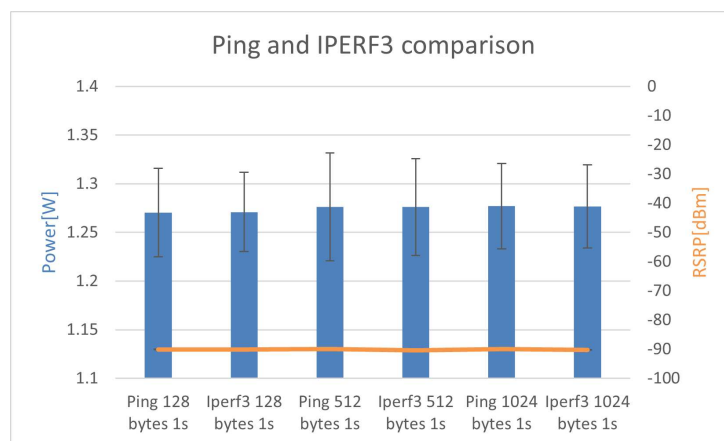


Figure 15 – Ping and iPerf3 Power usage comparison Source: Author.

In the results, which can be seen in Figure 15 there was no real difference, as the values only differed past the uncertain digit. Because of this, it was decided to use the ping protocol, since it was designed for single packet messages and would not have problems with the higher frequency tests.

#### 4.4.2 Test plan

The tests were to be executed on 5G showroom at IPT, due to the excellent signal propagation and low chance of disturbances. In there, the adequate measurement system discussed in Section 4.3 would be connected to the device, either via USB or directly to the power ports. Once the device is powered, a small test is conducted to check if the power was being measured correctly. With confirmation that the device is properly powered and the measurement system is working correctly, the device would be configured to connect to the network corresponding to the test. The tests of packet size would then be conducted, followed by the tests involving interval between packets also known as sending frequency. After this, the device would be shielded using metal sheets, as can be seen in Figure 16. This was done in order to reduce the signal strength it for the tests with degraded RSRP.

For the next test aiming for a better than average RSRP value, the device was positioned on a higher platform above the aforementioned showroom to both reduce the distance to the antenna and guarantee line-of-sight conditions. Extra care was also taken when aligning the device antennas in order to enhance the signal reception.

Any given test using the UM34C consisted of 1000 measurements and the ones using the INA219 consisted of 5000 measurements. These measurements were done

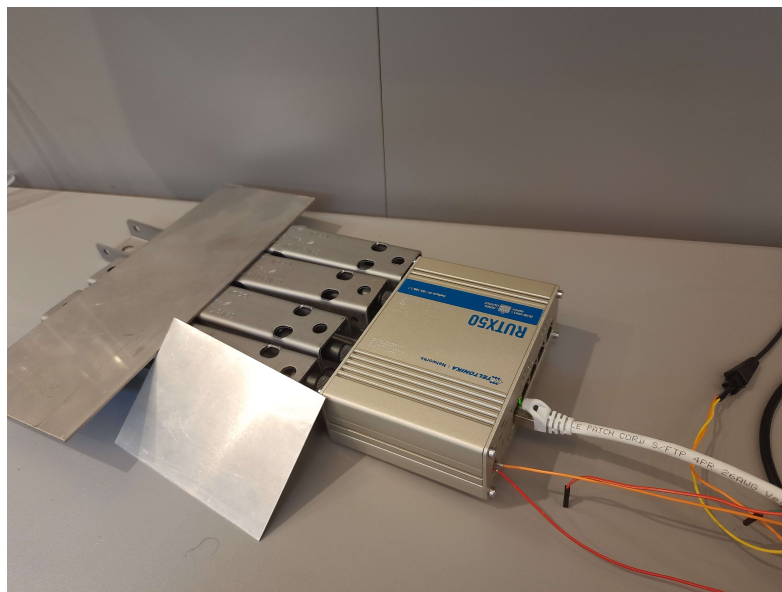


Figure 16 – Setup for testing the Siemens router with shielding Source: Author.

while a ping test was conducted with the packet size and sending frequency specified for that particular test. This was done by the use of a python script, present on appendix A. The RSRP value was extracted via AT commands for the USB powered devices, or via user interfaces for the remaining devices. To summarize, it was determined that 14 test scenarios for each network technology would take place. These scenarios would be applied to six different 5G transceivers. Five of these tests varying packet size, seven studying the interval between transmissions and two comparing the effect RSRP has on power usage. During these tests, the factors not being studied are fixed at 256 bytes for the packet size and a one-second interval for the sending frequency. The RSRP is always studied, with all tests not aiming to influence it being used to calculate the average and compare it to the last two scenarios. Two different measurement devices were to be used, the UM34C and INA219, depending on the 5G transceiver. The tests using the UM34C having 1000 measurements per test and those measured with the INA219 having 5000 measurements per test. The specifics of the setup of each device are discussed in their respective testing sections presented in the next chapter.

## 5 DATA ACQUISITION AND ANALYSIS

As discussed in Chapter 4, the parameters to test and the devices to be tested have been determined. Thus, this chapter presents the results and analysis of these tests. The tests of each device are presented in Section 5.1 along with an analysis of these results. In Section 5.2, a comparison of the results from all devices and networks is made. This comparison is also accompanied by an analysis of the best conditions and devices for use in applications with limited energy supplies.

### 5.1 TESTING

The tests were conducted following the test setup presented in Section 4.4.2 and are presented separately by device, following the same order presented in Section 4.2. Each subsection starts by discussing the setup, followed by the results, and analysis of the results from the tests on the SA and NSA networks.

#### 5.1.1 Quectel RM520-GL

The first device tested was the Quectel RM520-GL. This choice was made due to the ease of configuration and use of this device. This facilitated the initial testing of the parameters and verifying if any modification to the test plan would be in order for the other devices. The test procedure followed what was described in Section 4.4.2 and the resulting setup is shown in Figure 17. With the start-up finished, the QCOM



Figure 17 – Measurement setup for Quectel RM520-GL. Source: Author.

program, also provided by Quectel, was used to configure the device via AT commands. An image of the program interface with the commands and resulting log for connecting to the non-standalone network can be observed in Figure 18.

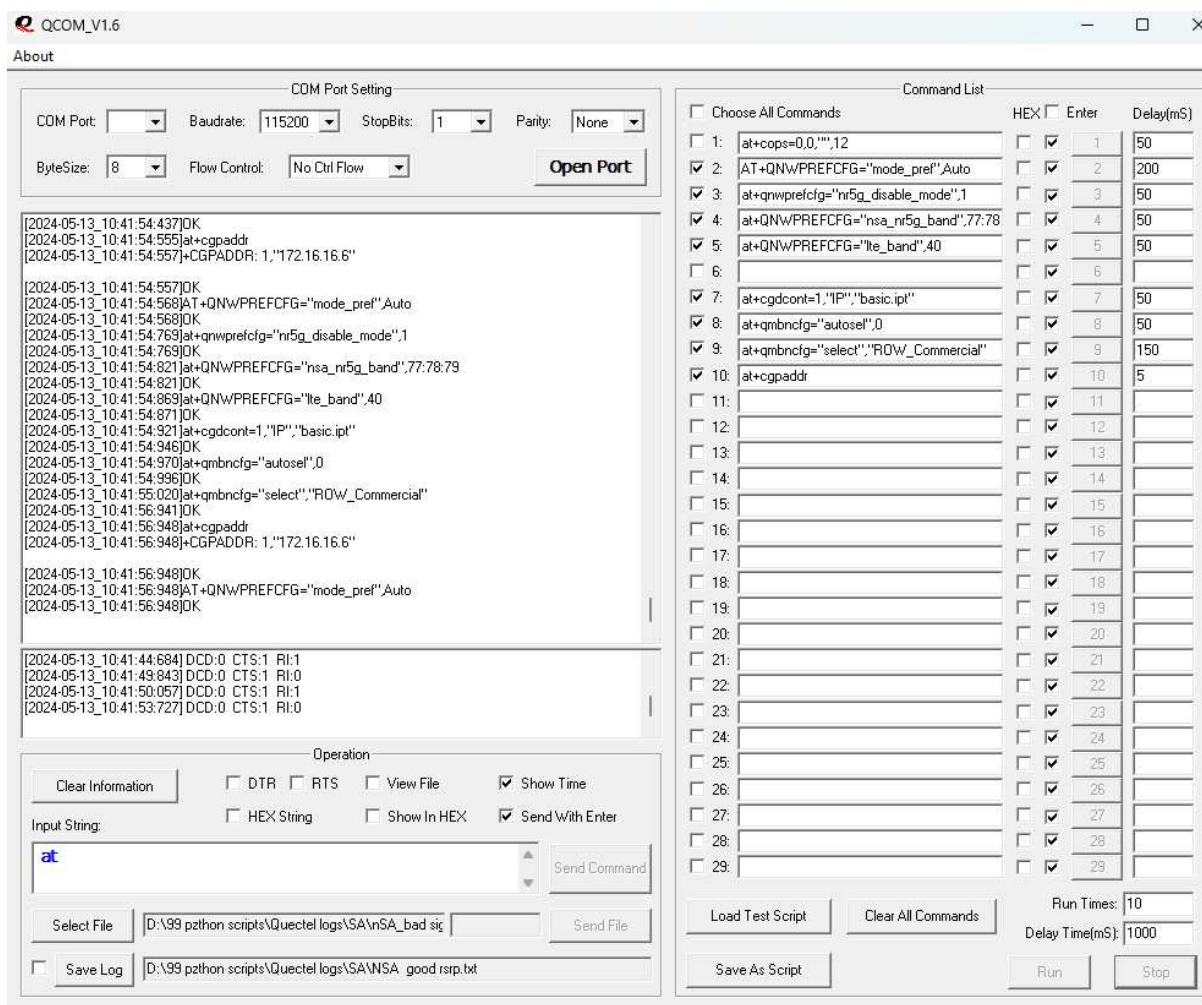


Figure 18 – QCOM interface during connection procedure with NSA network. Source: Author.

This same program was also used to obtain the RSRP value measured by the module via the command `AT+QENG="servicell"` as discussed in Section 5.1.1.

With everything set as shown in Figure 17, the measurements commenced. The device was then disconnected from the SA network and connected to the NSA network via AT-commands. This was done to avoid moving the device between the networks tests. Since the same antennas provided both SA and NSA communication, keeping the device static between tests minimized variation.

As described in Section 4.3, the data was extracted with the aid of python scripts. The scripts used to extract and format the Voltage and current measurements can be found in appendix B, C of this document. Once the results were in a more manageable form, they were analyzed and the graphs presented in Figures 19 and 20 were generated, one for SA and another for NSA. In the graphs, the average values of the measurements are presented, accompanied by the absolute error of the measured average in the form of error bars.

Observing the graph in Figure 19, it can be seen that for an RSRP of approxi-



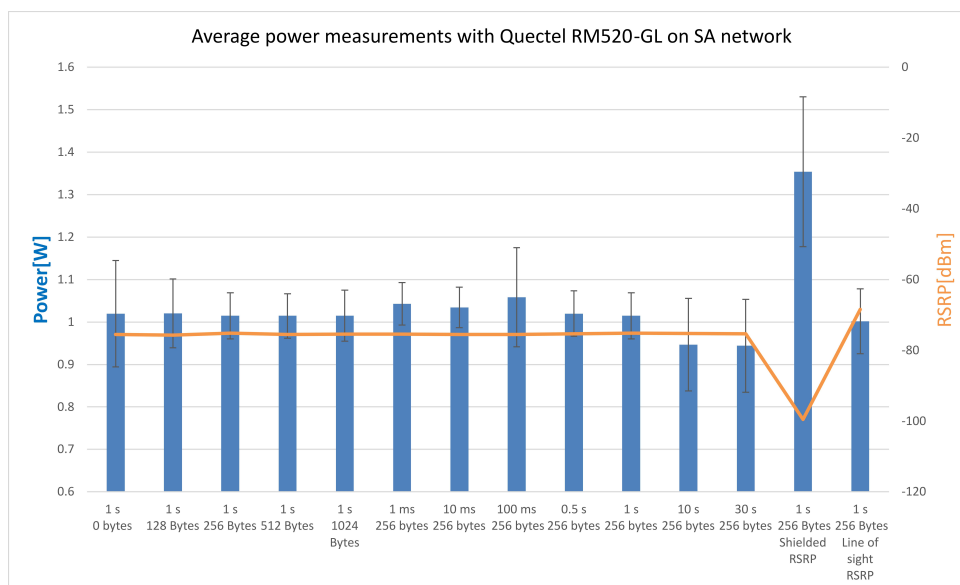


Figure 19 – Average Power measurements on Quectel RM520 on SA network. Source: Author.

mately  $-76$  dBm, the power usage stays close to 1 W. The lowest energy consumption is of  $(0.94 \pm 0.11)$  W, obtained in the test with 30-second intervals between pings. The highest power average can be observed in the “shielded signal” test scenario, as is clearly shown in the graph. This test involved one ping per second with packets of 256 bytes being sent over a link with an average RSRP of  $-99.5$  dBm, resulting in an average power usage of  $(1.33 \pm 0.17)$  W. Regarding the impact of the different parameters on energy consumption, the RSRP measure had the greatest influence by far. Following it, the frequency also has a noticeable impact, and lastly the payload size had a minor effect. Focusing on the effect of RSRP values, a reduction of 23.4 dBm resulted in an increase of around 33.4% in the average power usage. For the scenario with shielded RSRP, there is a difference of only 6.77 dBm and  $(0.02 \pm 0.15)$  W or 2% in power usage. This low difference and impact are results of  $-80$  dBm already being considered very good signal strength (PRAMONO et al., 2020), this small increase might not have much impact since the link remains strong. However,  $-99.5$  dBm is almost  $-100$  dBm, commonly the threshold for “bad” signal strength (PRAMONO et al., 2020), so this may explain the influence. Whether this is an isolated occurrence or not will need to be observed in the following tests.

Regarding frequency, the higher consumption for 1 ms intervals and the lowest for 30 s intervals was expected when considering how the router works. Each transmission must be amplified and sent to the antenna, which is often the most energy intensive part of communication. Thus, an increase in idle time would also result in a decrease in energy consumption.

Repeating the tests while connected to the NSA network yielded the results presented in Figure 20.

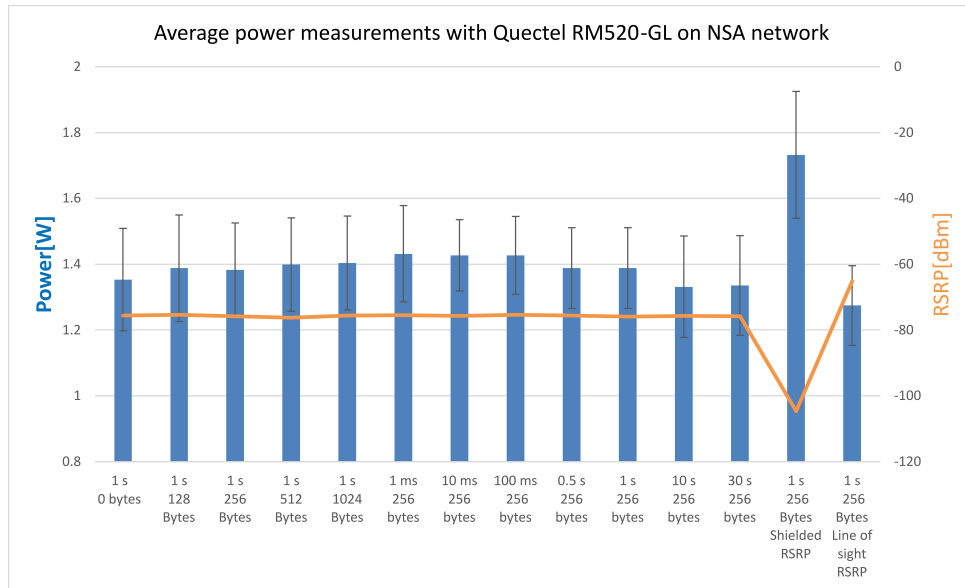


Figure 20 – Average Power measurements on Quectel RM520 on NSA network. Source: Author.

At first glance, there is a clear an increase in power consumption in all scenarios when compared with the tests in the SA network. Comparing each scenario on the two networks, there is an increase of approximately 40% in the required power. This difference is not due to the signal strength, since the differences in average signal strength between the respective tests are lower than 1 dBm. This increase may be evidence of how much the SA architecture has improved the energy efficiency of the communication for the end devices.

Focusing on the results themselves, just as in the SA network, the highest power consumption scenario is of “1 s 256 bytes shielded RSRP” with  $(1.73 \pm 0.19)$  W. Conversely to the previous test, the lowest result is now that of the higher RSRP value at  $(1.27 \pm 0.12)$  W. This may be due to the difference in RSRP being a slightly higher, now 10 dBm, however both are still in what would be considered very good to excellent. While RSRP was the most influential factor, the sending frequency still has an impact in both ends of the spectrum. While most results cluster around 1.38 W to 1.39 W the 10 s and 30 s intervals are lower, with a  $(1.33 \pm 0.15)$  W Power usage, resulting in a decrease of 50 mW. Looking at the tests with 1 ms and 10 ms intervals, there is also an increase of around 40% in the results.

### 5.1.2 Quectel RG255C

The second device to be tested was the RedCap device presented in section 4.2.2.

The testing followed the steps discussed in the test plan, with an added previous step of contacting support to activate the proper network configuration. Just as the

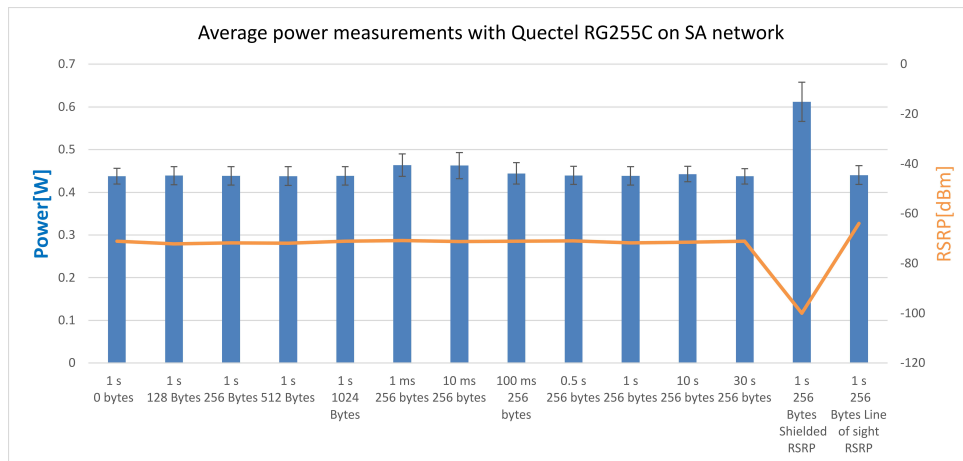


Figure 21 – Redcap power consumption in SA network. Source: Author.

previous Quectel module, the QCOM tool and at commands were used for configuration and RSRP logging. For the “shielded RSRP” scenario, shielding could not be used, since it resulted in large variations in the RSRP quality regardless of setup. The solution to this was to disconnect the two antennas. Surprisingly, the board was able to connect and transmit using only the attachment connectors, seen in gold at the bottom of Figure 9. This setup provided an average of  $-100$  dBm but with far more stable performance. The results are presented in the graph in Figure 21.

Initially, it is clear that there is a large improvement in the energy consumption when compared with the other Quectel module. All tests show a reduction of around 55% when compared with the respective results presented in Figure 19. However, this raises the debate if a 55% decrease in energy usage is enough to justify the 80% reduction in performance brought by the RedCap device. Considering the planned applications to be studied in this project are energy critical, there might not be the option of a choice.

Looking at the results, the highest power consumption was of  $(0.61 \pm 0.05)$  W for the “shielded signal” quality case. A significant difference that was also perceived when the strength of the signal was reduced via shielding or distance. Overall, a reduction of  $-28$  dBm or 39% from the average RSRP resulted in an increase of 39.5% in power consumption. Looking at the best result, the “better RSRP” is closely matched to the other results, this may be due to the small difference of just 6 dBm from the average. Another factor is that  $-71$  dBm indicates an excellent link, so there is very little room for improvement. In the better RSRP scenario, the power usage is of  $(0.44 \pm 0.02)$  W, although it is effectively tied with all the packet size scenarios, since the divergence only happens past the doubtful number. The only other tests that are not tied are the ones with 1 ms and 10 ms intervals, both having  $(0.46 \pm 0.03)$  W of power usage. What can be drawn from this test is that the device power consumption is remarkably stable for great links, but quickly degrades once the signal deteriorates.

Since the Reduced Capacity device is incompatible with the NSA network for the reasons discussed in section 4.2.2, tests were limited to the SA configuration.

### 5.1.3 WNC 5G NR sub-6 i- Router

The test setup was assembled as per the testing plan, this time using the INA219 assembly. Thanks to the power connectors of the device sharing the same pin dimensions of a common jumper cable, testing was facilitated. The device with the measuring system connected can be seen in Figure 22.

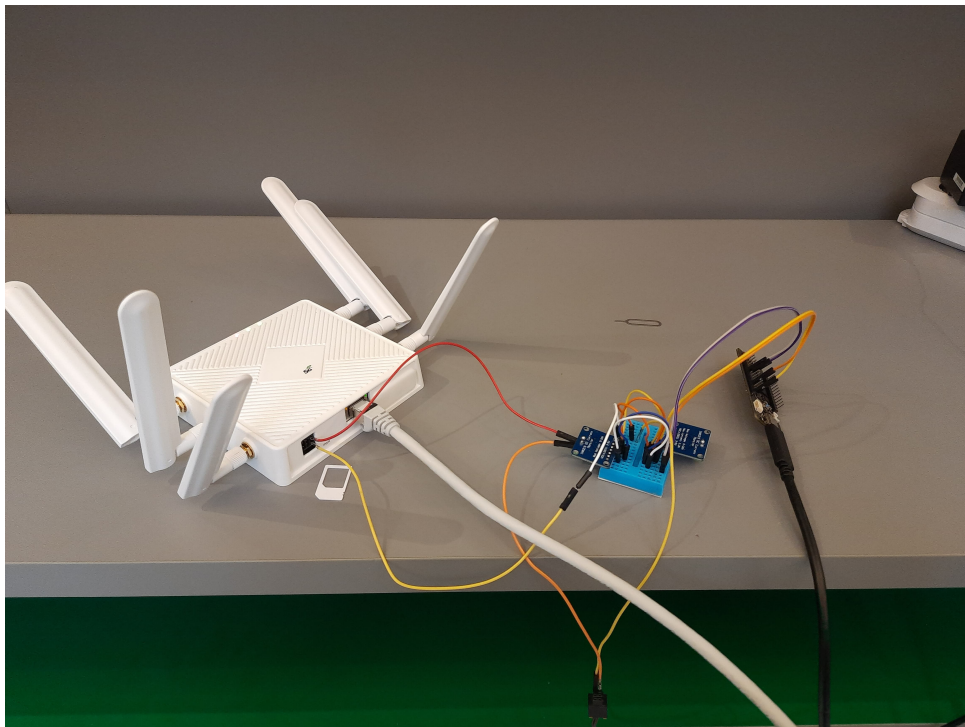


Figure 22 – Test setup for WNC. Source: Author.

Starting with the tests in the SA network, the results obtained are displayed in the graph in Figure 23. Observing the results, it can be seen that RSRP being the main factor in power consumption is not exclusive to the Quectel devices. The highest average coming from test “1 s 256 bytes shielded RSRP” with  $(3.76 \pm 0.41)$  W and the lowest average comes from the test with the best average RSRP, with  $(3.41 \pm 0.34)$  W. The values obtained are much higher than the ones from the Quectel modules, but considering this device has much higher capabilities and even runs a user interface, it is expected.

Looking at the full picture, the results mirror the ones obtained previously with one difference, the tests with time intervals higher than one second. The tests with 10-second and 30-second intervals have almost the same power usage as the tests with 0 bytes being transmitted. This may indicate that the device does not have any

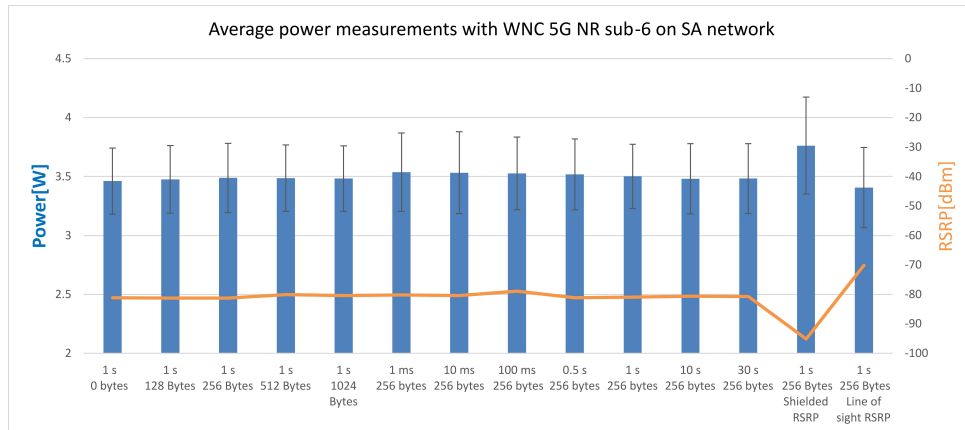


Figure 23 – Average Power measurements on WNC 5G NR sub-6 router in SA network. Source: Author.

mechanism to reduce power usage when idle, or has an incredibly long wait time before going idle.

Turning to the tests realized in the NSA network, the results obtained can be examined in Figure 24.

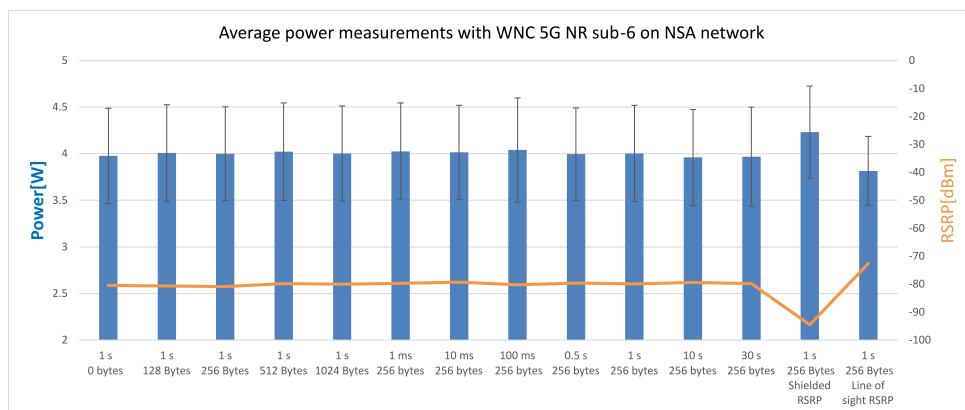


Figure 24 – Average Power measurements on WNC 5G NR sub-6 router in NSA network. Source: Author.

Comparing the results in the two networks, higher energy cost for communication in the NSA network is not unique to the Quectel devices. Comparing the results across both networks, there is an increase of around 14% in the power usage comparing the tests with equal RSRP values.

One thing that is apparent in the measurement is the high uncertainty of the results, reflecting instabilities in the network and the compounding effect of RSRP. Due to continuous instability at the moment of testing, the results have a higher distribution than would typically be expected for the device. While this complicates the analysis a bit, it does not make it impossible and also demonstrates the compounding effect of RSRP with the other aspects.

Just as in the SA network, the tests focusing on RSRP have the highest and

lowest power consumption at  $(4.23 \pm 0.49)$  W and  $(3.81 \pm 0.37)$  W, respectively. Focusing again on the scenarios with the 10 second and 30 second interval, there is very little reduction in power usage when compared to the 1-second test. The results again match the scenario with 0 Bytes of payload. A possible reason to explain this behavior would be that something other than the transmission is consuming the power. This can also be compounded by the device having no mechanism to automatically reduce the power usage over long times of inactivity and needs to be told by the network to go idle. In order to test this hypothesis, another test was done with the device being idle, but connected to the network. The result was a power usage of  $(3.90 \pm 0.49)$  W, around 50 mW above the tests mentioned previously. Considering no transmission happened during the idle test, another functions are the main causes of power usage. This implies that either the transmission has very little impact in the power consumption, or that power is rerouted during transmission.

#### 5.1.4 Phoenix contact: TC ROUTER 5004T-5G EU

The Phoenix Contact router followed the test plan with one difference. Due to this router having a power-saving mode, it required an extra cable connected to port three or input one to activate it. The signal that would activate the power saving mode was configurable, so it was set for I/O port one or the third pin from left to right. Said port was then connected to the circuit ground as seen in Figure 25 and the router was configured to activate this mode on a low input. Just as with the previous router, the

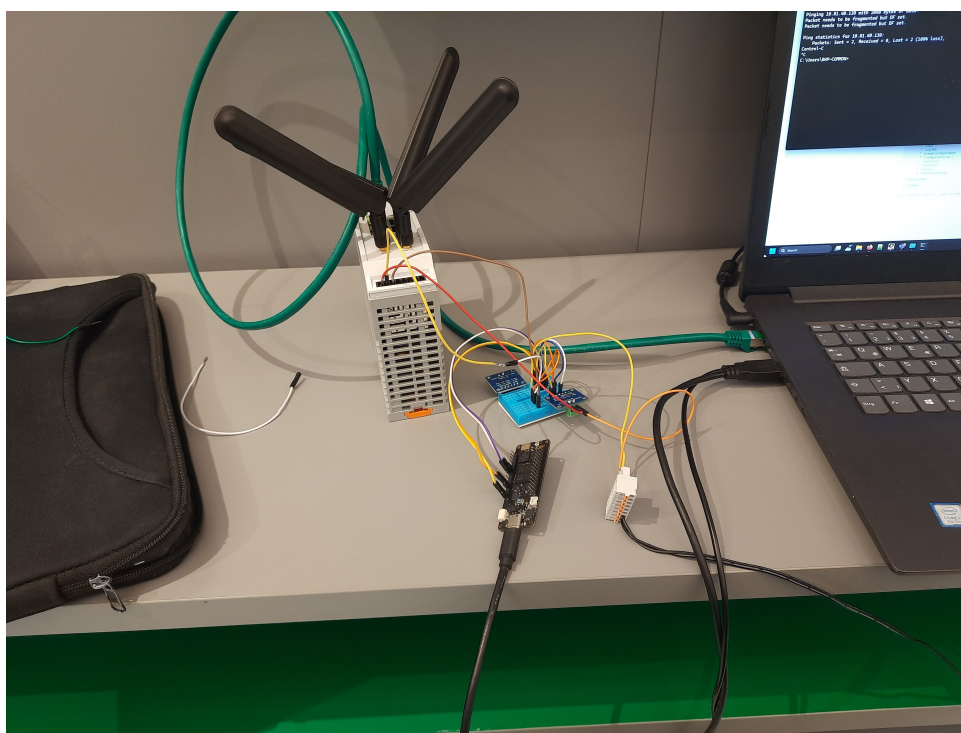


Figure 25 – Test setup for TC ROUTER 5004T-5G EU. Source: Author.

RSRP values referenced were obtained for the router's interface.

Upon testing, this device proved itself remarkably unstable, so much so that the very first battery of tests returned the set of results visible in Figure 26, with errors up to 18%.

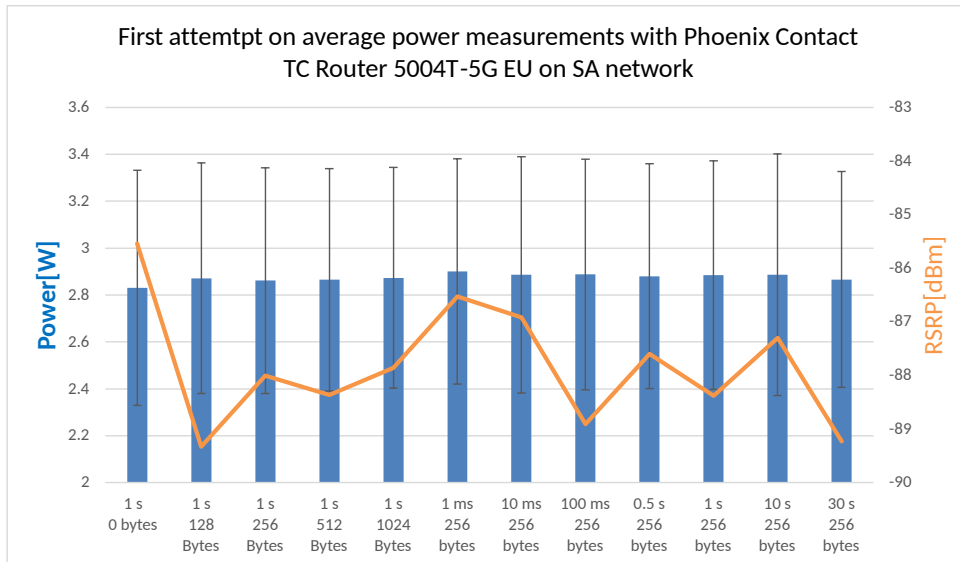


Figure 26 – First attempt at Average Power measurements on TC ROUTER 5004T-5G EU on SA network. Source: Author.

As can be seen, there is overwhelming uncertainty in the measurements, this was tracked to two sources. The first was the power source, which was not original and was found out to be of subpar quality, leading to its replacement. However, the biggest contributor to the uncertainty was the sensitivity of this device to fluctuations in the signal strength. Upon verification, the measured RSRP value in this device varied upwards of 5 dBm above or below the average. For the other devices, the variation was at most of 2 dBm, with any more indicating instabilities in the network itself.

The solution to this was the alteration of the test setup in order to provide the device with a direct line of sight to the antennas. This improved the RSRP received by the router to values that more closely matched those obtained by the other devices and greatly reduced the oscillations in the measurements. Now that values had a more acceptable, although still high, variation, the remaining tests were conducted and the results are presented in Figure 27.

As visible in Figure 27, the precision of the measurement is now at acceptable levels. As expected, the highest power usage belongs to the test with “shielded RSRP”, consuming  $(2.82 \pm 0.37)$  W with a RSRP of  $-91$  dBm. On the other hand, the lowest power usage was that of the 30-second interval, with  $(2.57 \pm 0.25)$  W used. It was followed by the test with a 10-second interval with  $(2.59 \pm 0.24)$  W and just then the good RSRP, with  $(2.62 \pm 0.27)$  W. Considering how susceptible this device is to variations in the signal quality, this result is sensible. The average case of 256 bytes and one second

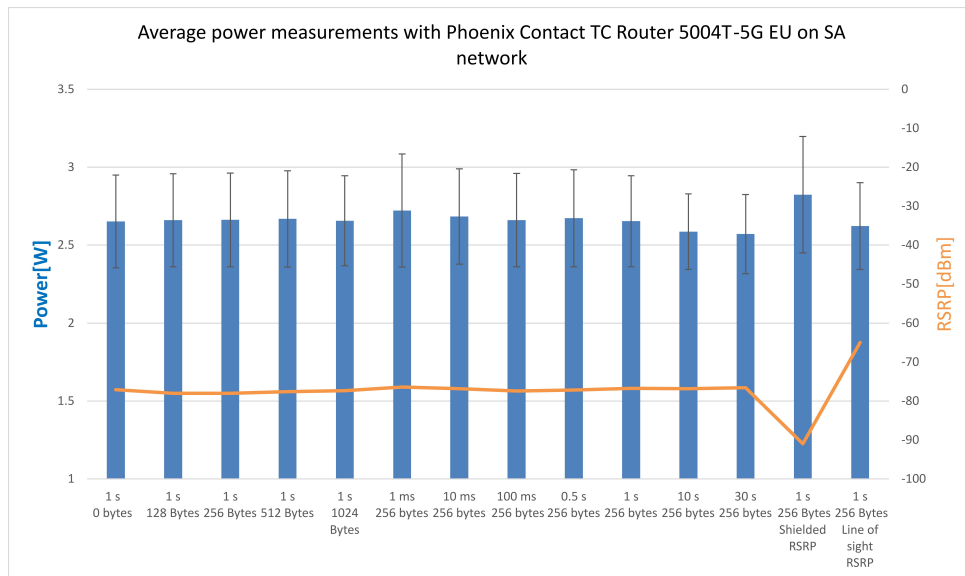


Figure 27 – Average Power measurements on TC ROUTER 5004T-5G EU on SA network. Source: Author.

consumed ( $2.65 \pm 0.29$ ) W, so a value slightly above this would be required in order to power this device in most scenarios.

For the packet size, the only notable detail is the reduction for the 0 bytes scenario. There are no mentions in the manual for any optimizations for small or header only packets. Repetition of the test still showed this small reduction. Although it could still be a coincidence, since only two repetitions were done, this may indicate some optimization for short messages at play due to the energy saving mode in this device.

Regarding testing on the NSA network, it was not possible. It was discovered that while the device is compatible with NSA technology, it was compatible only up to band 77, whereas IPT NSA network uses band 78. This came as a surprise to the author, as the device allegedly was able to connect to band 78 in the past. However, the device had since needed to be factory reset to fix an unrelated problem. Despite efforts to enable the band, it was not possible and the tests in the NSA network with this device were canceled until a firmware upgrade enabling this functionality becomes available.

### 5.1.5 Teltonika RUTX50

For this router, the physical assembly described in the test plan was greatly facilitated by the fact that the internal connectors of the power source and socket shared the same standard as the jumper tips being used. This assembly can be seen in Figure 28.

On the other hand, the tests with this device had major delays due to a problem in its configuration, impeding its connection to the NSA network. This problem even prompted the author to contact the company that provides and administers the network



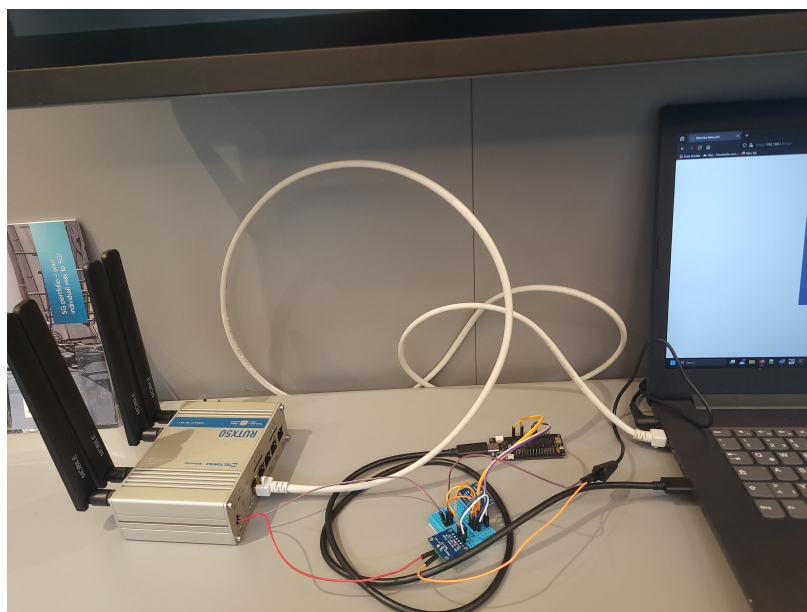


Figure 28 – Test setup for RUTX50. Source: Author.

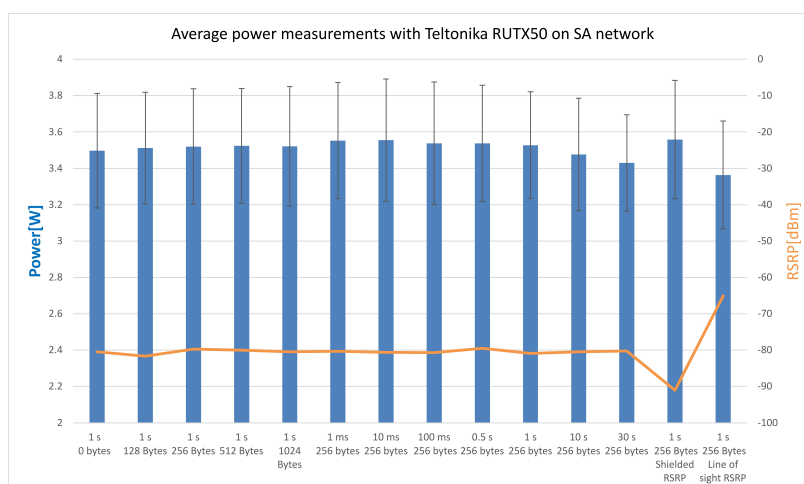


Figure 29 – Average Power measurements on Teltonika RUTX50 on SA network Source: Author.

to verify if it was somehow incompatible with the NSA network. The provider, despite their efforts, could not determine anything other than the problem being in the device itself. This resulted in testing being executed only on the Standalone network for this device.

Despite the problems, all tests were possible in the SA network, and the results obtained can be examined in the graph in Figure 29.

Observing Figure 29, it is notable that, for the first time, the highest value does not clearly belong to the test with the higher RSRP. Rather, there is an effective tie between that scenario and the ones with 1 ms and 10 ms intervals between pings. The test with the 1 ms and 10 ms intervals between pings have an average power consumption of  $(3.55 \pm 0.32)$  W and  $(3.56 \pm 0.34)$  W respectively. For the tests with

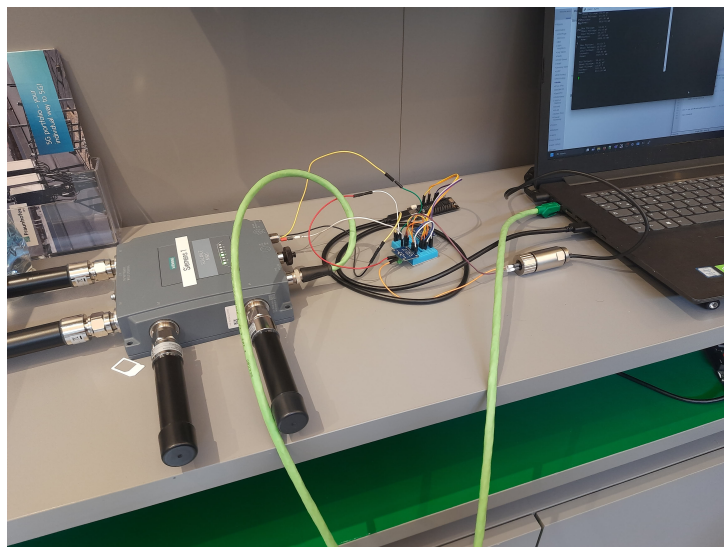


Figure 30 – Test setup for Siemens Scalance M800. Source: Author.

the higher RSRP, the average power usage is of  $(3.55 \pm 0.32)$  W. Since the differences are in the uncertain digit, there is no point in saying one is higher than the others. This result is very interesting, showing that for this device that claimed highly stable connections indeed does so, to the point where a difference of 11 dBm has the same effect as multiplying the communication frequency by a thousand.

Looking at the opposite side of the spectrum, the benefits of an excellent link are still undeniable, although by a far smaller margin than in the previous devices. The lowest average is that of the best RSRP, with  $(3.36 \pm 0.30)$  W of power consumed. Considering there is an improvement of 16 dBm between this scenario and the average, it is safe to say that this device is less affected by fluctuations in the quality of the signal.

The conclusion that can be drawn for this test is that in case the signal quality is expected to oscillate or be of poor quality, this device may be the solution. That is, in cases where the almost 3.5 W of power required can be supplied.

### 5.1.6 Siemens Scalance M800

As can be seen in the Figure 30, following the test plan required a bit of adaptation. The main problem was to guarantee the airtight seal in the power plug during normal use, the internal connectors were rather short. The solution to this was to chain wire tips to both reach the connector and keep positive and negative isolated. All components used were rated for voltages and currents higher than those that could be provided by the power source, resulting in a safe, although time-consuming assembly.

For the RSRP measurement, as with the other routers, the information was extracted from its interface, as visible in Figure 31.

With those points addressed and the setup complete, the tests were conducted without major problems, however, due to issues in the network the tests in the SA and



Figure 31 – Siemens Scalance M800 information. Source: Author

NSA networks were conducted on different days.

The testing in the Standalone network culminated in the graph in Figure 32.

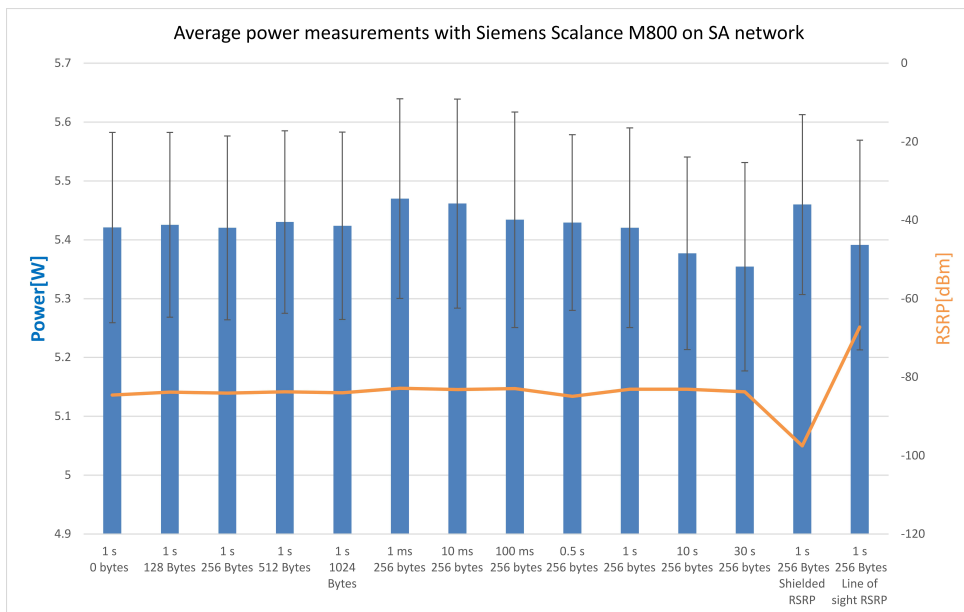


Figure 32 – Average Power measurements on Siemens Scalance M800 on SA network. Source: Author.

The testing itself showed that the current usage of this transceiver is far more

stable than the others, resulting in the smallest error percentages between the routers.

As can be seen in Figure 32, the data follows the pattern shown by the previous tests with one exception. While the RSRP proves itself again as the most influential factor in both increasing and decreasing the power usage, the reduction is matched by the higher intervals.

The lowest average of the scenarios is of  $(5.35 \pm 0.18)$  W for the 30-second interval test, followed by  $(5.38 \pm 0.16)$  W for the scenario with 10-second intervals. While the Siemens Scalance M800 is capable of hibernation, such an impact was not expected. In any case, this result shows great promise for applications that can tolerate big intervals between updates. Even better, considering the Scalance M800 also has the highest energy consumption of all routers. Something that was expected since it required 24V to operate, double that of the other routers with power sources meant to connect to AC power outlets.

On the other end of the frequency spectrum, the higher rate of transmission continues to take its toll, having the highest energy use of all tests scenarios at  $(5.46 \pm 0.15)$  W. Just like the Teltonika RUTX50, frequency had an influence equivalent to that of the power received. This may be due to the fact that these two routers already require a large amount of power to work and thus have more resources to counteract the effects of fluctuations in the signal quality.

Another conclusion that can be drawn with certainty with these results is that in case a large amount of data must be transmitted, sending multiple large packets would be more efficient than fragmenting the data in smaller packets.

Focusing now on the tests in the NSA network, the test results can be seen in Figure 33. Again, it is possible to see the increase in power usage brought by the use of the NSA network.

This increase is 7% on average across the tests, however, the NSA tests had an average RSRP almost 4 dBm lower than in the SA tests. While an attempt was made to provide the same signal strength for both scenarios, it was not possible without changing the test plan and providing line of sight with the antenna. Therefore, it was opted to follow the original plan and realize the tests without moving the device.

The transceiver requires between  $(5.72 \pm 0.17)$  W and  $(5.92 \pm 0.16)$  W, with these being the test cases with good and bad signal strength respectively. This places the Siemens Scalance M800 on NSA as the most power-intensive setup in this study. Comparing the effects of RSRP with those of frequency, as in the SA test, they are clearly matched. For the scenario with 30 second intervals, the power usage is  $(5.73 \pm 0.16)$  W, a difference of only  $(0.01 \pm 0.33)$  W. On the higher side, there is a similarly small difference between the scenario with shielded RSRP and the one with the lowest interval between communications. This reveals that this behavior was not partial to the SA network, but rather from the device itself. Although there can be many sources for

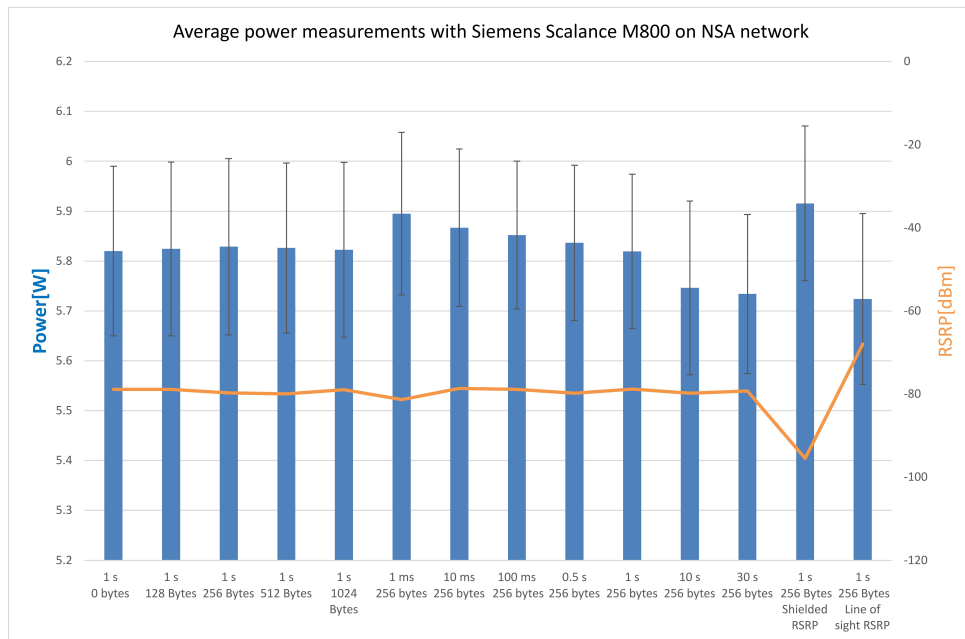


Figure 33 – Average Power measurements on Siemens Scalance M800 on NSA network. Source: Author.

this result, the most likely is that due to the intended use in hazardous environments, special care was taken to minimize the effects of variations in the signal.

The only aspect that does not show a significant impact is that of the packet size. These scenarios have their power usage in an effective tie around  $(5.82 \pm 0.17)$  W.

What can be drawn in conclusion to these results is that for cases where the interval between packets can be increased above one second, it might be a viable strategy to compensate for low signal strength. This would also have the added benefit of giving more time for the batteries to charge in applications involving energy harvesters.

## 5.2 RESULTS DISCUSSION

With the data collected, it comes time to compare the results from each device, to see how they fare against one another in their performance. One thing to keep in mind in this section is the large differences in construction and function between the devices. While the results may vary greatly, one cannot be determined as a clear winner, since they are all tools with different uses. While the RedCap device may have the lowest energy consumption, its maximum throughput and security pales in comparison to devices like the Scalance M800 or RUTX50.

In order to make a comparison possible, Tables 2 and 3 were created. Figure 36 also presents a comparison graph of the results in the SA network.

As discussed through Section 5.1, the two factors with the highest impact were the network technology and the RSRP value. However, the total power consumption of the device also appears to influence how much each of the factors impacts the energy

Table 2 – Power Consumption values on RSRP scenarios.

Device	Network	Better RSRP scenario	Average test scenario	Worse RSRP scenario
Quectel RM520-GL	SA	1.00 ± 0.08	1.02 ± 0.05	1.35 ± 0.17
Quectel RM520-GL	NSA	1.27 ± 0.12	1.39 ± 0.12	1.73 ± 0.19
Quectel RG255C	SA	0.44 ± 0.02	0.44 ± 0.02	0.61 ± 0.05
WNC 5G NR sub-6	SA	3.40 ± 0.34	3.50 ± 0.27	3.76 ± 0.41
WNC 5G NR sub-6	NSA	3.82 ± 0.37	4.00 ± 0.52	4.23 ± 0.49
P.C. TC Router 5004T-5G EU	SA	2.62 ± 0.28	2.65 ± 0.29	2.82 ± 0.37
Teltonika RUTX50	SA	3.36 ± 0.30	3.53 ± 0.29	3.56 ± 0.33
Siemens Scalance M800	SA	5.39 ± 0.18	5.42 ± 0.16	5.46 ± 0.15
Siemens Scalance M800	NSA	5.72 ± 0.17	5.82 ± 0.16	5.92 ± 0.16

Source: Author

consumption. For example, there is a difference of 40% in the power usage between SA and NSA with the Quectel device, while the WNC device, which required on average 3 to 4 times as much power only shown an increase of 14% from the average. The same applies for the Effects of RSRP variations. For the Quectel RM520-GL, a decrease of 14.5 dBm resulted in an increase of 33% in power consumption on the SA network and of 24% on the NSA. Looking at the other two routers, neither had an increase higher than 10% due to this factor.

For the network type, the discrepancy may be due to the greater processing power of the WNC and Siemens routers, as on the SA network, a greater part of the communication processing is done by the 5G core compared to the 4G. There may also be an influence of the signal power of two networks, as instabilities in each of them could lead to higher power consumption. In the RSRP aspect, since the minimum receiver sensitivity is linked to the device maximum throughput, devices with higher capabilities are by default more resistant to the effects of low RSRP.

Focusing on the network technology, a comparison between the results in SA and NSA for devices tested in both networks can be seen on Figure 34, considering only the devices tested in both networks.

Clearly, the SA network (in blue) is more energy efficient than the NSA network (in red) for the test scenarios studied. This is not a peculiarity of the device type, since the Quectel, WNC 5G NR sub-6 i-Router, and Siemens Scalance M800 differ significantly in their construction, even sporting different types of antennas. This is expected, as discussed in Section 4.1.1 due to the multiple improvements made to the SA network to improve the efficiency of the technology. If possible, it is advisable to work in the SA network, both because of the energy efficiency but also due to the higher performance brought by it.

The other impactful factor is the sending frequency, which is the interval between transmission. It is reiterated that the sending frequency does not have any relation to the frequency bands in Hertz used by the transceivers. To offer a comparison, Figure

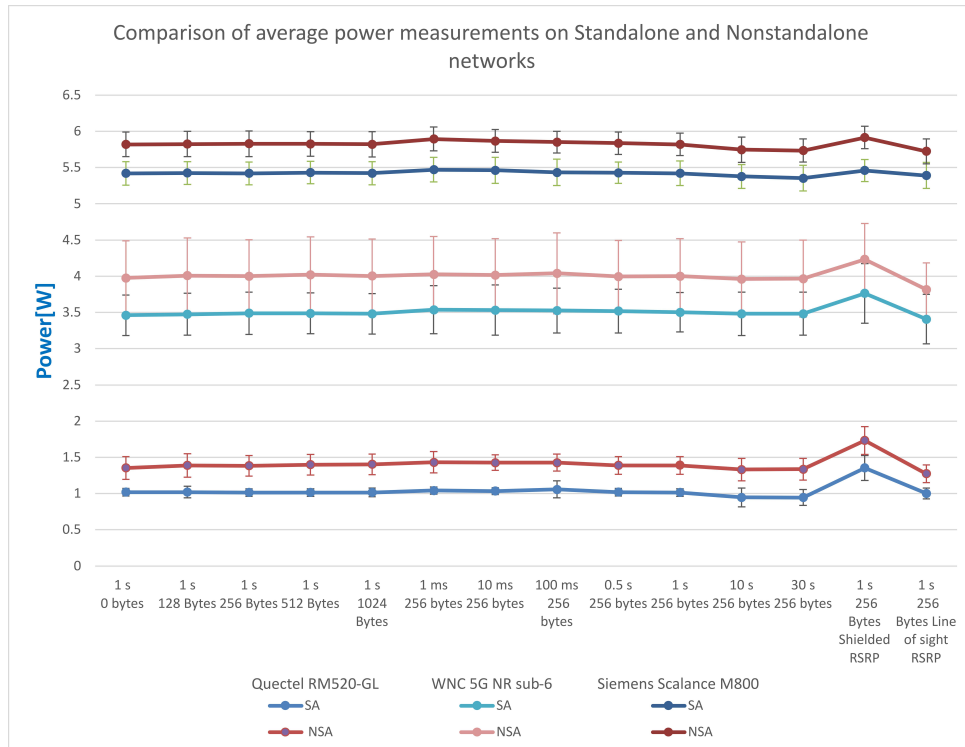


Figure 34 – Comparison of average power measurements on SA and NSA networks. Source: Author.

3 was made presenting the results for the 1 ms and 30 s second scenarios with the 1 s 256 bytes scenario from the sending frequency battery of tests also added for reference as the average case.

Device	Network	1 ms 256 bytes	1 s 256 bytes	30 s 256 bytes
Quectel RM520-GL	SA	1.04 ± 0.05	1.02 ± 0.05	0.94 ± 0.11
Quectel RM520-GL	NSA	1.43 ± 0.15	1.39 ± 0.12	1.34 ± 0.15
Quectel RG255C	SA	0.46 ± 0.03	0.44 ± 0.02	0.44 ± 0.02
WNC 5G NR sub-6	SA	3.537 ± 0.333	3.502 ± 0.272	3.483 ± 0.296
WNC 5G NR sub-6	NSA	4.233 ± 0.493	4.002 ± 0.517	3.816 ± 0.370
P.C. TC Router 5004T-5G EU	SA	2.721 ± 0.364	2.653 ± 0.293	2.570 ± 0.254
Teltonika RUTX50	SA	3.553 ± 0.320	3.528 ± 0.294	3.430 ± 0.265
Siemens Scalance M800	SA	5.470 ± 0.170	5.420 ± 0.156	5.354 ± 0.177
Siemens Scalance M800	NSA	5.895 ± 0.163	5.819 ± 0.155	5.734 ± 0.159

Figure 35 – Power Consumption values on some variations scenarios. Source: Author.

Looking at the values in Figure 3, there is no doubt about the impact of this factor and comparing the results with those presented in Figure 2, lower sending frequencies may be a viable strategy to counteract the effects poor signal strength has on power

consumption if the application allows for it.

The last tested factor is the packet size, however, it has proven to have little to no impact. This can be seen clearly when looking at the comparative graph of the results in the SA network presented in Figure 36. This conclusion is also valid for the NSA network, as can be seen in figure 34.

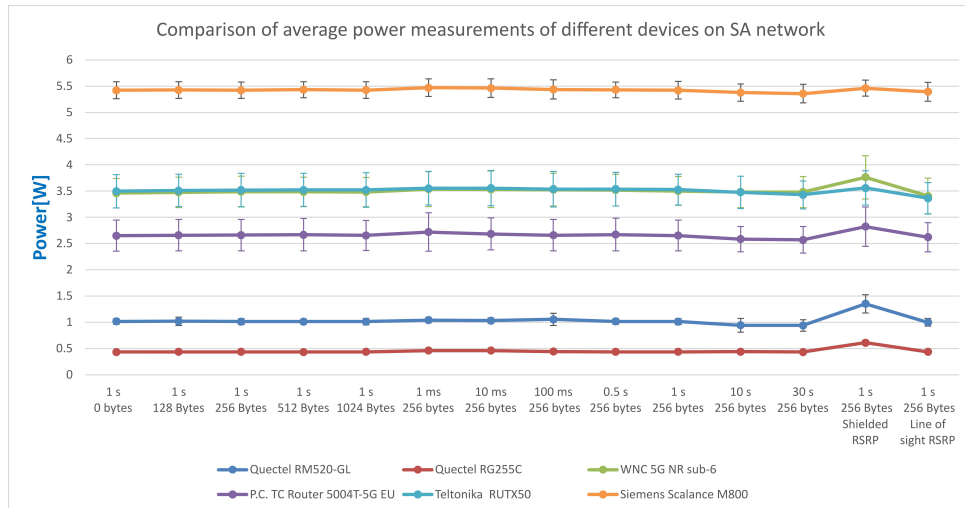


Figure 36 – Comparison of average power measurements on different 5G devices on SA network. Source: Author.

Table 3 – Power Consumption values on some variations scenarios

Device	Network	1 ms 256 bytes	1 s 256 bytes	30 s 256 bytes
Quectel RM520-GL	SA	1.04 ± 0.05	1.02 ± 0.05	0.94 ± 0.11
Quectel RM520-GL	NSA	1.43 ± 0.15	1.39 ± 0.12	1.34 ± 0.15
Quectel RG255C	SA	0.46 ± 0.03	0.44 ± 0.02	0.44 ± 0.02
WNC 5G NR sub-6	SA	3.54 ± 0.33	3.50 ± 0.27	3.48 ± 0.30
WNC 5G NR sub-6	NSA	4.23 ± 0.49	4.00 ± 0.52	3.82 ± 0.37
P.C. TC Router 5004T-5G EU	SA	2.72 ± 0.36	2.65 ± 0.29	2.57 ± 0.25
Teltonika RUTX50	SA	3.55 ± 0.32	3.53 ± 0.29	3.43 ± 0.27
Siemens Scalance M800	SA	5.47 ± 0.17	5.42 ± 0.16	5.35 ± 0.18
Siemens Scalance M800	NSA	5.90 ± 0.16	5.82 ± 0.16	5.73 ± 0.16

Source: Author

In any case, it is clear from the results presented that the preferred devices for applications with limited energy supplies are the Quectel modules. Their small energy consumption as well as small size and ease of use make them ideal for integration, at the cost of not having more advance features.

What can be concluded is that in order for applications involving energy harvester to be successful, some aspects must be considered at the time of designing the installation. Special care must be taken in ensuring a high quality link between the device and the antenna, preferably with line of sight, in order to avoid spikes in power usage. The communication must be tailored to be done in as few messages as feasible. In cases delays are tolerated by the system, it may be better to send multiple measurements at a time rather than as they are done. Overall, the data requirements of the use



case may limit the devices that can be chosen, but even for those with higher power usages, these techniques are still impactful, and may be what turns energy autonomy into a possibility.

## 6 ENERGY AUTONOMY VIA ENERGY HARVESTING

The data presented in Chapter 2 shows how much power each device requires on average in order to function and the conditions that may influence it. This knowledge may be used to design ways to power each device when not connected to the power grid. While batteries are an obvious choice, they are limited in their lifespan. This brings us to a complementary solution, energy harvesting systems in their many forms. With this conglomerate of technologies, it may be possible to achieve energy autonomy, which could make a battery last indefinitely in theory. While in practice the battery will degrade and eventually need to be replaced, the time required for that to happen is significantly longer than the time for it to simply discharge. Such development would be of great use in both reducing costs and idle time due to battery swapping in processes that depend on the transmission of data by battery powered 5G devices.

The idea of this investigation is to see how viable it is to power only the 5G transceiver, as they are the most power intensive component in any 5G sensor module and thus the biggest concern (DIAKHATE et al., 2020). In a real use case, which will be discussed later, other components, such as the sensors themselves as well as a microcontroller to interpret their measurements would be required. In order to have both a battery and a harvester working in tandem, a power management unit is also required. A case can be made that if the harvester can generate enough energy to fully power the sensor unit, the battery and energy administrator may not be required. However, it would make the system very susceptible to disruptions in the power supply. For example, a system powered by photovoltaic cells may be shut down if a light bulb dims or a worker passes in front of it, casting a shadow. Since the components and their configurations would vary depending on the use case, they will not be considered until Section 6.2.1. Regardless, the same methods used to estimate the amount of energy harvesters required to power the 5G transceiver can and were used to do so for the entire system.

In order to make these comparisons, the bachelor thesis of a colleague will be used as a source for the data of the energy harvesters. The bachelor thesis from Lauscher (2022) involves the evaluation of three different methods of energy harvesting, evaluating how much power was available in different factory setups and how much power different models of energy harvesters generate in those conditions.

With the information from Lauscher (2022), it was possible to compare how feasible it would be for each of the three technologies to power the 5G devices, as presented in Section 6.1. Since there is often more than one possible energy source for harvesting in most use cases, Section 6.2 discusses the application of multi-source energy harvesting, presenting a theoretical use case as an example.

## 6.1 SINGLE SOURCE ENERGY BALANCE FOR 5G DEVICES

As discussed in Section 3.2, there are many forms of energy harvesting that can be used alone or in conjunction. Initially, the focus will be on whether any of them could provide enough energy to supply one of the devices. Considering the elevated power requirements of some of the devices, there will also be comparisons where part of the power is being supplied by a battery instead of it being only a backup.

In order to do these comparisons, only the results in the standalone network will be considered for two reasons. The first is that the performance in the SA network was better across the board. SA networks are also faster and more capable, while the NSA architecture was created to be transitional. Future applications are more likely to use the simpler installation rather than one that requires two networks. The second reason is that due to the difference in scale between the RedCap device and Siemens, most NSA results end up very close together with the SA lines. This made the graphs including all datasets hard to read due to overlapping data. Another compounding effect is the fact that only 3 of the 6 devices have results for the NSA network, so a separate analysis of the two networks is not very productive.

### 6.1.1 Photovoltaic powering comparison

The first method studied was photovoltaic cells, also known as solar panels. The generation of a photovoltaic cell depends on many factors, with the main one being the incidence of light. In Lauscher (2022), there are three scenarios to be considered. The first considers the average incidence of light inside the machine hall at Fraunhofer IPT. The second and third consider that the recommended 1000 lx reaches the panel with fluorescent and LED lights, respectively.

For the first scenario, 12 measurements of illuminance were taken around the machine hall, arriving at an average of 514 lx in the area. This resulted in a maximum power production of  $(1.288 \pm 0.062)$  mW with a photovoltaic cell of model “Seeded 313070003 monocrystalline”. Said photovoltaic cell is presented in Figure 37 for reference.

Although this is far too little to power even the best case of the RedCap device, this value was obtained using only one cell with  $144 \text{ cm}^2$  of area. Even in the original work, it was suggested to add together multiple cells in order to provide enough power. Thus, it is necessary to verify how much area would be required to provide power for each device in each scenario.

In order to do so, the energy density of this energy harvester was calculated as  $(0.089 \pm 0.012) \text{ W/m}^2$ . With this data, it is possible to plot how many square meters of area would be required to power each device fully, the result can be seen in Figure 38. One thing to remember is that while the error bars may appear overtly imprecise, we



Figure 37 – Photovoltaic cell model “Seeded 313070003 monocrystalline”. Source:Marutsu (2024).

must consider they are also influenced by the original scale of the values.

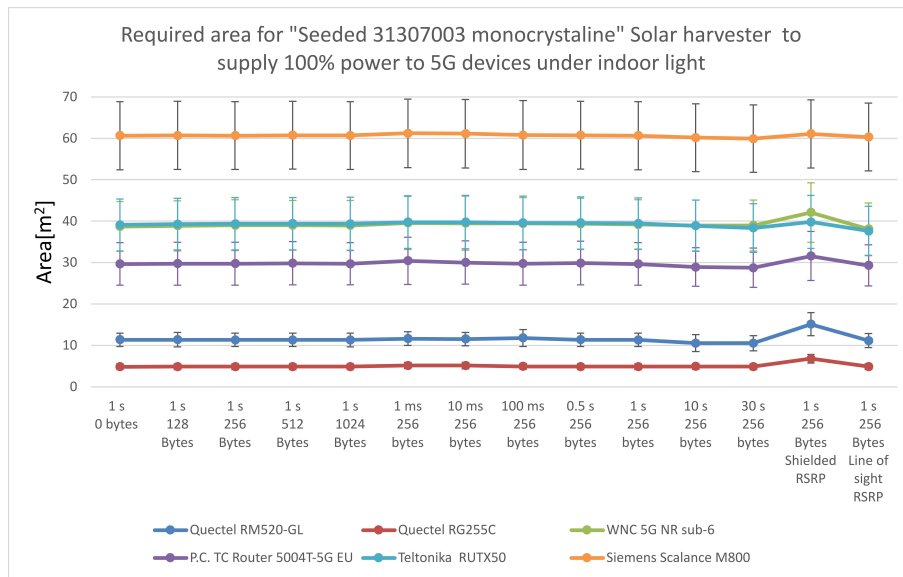


Figure 38 – Area required to supply the devices with the “Seeded 313070003 monocrystalline” solar harvester. Source: Author.

As expected, looking at the scale, it would not be possible to fully power any of the devices with such a low energy density. Even the most energy-efficient device requires almost five square meters of cells, which would be bigger than some commercial solar panels. However, while energy autonomy is relevant, extending the battery life would already have a significant impact.

To evaluate the possibility of partial powering the area required to provide only 10% of the required power device, it would still not be feasible. In order to power the

average case with the lowest power consumption, that of the Redcap device, it would require an area of  $(0.483 \pm 0.068) \text{ m}^2$ , which would necessitate 34 of the measured photovoltaic cells. This is by no means viable, and that does not consider the fact that the voltage being generated by this cell is only  $(2.955 \pm 0.069) \text{ V}$ . The low voltage may be counteracted by associating multiple cells in series, however, this may overload circuits for administering the energy or the sensors themselves.

While the initial prognosis is not very optimistic, this is not the only situation involving photovoltaic cells studied in the original thesis. While the radiance obtained in the Machine hall was only 514 lx, the types of cells studied are designed with irradiation of 1000 lx or more in mind. These comparisons were done considering fluorescent and LED lights, since the different sources had an impact on the results.

A comparative study of different power cells considering varying levels of irradiation and color temperature for LED lights can be seen in Figure 39 for context. In

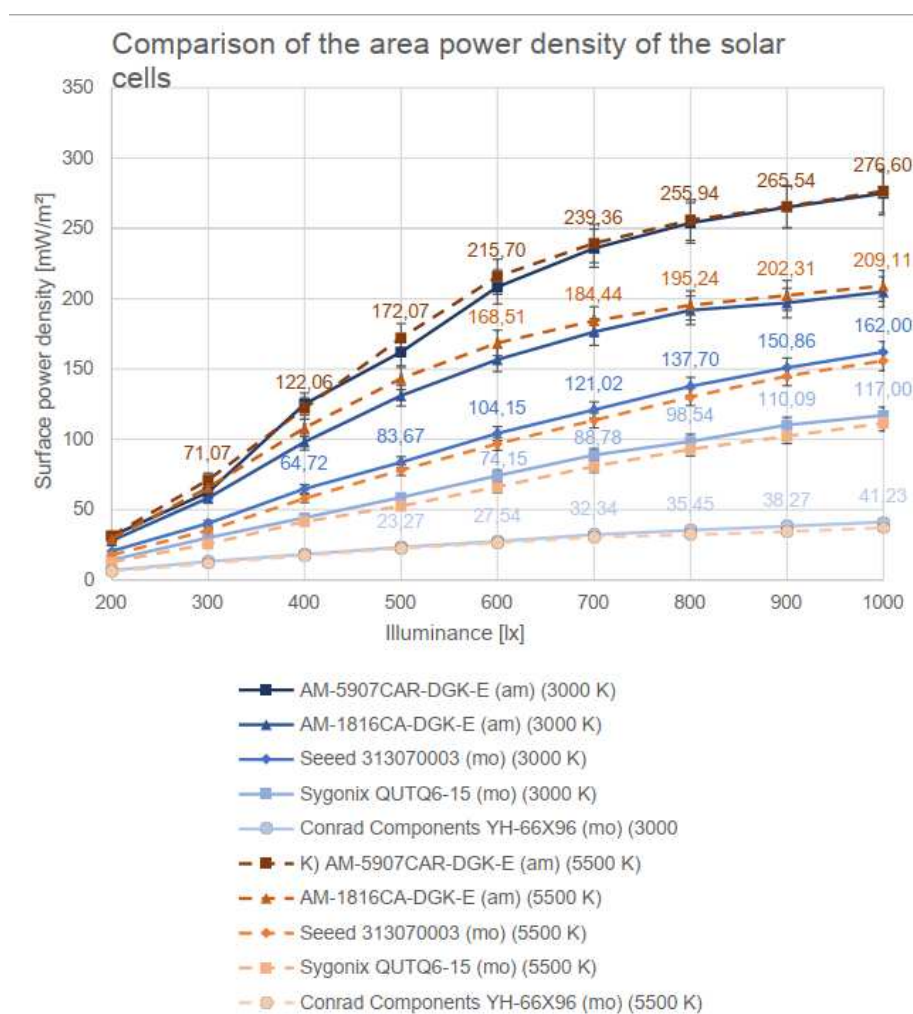


Figure 39 – Comparison of the area power density of the solar for LED lights. Source:Lauscher (2022)

the study, the configuration with the best performance was the scenario involving the amorphous photovoltaic cell of model “AM-5907CAR-DGK-E” receiving 1000 lx with a

color temperature of 5500 K. For context, this cell has an area of  $41.3 \text{ cm}^2$  and could generate a voltage of  $(5.04 \pm 0.12) \text{ V}$ .

Considering this best scenario, the energy density available is of  $(276.6 \pm 15.5) \text{ mW/m}^2$ . Repeating the last comparison, aiming to supply only 10% of the power demanded by the devices, the required areas can be seen in the graph in Figure 40.

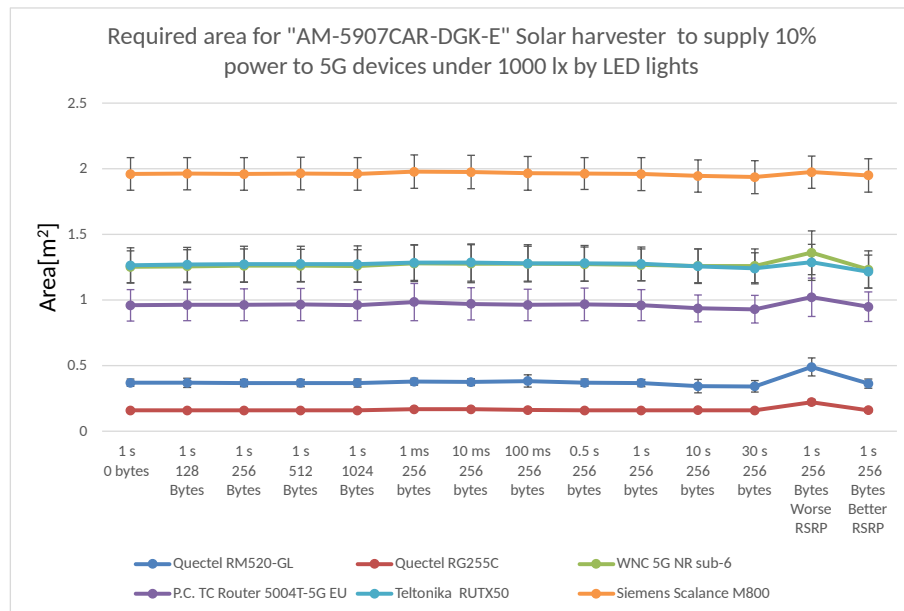


Figure 40 – Required area for “AM-5907CAR-DGK-E” harvester to supply 10% power to 5G devices under 1000 lx. Source: Author.

While this is an improvement, it would still require  $(0.156 \pm 0.012) \text{ m}^2$  to supply the average case of the least power-intensive device. This is still too much, as it would require  $(38 \pm 3)$  panels in order to cover this area. This would an area equivalent to a 22-inch TV screen would be required in order to be able to extend the battery life by only 10%. And that does not consider the energy costs of the sensors and energy administrator that would be required. At least, in this scenario, the voltage provided by the energy harvester is capable of supplying the Quectel modules, which would ease integration if they are used.

Unfortunately, photovoltaic cells, even under the best conditions, cannot supply a device during operation. The technology would still be useful in cases where the system has long periods of inactivity, allowing for the power to be replenished over time. In case the other technologies perform better, it can also be paired with them in order to cover eventual fluctuations on their power supply.

### 6.1.2 Thermoelectric powering comparison

Considering now thermoelectric energy harvesters, as discussed in Chapter 3, the power is generated by a difference in temperature between two parts of the

harvester. Because of this, there must be a significant temperature gradient in order to use this type of harvester.

Referring again to (LAUSCHER, 2022), it is possible to obtain the power generated by four different models of thermoelectric harvesters. These harvesters are actually Peltier thermal cycling systems. The Peltier effect is the phenomenon where current flow can be used to move heat between two conductors and vice versa, being the main principle of many thermocouple devices (SANIN-VILLA, 2022). In order to illustrate their appearance, the model used in the future comparisons is presented in Figure 41.

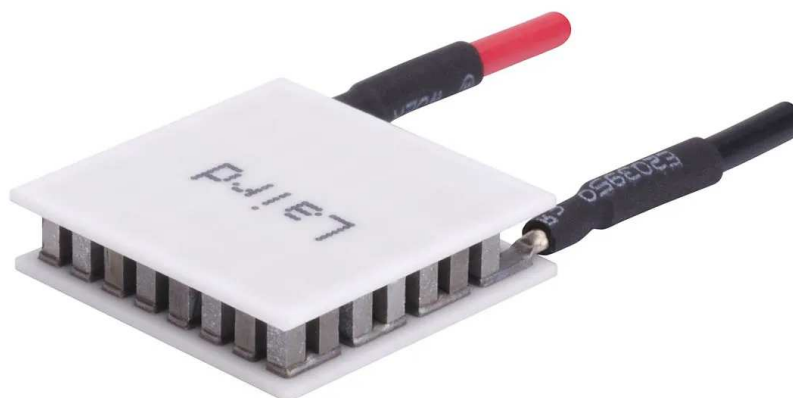


Figure 41 – Thermoelectric harvester model Laird 387005695 Source: PITCH Technologies (2024).

These models were studied assuming cooling via heat sinks would be present in order to maximize their generation. They also were proven to be very sensitive to movements in the air. This influence increased the uncertainty of the measurements, but would also increase the total power generated. The graph with the power measurements done in (LAUSCHER, 2022) is shown in Figure 42.

From the graph, it can be observed that the best scenario would be a temperature gradient of  $115^{\circ}\text{C}$  using the harvester of model “Laird 387005695”, by Laird Thermal systems. This device can generate up to  $(0.37 \pm 0.03) \text{ mW}$  and  $(213 \pm 11) \text{ mV}$  in these conditions. While these values may be low, even the company providing them suggests the use of multiple units in order to counteract these drawbacks.

Considering this device has an area of  $16 \text{ cm}^2$ , it is possible to calculate its power density as  $(0.148 \pm 0.012) \text{ W/m}^2$ . For the sake of comparison, the graph presenting the areas required either to have energy autonomy or to supply only 10% of the energy demand were generated considering this power density and can be seen in Figures 43 and 44.

For the energy autonomy scenario, it can be clearly seen that it would not be feasible to supply any of the devices. In reality, it would be necessary to mount 1244

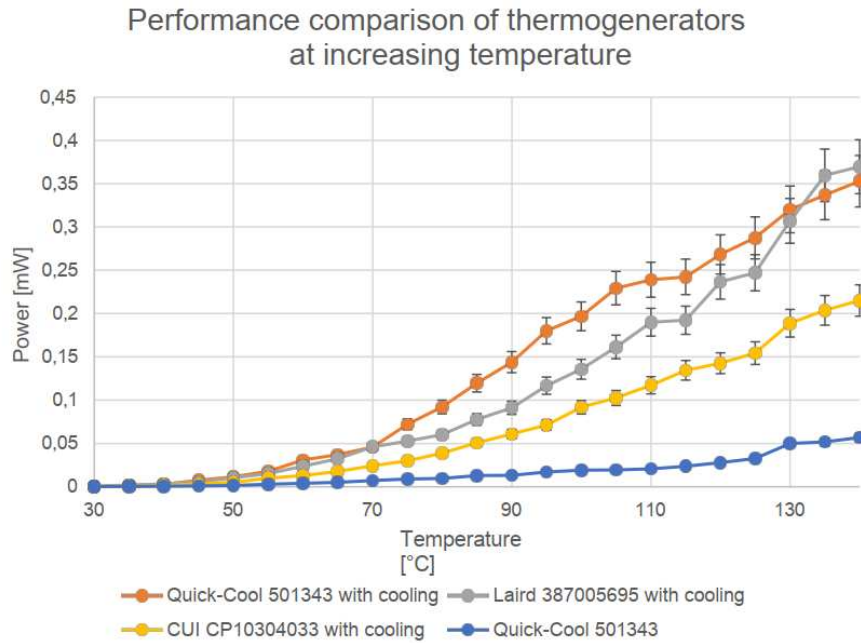


Figure 42 – Performance comparison of thermogenerators at increasing temperature. Source: Lauscher (2022).

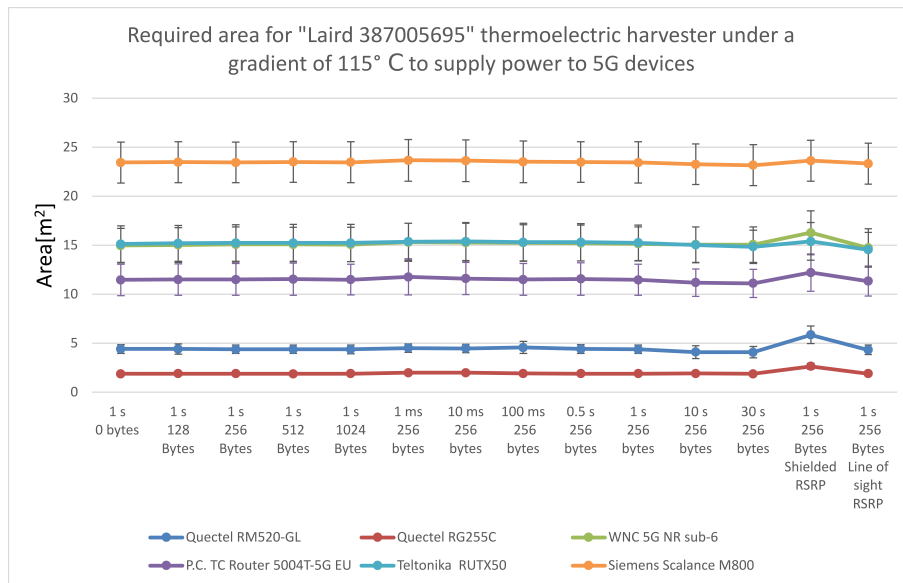


Figure 43 – Required area for “Laird 387005695” thermoelectric harvester under a gradient of 115 °C to supply full power to 5G devices. Source: Made by the author.

devices in order to supply the Quectel RG255C in the average case of 256 packets every one second. This is due to the requirement of an area 1.991 m<sup>2</sup> to generate enough energy. In case it was decided to attempt to fully power the Siemens Scalance M800 router with this device, it would require an area of 23.463 m<sup>2</sup>, which would likely surpass the heated area of any machines this system may be mounted to.

Since energy autonomy is far from being achieved, it is better to focus again on the reduced scenario of only 10% of energy coverage, which is presented in Figure 44.



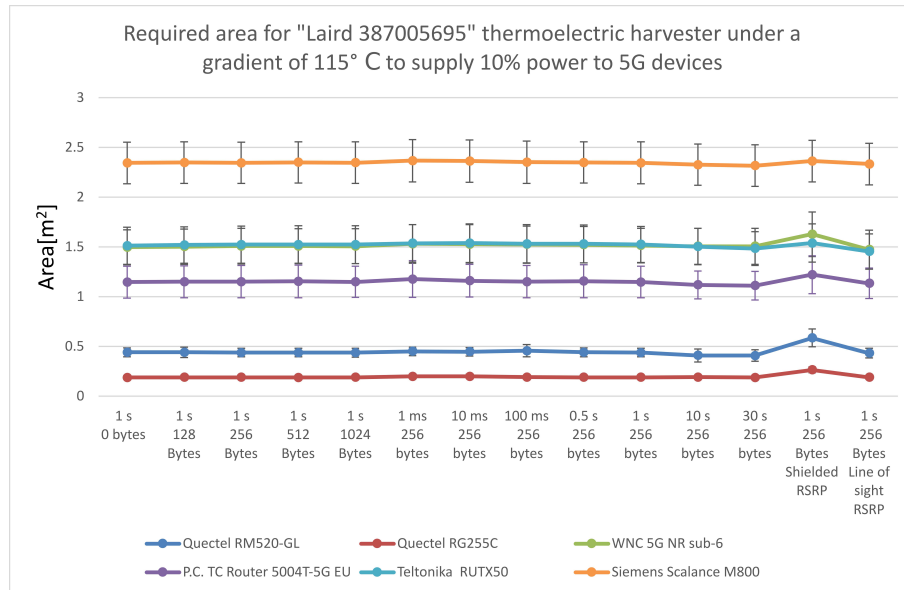


Figure 44 – Required area for “Laird 387005695” thermoelectric harvester under a gradient of 115 °C to supply 10% power to 5G devices. Source: Author.

With this reduction, an area of only  $(0.199 \pm 0.019) \text{ m}^2$  is required for the average scenario. This would mean 119 units of this harvester must be installed for this generation to be achieved. Despite the cost such installation would have, since this type of energy harvester must be installed at the heat sink or between it and the heated device, it could compromise the cooling of the machine from which the energy is being harvested. This also does not consider the losses that could happen to connect such a large amount of devices, especially with the wires being very close to elevated temperatures, which would increase their resistance. To summarize, such an installation might be possible, but it would have a high cost and complexity, besides requiring a large heated area to be available.

In any case, there must be an evaluation of whether the cost of the installation would justify the application. Regardless of the size of the final installation, the application of this technique will prove beneficial to the battery life. This is especially valid for systems with large periods of inactivity, where the 5G transceiver can be turned off, enabling the battery to be charged.

### 6.1.3 Kinetic powering comparison

Turning the focus to kinetic energy harvester, two varieties are mainly used in industry, piezoelectric and electromagnetic. Piezoelectric harvesters take advantage of piezoelectricity as their name implies. Electromagnetic harvesters, on the other hand, use a permanent magnet surrounded by a coil and the effects of induction to generate a voltage difference. Kinetic harvesters are designed to work in a limited band of frequencies. However, modern manufacturers are capable of producing harvesters for many

varieties of frequencies, which makes them preferable if the frequency of vibration is known and almost constant. This does not imply that they do not work outside of their designed frequency band, but rather that their efficiency is compromised. Both types generate alternating currents instead of continuous, thus requiring the use of a rectifier in order to power the devices.

In order to make comparisons, the data presented in (LAUSCHER, 2022) will be used again. In its experiments, a total of 4 kinetic harvester were tested, two piezoelectric and two electromagnetic. The vibrations in the tests did not come from a real machine, but from a modal vibration test system from TIRA, of model TV 51110.

This test system was configured to be controlled by voltage, and that is the metric used by the author to classify the intensity of vibration. However, the device controller maximum RMS voltage is known, being of 22 V<sub>RMS</sub>. Considering the maximum force of the vibration that can be generated as by the device is 100 N and the device is linear, it is possible to estimate the force used in the tests in newtons in order to have a frame of reference. Following this logic, there was an intensity of around 4.54 N in the initial case of 1 V and for the 6 V cases that will be focused on, an intensity of around 27.27 N was applied to the harvester. This approximation is based on both the datasheet of test system and the content in (LAUSCHER, 2022). The values obtained also explain the problems with stability reported on (LAUSCHER, 2022) when applying the highest vibration configurations.

Looking first at the electromagnetic harvesters tests, the models “ReVibe Energy 00204” and “Xidas VEG-50 10- 301200” were tested in (LAUSCHER, 2022). Both of these models are optimized for an oscillation frequency of 50 Hz but were tested for frequencies between 35 Hz and 100 Hz. The best result was of the ReVibe Energy 00204 model ( $197.47 \pm 9.87$ ) mW at 51 Hz. One thing that must be considered in order to calculate the energy density is that these devices are not flat panes, but rather cylinders that are supposed to be attached directly to the machine. Since in order to operate, the bottom of the cylinder must be perpendicular with the vibration force, it is designed to have the bottom glued or side attached to the lateral of the machine. With that in mind, the area of the bottom of the cylinder was considered for calculations of energy density.

Because this model has an area of 22.94 cm<sup>2</sup>, the energy density available is of ( $86.081 \pm 4.303$ ) W/m<sup>2</sup> (LAUSCHER, 2022). However, this energy density does not consider the losses incurring to the rectification of voltage generated by this type of harvester. Since the effective voltage is ( $8.22 \pm 0.33$ ) V in this best scenario, it would be possible to estimate the effectiveness of a rectifier bridge. This estimation however heavily depends on the bridge rectifier efficiency. Depending on the energy administrator board used it may even be built into the board and taken into account in the total efficiency of the administrator. As discussed at the start of this section, this

aspect will not be considered in order to keep the analysis general. In Section 6.2.1, a rectifier will be chosen and their losses incurring from its usage will be considered.

In order to compare this device performance with the other harvesters, a graph presenting the area required to fully power the devices was made and can be seen in Figure 45.

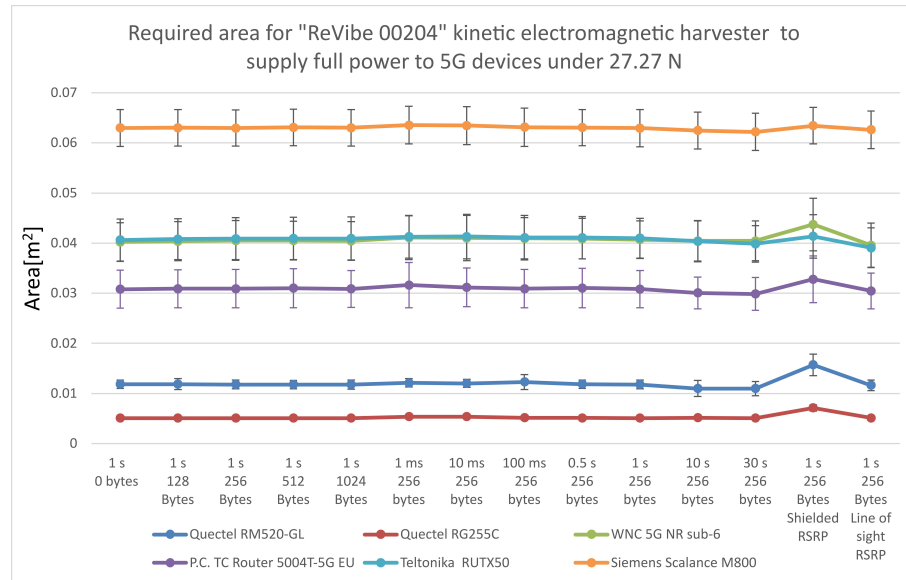


Figure 45 – Required area for “ReVibe 00204” Kinetic electromagnetic harvester to supply power to 5G devices under vibrations of 27.27 N. Source: Author.

As can be seen by the scale, this is the most promising result obtained so far. In order to power the RedCap device in its average case, an area of only  $(0.00501 \pm 0.00035) \text{ m}^2$  or  $(50.1 \pm 3.5) \text{ cm}^2$  is required. This area can be covered by three harvesters of this model. In reality, only 2.2 but the device cannot be divided in this manner. This is by no means a detriment since using three devices, an area of just  $68.82 \text{ cm}^2$  is covered. If the worst case is considered, the one with poor RSRP,  $(0.61 \pm 0.05) \text{ W}$  must be provided, which is not possible with 3 generators for  $0.01 \text{ W}$ . However, the addition of a fourth harvester even without receiving the full vibration intensity can easily solve this problem. Together 4 harvesters of this model can generate enough to power all the scenarios involving the Quectel RG255C, in other words, energy autonomy is achieved in this setup. However, there is one problem with this setup, and that is the voltage generated by the device. In these conditions, the device generated a voltage of  $(8.22 \pm 0.33) \text{ V}$ , and the Quectel modules operate at only  $5 \text{ V}$ . This poses a problem, while the voltage can be reduced, it would generate losses. A transformer could be used in order to lower the voltage, however, since the apparent power is less than  $1 \text{ VA}$ , the efficiency would be of less than  $50\%$ . A step-down converter, but that would also incur into significant losses. Another option would be to operate the battery and energy manager at this voltage and connect the step-down unit directly to the 5G device, microcontroller and sensors if needed. What would be the best approach is discussed

in Section 6.2.1, where a theoretical use case is defined, since there are too many variables at play for a general scenario.

Focusing on the other devices, Table 4 presents the area and number of devices that would be required to power each of them. The average use case assumed is the 1 s 256 bytes from the sending frequency series of tests, as it contains the values in the default configuration for this test and approximates the actual average consumption across the tests.

Table 4 – Area measurements and required number of units to guarantee power to the 5G devices.

Name	Area required (cm <sup>2</sup> )	Units required to power the default case
Quectel RG255C	50.1 ± 3.5	3
Quectel RM520-GL	115.8 ± 8.5	6
WNC 5G NR sub-6	407 ± 37	20
P.C. TC Router 5004T-5G EU	308 ± 37	16
Teltonika RUTX50	410 ± 40	20
Siemens Scalance M800	630 ± 37	30

Source: Author

As can be extracted from Table 4, there could be enough power generation to fully supply the Quectel modules with this harvester, provided that enough vibrational energy is present. This still leaves the problem of the voltage surpassing the safe values for the modules. As long as there is more energy and space available, more units can be added to compensate the losses during conversion.

For the remaining devices, it would be more challenging, since they would require 16 or more harvesters, depending on the model. This is a problem because each harvester will act as a dampener, reducing the total efficiency of the others. There would also be challenges in order to manage the energy generated by so many different devices, especially considering the current generated by them is alternating. In case the devices are not assembled in a way that the vibration signal matches between them, the harvester may cancel each other generation or require one rectifier bridge per harvester in order to avoid this problem all together. In any way, this shows that even for the more power hungry devices, partial supply is viable.

However, this result is a best case scenario that assumes enough kinetic energy is being propagated into the harvesters. From the original study, there are other 5 cases with lower vibrations that were considered. The raw data from these experiments with this harvester was provided by the local Supervisor, Sarah Schmitt, after she contacted the author of Lauscher (2022). This provided the capability to generate the graph in Figure 46, where the area required to power the RedCap device with each intensity is presented.

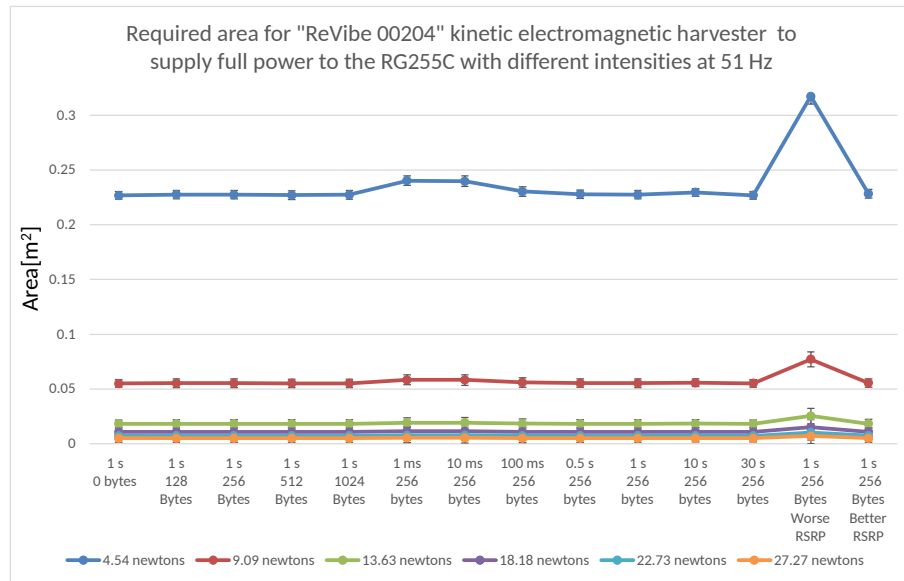


Figure 46 – Required area for “ReVibe 00204” Kinetic electromagnetic harvester to supply power to under different intensities of vibration at 51 Hz. Source: Author.

Although it is hard to see, even two thirds of the intensity, there is a reduction of 52% in output. However, these results are not the optimal power generation at each intensity, since as the intensity increases, so does the most effective vibration frequency. This variation in efficiency still stays close to the theoretical 50 Hz for this model of harvester. For example, for the intensity of 18.18 N, the highest value is of  $(105.95 \pm 5.29)$  mW at 49 Hz. In order to have an equal comparison, the values at 51 Hz were used, as this is the best scenario that would have the device be designed for. For this frequency, the generation is of  $(93.14 \pm 3.23)$  mW. In case the comparison is done using the best frequency, the results are even better. While this proves that proper fixation and configuration of the harvester for the expected conditions is paramount for the best results, such reduction does not invalidate the results obtained. Energy autonomy may require the addition of extra harvesters or not be possible altogether, but an increase in battery life of more than 50% is by no doubt relevant and can be worth the investment.

To summarize, even for lower intensity situations, partial supply would still be possible for this type of harvester, or even full power with the addition of extra units. This is very promising for applications where kinetic energy is available in the environment.

Turning to the piezoelectric harvesters that were also studied in (LAUSCHER, 2022), the two models tested were “S452-J1FR-1808XB” and “S128-H5FR-1107YB”, both tuned for 20 Hz. For illustration purposes, the “S452-J1FR-1808XB” device is presented in Figure 47.

The tests revealed that the first model had a better performance, generating a maximum of  $(4.48 \pm 0.18)$  V and  $(0.733 \pm 0.038)$  W. The area of the device, however, is



Figure 47 – Enter Caption

a complicated subject. The device itself needs to be attached to a stationary point, so the actual area occupied by the device and its anchor may vary. In order to make calculations possible, only the area of the device itself, being  $17.75 \text{ cm}^2$ , will be considered. With this area, the calculated energy density of this device is of  $(0.409 \pm 0.021) \text{ W/m}^2$ . For ease of analysis, the graph in Figure 48 was generated showing the area required to power the devices with this density.

In contrast to the performance of the electromagnetic harvester, it would require  $(1.054 \pm 0.075) \text{ m}^2$  to fully power the average case of the Quectel RG255C. Considering the harvester device has only  $21.24 \text{ cm}^2$  and would still require an anchor, such installation would not be possible. If the least demanding device cannot be powered, the remaining ones would also not be viable.

For the sake of brevity, a new graph for the 10% scenario will not be presented. Since it would require  $(0.1054 \pm 0.0075) \text{ m}^2$  to power the average case of the Quectel RG255C. This would imply in the installation of 50 units of these harvesters. This would also require the installation of supports for them to be connected rigidly enough to not oscillate alongside this many harvesters. In reality, this many connection points would likely dampen the vibrations significantly, reducing the generation of all harvesters.

While such a large installation may be possible in an oil pipeline due to its size,

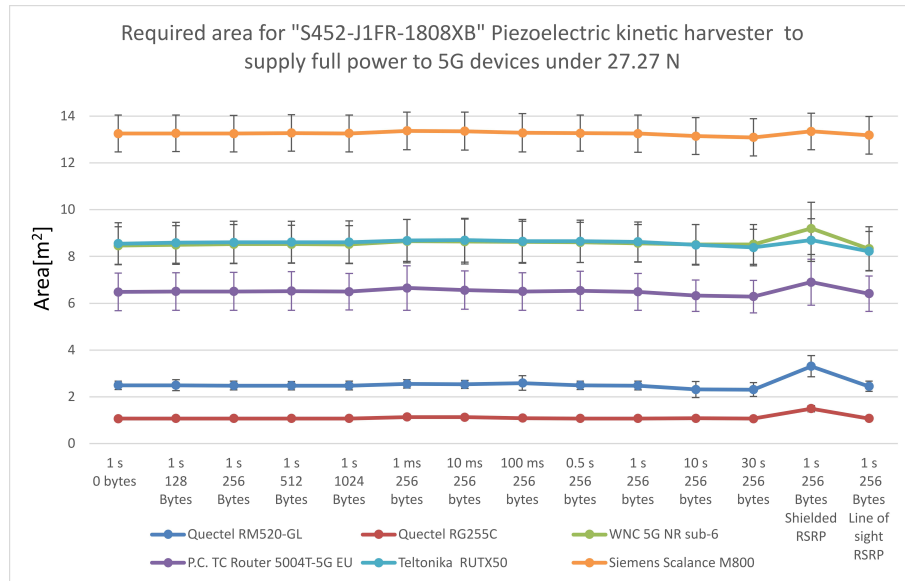


Figure 48 – Required area for “S452-J1FR-1808XB” Kinetic piezoelectric harvester to supply power to 5G devices under vibrations of 27.27 N. Source: Author.

it is safe to say it would not be cost-effective, and that the electromagnetic harvesters would be a better solution.

## 6.2 EXAMPLE FOR MULTI-SOURCE CONFIGURATION

As seen in Section 6.1, a single energy harvester may not be sufficient to sustain a 5G transceiver during operation. However, a possible solution to this may be to combine different energy harvesters in order to supply the required power. In order to make this comparison, it would be necessary to consider in what situations would it be possible to apply the energy harvesters, since the conditions of a given use case are going to dictate the viability of application.

First and foremost, there must be a study of the use cases involving 5G to check which would be suitable for the implementation of multi-source energy harvesting. Once the suitable use cases are decided upon, the remaining aspects such as the real-life environment for their application may also be determined. From the constraints that the use case brings it will be possible to determine what could be the remaining components, such as the sensors to be powered, the microcontroller, and the power management units. Lastly, the real world application also provides a notion of the area which would be available for the installation of the harvesters and the conditions they would be subjected to. As presented in Section 6.1, this is a critical component due to the low energy density of the harvesters compared to the consumption of the 5G devices.

Starting on the possible use cases, the diagram presented in Figure 6 can be used as a basis. It presents a total of 5 groups of use cases, although not all of

them are viable or practical to have energy harvesting installations for 5G on them. In order to summarize which use cases would or not be viable, Table 5 was created. The detailed explanation of why the use cases were partially or fully excluded is presented afterwards.

Table 5 – Use Case Table with Viability Considerations

<b>Use Case</b>	<b>Considered</b>	<b>Multi-source harvesting viable</b>
Motion control	Yes	Yes
Control to control	Yes	Yes
Process automation	Yes	Yes
Mobile robots	No	No
Human centered monitoring	No	Yes

Source: Author

In the case of automated vehicles, they will already be battery operated. This means that any employment of energy harvesting would be focused on charging the robot itself, which would be outside the scope of this project. Regarding human-centered monitoring, achieving energy autonomy of a 5G device would be very hard under the conditions of these use cases. These use cases belong mostly to indoor applications, limiting the amount of light and thus the generation of photovoltaic cells. Another problem is that for handheld or wearable devices, they may not be properly aligned with the light source at all times, further reducing their efficiency. These two factors would require large areas to compensate, which would not be available in these types of devices or would make them very cumbersome. Thermal harvesters can use a person's body temperature to generate power, but as discussed in Section 6.1.2, it would not be possible to have enough generation for a transceiver without a gradient of more than 100 °C. Since human body temperature is around 37 °C, an even larger area would be required, so this technique would not be able to generate enough power. For the kinetic generation, while vibrations from human movement can be harvested, they would not have the necessary strength or regularity required for energy autonomy to be reliably achieved.

This does not mean that energy harvesting on handheld devices is not viable. The problem is the amount of energy required for the 5G transceivers to work. For less power hungry applications, these systems can be very successful. But the higher power demand brought by the 5G transceivers would require near ideal conditions, which leads to this use case being disregarded.

This leaves three types of use cases available. However, only the use cases involving process automation mirror the previous tests in their little to no mobility. While the aspects found in the tests would apply to moving devices, it would not be a fair comparison. Another benefit of the process automation use cases is their large variety, leaving ample room to look for specific use cases that are compatible with energy



harvesters. As the engineering course of control and automation proves, there are very few processes that cannot benefit from closed-loop controls or at least monitoring.

Nevertheless, from the point of view of the device, the three use cases in this type are virtually the same. Each of them consists of sensor arrays that transmit data to a central processing unit. The purpose of the data, whether as input for control systems, monitoring, or plant status assessment, is inconsequential (5G ALLIANCE FOR CONNECTED INDUSTRIES AND AUTOMATION (5G-ACIA), 2019).

### 6.2.1 Use case: Process monitoring

In order to simulate this use case, 5 elements need to be determined in order to bring the abstract into a physical use case to be discussed. These elements are:

- Sensor(s);
- Microcontroller;
- 5G transceiver;
- Harvesters;
- Energy administrator.

After careful study and deliberation, the use case decided upon was that of milling operations. It was chosen for two main reasons, the first being the large availability of kinetic energy and light depending on the machine and procedure. Temperature gradients may also be present, but would be tricky to collect as there is a need to cool the piece in order to avoid deformation and internal stresses. The second reason is that it is a process that has already seen many attempts to implement energy harvester powered sensors, such as the implementation described in Chung et al. (2016). This happens because the process of milling must be enclosed in order to both protect workers and equipment. This enclosure complicates the process of adding new sensors to old machinery, as the installation of cables would require costly or difficult modifications to the enclosure. Cables also pose a risk since they can be caught by the machinery, destroying the sensor and possibly damaging the machine.

Before any more discussion can be done, some assumptions must be made. These are that there is enough energy to be converted by the harvesters to match the values discussed previously. Another is that the signal strength from the previous tests can also be provided inside the machine. Considering that non-metallic materials have very little influence in the signal and many machines have large windows to provide a way to observe the process, this assumption is reasonable.

Turning back to the items on the list, starting by the sensors, the most logical data to be collected would be that of vibration. This would require one or more accelerometers. One possible accelerometer model to be used is the ADXL345. It is a low-power 3-axis accelerometer with relatively high precision, large configurable scale going up to  $\pm 16$  g, and I2C capabilities, which would facilitate communication with the microcontroller. Said sensor can also be powered with voltage values between 1.8 V to 3.6 V, which would make it easier to match it with a microcontroller. The datasheet for this device states that for normal function, it requires 160 mA while receiving 3.3 V (DEVICES, 2022b). This translates to a power of 0.528 mW for each unit of this sensor used. In order to simplify the comparison, it will be assumed that only one sensor is used.

With the source of the data defined, there must be a device to process it, a microcontroller. This component however can come in many shapes with many capabilities. After analysis, the microcontroller chosen was the STM32L051RBt6, for its low power consumption and also for have already been used in (KONGARA, 2023), which is being used as a basis for the development of this use case. The STM32L051RBt6 is an ultra low power microcontroller with 64 kbyte flash memory with Error-Correcting Code (ECC) and 8 kbyte RAM. It has 51 I/O ports, sleep and low power sleep capabilities, making it ideal for an energy critical operation. It also has 12-bit Analog-to-Digital Converter (ADC) on up to 16 channels, and 7-channel (Direct Memory Access) DMA controllers (STMICROELECTRONICS, 2019). This means that protocols like the I2C used by the ADXL345 are understood by the sensor, and would even allow for two of the sensors to be implemented. During normal operation, the current drained by the microcontroller is mapped in Table 25 of the datasheet, presented in Figure 49.

IPs	Run/Active	Sleep	Low-power run	Low-power sleep	Stop	Standby
					Wakeup capability	Wakeup capability
Consumption $V_{DD}=1.8$ to $3.6$ V (Typ)	Down to 140 $\mu$ A/MHz (from Flash memory)	Down to 37 $\mu$ A/MHz (from Flash memory)	Down to 8 $\mu$ A	Down to 4.5 $\mu$ A	0.4 $\mu$ A (No RTC) $V_{DD}=1.8$ V	0.28 $\mu$ A (No RTC) $V_{DD}=1.8$ V
					0.8 $\mu$ A (with RTC) $V_{DD}=1.8$ V	0.65 $\mu$ A (with RTC) $V_{DD}=1.8$ V
					0.4 $\mu$ A (No RTC) $V_{DD}=3.0$ V	0.29 $\mu$ A (No RTC) $V_{DD}=3.0$ V
					1 $\mu$ A (with RTC) $V_{DD}=3.0$ V	0.85 $\mu$ A (with RTC) $V_{DD}=3.0$ V

Figure 49 – Current use by the STM32L051RBt6 Microcontroller during normal operation Source:STMicroelectronics (2019)

There is no mention of the typical values for sleep mode, only that they can be down to 37 mA MHz<sup>-1</sup> of clock for normal sleep mode. For the low power sleep mode, it can be as low as 4.5 mA. However, the low power sleep mode requires a special signal to be exited. Since there is no physical connection to the device, it would need to be woken up by the sensor, which cannot produce the required signal.

For the 5G transceiver, the most viable option would be Quectel RG255C, due to its low power requirements. Considering it is capable of 50 Mbit throughput, the device is more than capable to fulfill this use case requirements. One aspect to be considered is its voltage, as it requires 5 V instead of 3.3 V used for the sensor and microcontroller. Considering a battery of 5 V can be used, and the voltage conversion can be done by the energy admin, the microcontroller can be powered directly by the battery. In order to save power when not operating, power can be turned on or off by the microcontroller by the use of a transistor as a switch.

Regarding the harvesters, two of the three types discussed can safely be implemented: kinetic and photovoltaic, one that would use the vibrations inherent to the milling process and the other that would collect light coming from the windows that allow the process to be observed. Unfortunately, it would not be possible to generate the massive temperature gradients discussed previously in a safe manner in this use case. While it can be argued that the motor rotating the tool would generate enough heat, the main idea is not to modify the original machine, so there may not be access to an actual heat sink inside the work area. Collecting heat from the work piece itself is also not realistic. The piece would be actively cooled in cases where enough heat waste would be generated, and the placement of the harvester would also be dangerously close to the piece.

One aspect that must be considered is that there would only be vibrations during operation. This would mean that the only time the kinetic harvesters would be active would be when the process is ongoing and data is required. Nevertheless, the photovoltaic generators would always be active to some extent in an indoor installation, as the lights must be on when workers are in the premises. This constant source of power would allow the batteries to be charged during idle times in the process, even if the generation cannot generate enough to supply the transceiver during operation.

In order to be able to regulate where the energy is used, a power manager circuitry is required. This circuit must be used in order for a battery to be viable, and since vibrations may oscillate and the solar cells may be covered accidentally, a battery is needed to ensure uninterrupted function. This circuit as its name suggests will direct the collected energy either into the battery or into the circuit as needed, allowing both sources to operate together as needed. Since multiple energy harvesters are being used, multiple energy power managers would be required, at least one for each source.

While there is not a commercial alternative presenting multiple power managers, there have already been studies in order to either produce them or bypass the need of a power manager. An example of their joint usage is the study of Kongara (2023). In this master thesis, a proof of concept using multiple power management boards in parallel was created.

Focusing on Kongara (2023), while there is no data about the efficiency of this

design since it was not assembled, the proof of concept cases already provide very valuable information. In case 3, which considers the circuit diagram in Figure 50, one harvester is responsible for powering the device and the battery if needed and the second harvester focuses only on charging the battery. The experiment proved that this setup worked, and alongside the following cases proved that even if one of the harvesters became offline, the battery and/or the other harvester could still supply the microcontroller.

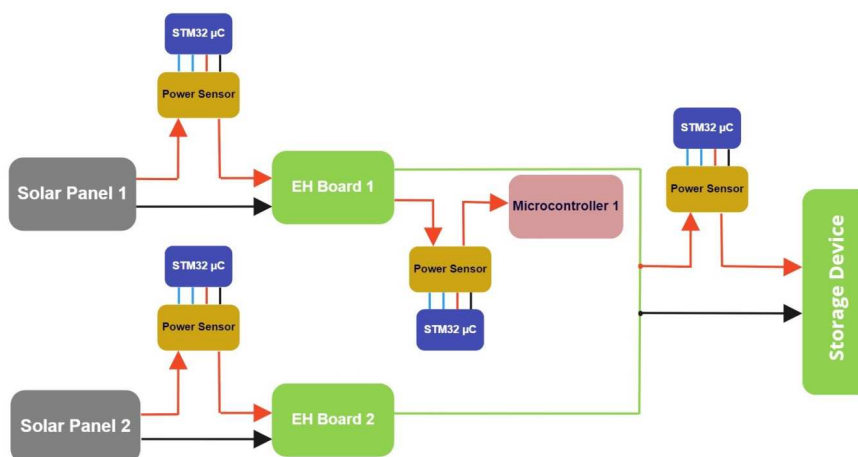


Figure 50 – Circuit diagram for Multi source energy harvesting test case. Source: Kongara (2023).

This experiment was used as a reference and basis. A kinetic electromagnetic harvester assembly can be designed to power the communication system while the process is ongoing, they would take the role of solar panel 2 in the schematic. As discussed previously, kinetic energy is only available during the process, this means that the solar cell harvester can be designed with only the microcontroller idle power consumption in mind, with any extra charging the batteries. In the schematic, this photovoltaic cell would take the role of solar panel 1.

It was decided to use the same scheme and power manager circuits as used in the validation case, in order to assure that the project would be viable in case it one day is implemented. This would mean the use of 2 ADP5091-Evalz boards, one for each harvester assembly. This board, which can be seen in Figure 51, is a power management unit using the ADP5091 energy manager chip. It can receive an input between 0.38 V and 3.3 V and requires only 6 mW for a cold start at the minimum voltage. Regarding the outputs, it can charge a battery cell with up to 5.2 V and 1 A, so it can safely power the Quectel device and charge the battery simultaneously (DEVICES, 2022a). It also has a regulated output between 1.5 V and 3.6 V with up to 150 mA. Since this current would be enough to power the Quectel RG255C, it is safe to assume that it will be enough to power the sensors and microcontroller.

This creates two situations that must be supplied by each harvester board, idle



Figure 51 – ADP5091-1-EVALZ board. Source: Devices (2022a)

and operation. For the idle case, the microcontroller will need to be in the default sleep mode, since it needs to be awakened by the sensor. The low power sleep mode requires a special signal to be sent, and since the transceiver would be powered off, it cannot provide this signal. This leaves the accelerometer as the only source of input inside the enclosure, which would also not be able to provide the special signal in the wake-up pin. The microcontroller STM32L051RBt6 requires around  $37 \text{ mA MHz}^{-1}$  of clock to stay in sleep mode while being able to run up to 20 instructions. Assuming the frequency used is of 2 MHz in order to save power, and it will be powered at 3.3 V in order to match the sensor, it would require a power of 0.224 mW. Adding this value with the power required by sensors, the idle state requires 0.752 mW.

As discussed in Section 6.1.1, a single “Seeded 313070003 monocrystalline” panel could generate  $(1.288 \pm 0.062) \text{ mW}$  with the average indoor illuminance in the factory hall (LAUSCHER, 2022). Considering the ADP5091 has a medium efficiency of 88% (ZHOU et al., 2021),  $(1.133 \pm 0.055) \text{ mW}$  would reach the system. The average efficiency is being used because efficiency examples presented in the datasheet from the power manager assume a lower battery voltage and current input, thus not offering a good reference for this specific case. The solution was to use the experimental results obtained in Zhou et al. (2021) as a basis for this efficiency value. The values obtained in the paper are equal or below the efficiency presented in the datasheet. It is better to underestimate the available power than finding it insufficient if this system is ever implemented. In any case, the effective value is more than enough to both power the sensor and microcontroller, while leaving  $(0.381 \pm 0.055) \text{ W}$  to charge the battery.

For the active state, the current needed by the microcontroller is of 290 mA, resulting in 0.957 mW. This would be added to the 0.528 mW of the sensors and  $(460 \pm 20)$  mW required by the RedCap device assuming 10 ms interval between messages, as dictated by the process monitoring use case. The final result is that  $(461 \pm 20)$  mW need to be generated. However, the ADP5091 has a maximum input of 3.3 V, which would be surpassed by the ReVibe 00204 energy harvesters, so a buck dc-dc converter must be used after rectification in order to lower the voltage. In order to simplify calculations and placement, it will be assumed that each device has its own rectifier bridge.

Since the effectiveness of the harvesters will heavily depend on the rectifier bridge, it was decided to assemble one from the STPS10L25 Low drop power Schottky rectifiers. These are diodes with very low forward voltages, 0.3 V in the case of this model, making them ideal for low power rectification (STMICROELECTRONICS, 2016).

In order to estimate the efficiency of the bridge, the difference between the peaks in input and output voltage is needed. The input voltage peak or  $V_{in, peak}$  can be obtained via equation (5).

$$V_{in, peak} = V_{rms} \doteq \sqrt{2} \quad (3)$$

$$V_{in, peak} = 8.2 \doteq \sqrt{2} \quad (4)$$

$$V_{in, peak} = 11.6 \text{ V} \quad (5)$$

And with it and the forward voltage, it is possible to calculate the output voltage peak on equation (7).

$$V_{out, peak} = V_{in, peak} - 2V_F \quad (6)$$

$$V_{out, peak} = 11.6 \text{ V} - 2 \times 0.30 \text{ V} = 11.0 \text{ V} \quad (7)$$

Where  $V_{out, peak}$  is the output voltage peak and  $V_F$  is the forward voltage of each Schottky diode.

With both peak voltage values, it is possible to estimate the efficiency of the rectifier using equation (9). However, this method does not consider the losses due to ripple or other effects. Unfortunately, it was not possible to find a suitable device that provided this information without it being made for much larger currents and voltages, resulting in exacerbated losses.

$$\eta = \frac{V_{out}}{V_{in}} \quad (8)$$

$$\eta = \frac{11.0 \text{ V}}{11.6 \text{ V}} \approx 0.948 \quad (9)$$

Knowing that this rectifier setup would have an approximate efficiency of 94.8%, it is possible to calculate that the actual available power from the ReVibe 00204

Harvester under 27.27 N as  $(187.20 \pm 9.36)$  mW resulting in an energy density of  $(81.60 \pm 4.10)$  W/m<sup>2</sup>. Also, due to the losses, the effective voltage is 7.78 V<sub>RMS</sub>.

Any method to reduce the voltage would need to be able to lower 7.78 V to 3.3 V, while providing an output current of around 140 mA in order to provide the power required. In order to achieve these requirements, the MINI-360 Buck Converter Module was chosen, due to both its performance and its datasheet presenting the efficiency for an output of 3.3 V. While the datasheet did not offer a curve for an input of 8 V, it did offer it for 7 V and 9 V, so it was possible to estimate that the efficiency would be around 88% for the output current of 140 mA (ELECTRONICS, 2016). Considering the ADP5091 also has an efficiency of 88%, the total efficiency can be calculated as:

$$\eta = B_{eff} * ADP_{eff}, \quad (10)$$

$$\eta = 0.88 * 0.88, \quad (11)$$

$$\eta = 0.7744 = 77.44\%, \quad (12)$$

where  $\eta$  is the efficiency,  $B_{eff}$  is the efficiency of the buck dc-dc converter, and  $ADP_{eff}$  is the efficiency of the ADP5091 energy administrator.

Only 77.44% of the power collected by the harvester will be available for powering the system. This allows to calculate how much power needs to be generated in order to supply the aforementioned  $(461 \pm 20)$  mW consumed by the system as

$$P_{total} = \frac{461.5 \pm 20.0}{0.7744}, \quad (13)$$

$$P_{total} = 596.0 \pm 25.8, \quad (14)$$

with  $P_{total}$  being the total required power, in milliwatt, that must be generated in order to power the system, considering the losses due to efficiency.

This means that  $(596.0 \pm 25.8)$  mW must be generated in order to power the device, assuming no significant losses occur in the cables and connectors. One disclaimer that must be made is that it is assumed that the uncertainty of the required power will scale at the same rate as the base value. The actual uncertainty values of the instruments used and the measurements themselves are not known. Due to this, the worst-case scenario was chosen as a guarantee.

Since each ReVibe Energy 00204 provides  $(187.20 \pm 9.36)$  mW under the stipulated conditions, a total of four units are needed in order to provide more than  $(596.0 \pm 25.8)$  mW. This results in  $(748.80 \pm 100.36)$  mW being generated guaranteeing energy autonomy to the system. Considering the losses for efficiency up to the battery,  $(118.38 \pm 28.98)$  mW are available to charge it or supply any peaks in consumption, such as during transmission with worse than normal RSRP.

To summarize, the final setup would consist of one solar panel of model “Seeded 313070003 monocrystalline” and 4 kinetic electromagnetic harvesters “ReVibe 00204”.

Each technology is connected to an energy admin board in order to safely charge the battery and power the other components. They would power a Quectel RG255C, as well as one Microcontroller and one 3-axis accelerometer. A diagram of the proposed connections can be seen in Figure 52.

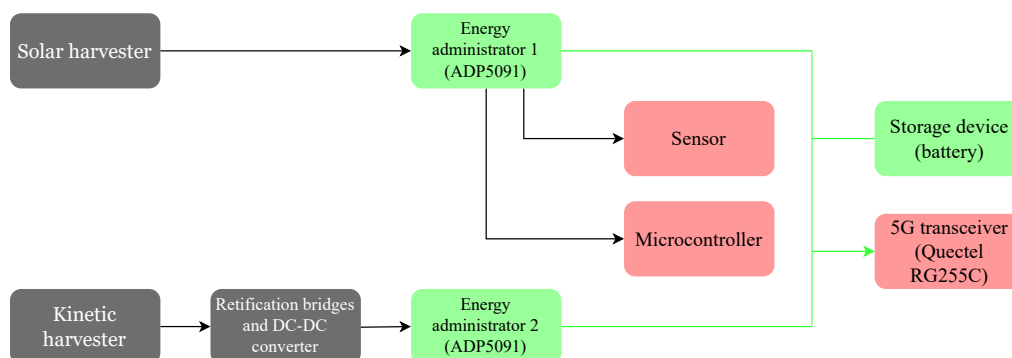


Figure 52 – Diagram for the theoretical use case circuit. Source: Author.

In the circuit, the flow of energy during the idle time of the operation, the microcontroller is in sleep mode, and since the milling operation is not active, only the solar generation is present, powering the microcontroller and sensor while charging the battery. Once the milling operation starts, the sensor measurements wake up the microcontroller, which in turn activates a transistor or similar key to turn on the RedCap device. With the milling operation generating vibrations, the kinetic harvesters engage, powering the entire system and charging the battery if enough kinetic energy is available or just supplementing the battery power if it is not.



## 7 CONCLUSION

In order to evaluate the power consumption of 5G transceivers, a test plan and the experimental evaluation of six models of 5G transceivers were done considering changes in factors such as the network technology, sending frequency, packet size, and signal strength. These tests used the ping tool to generate traffic under different test scenarios considering the combination of the factors already mentioned and measured the power consumption of the devices.

The factor with the highest impact on the power consumption is the network technology, since all the tests with the NSA network showed larger consumption than those performed with SA networks. Particularly, the use of the NSA network increased the power consumption of the Quectel RM520-GL in around 40% across all scenarios. For other devices, the increase was 14% for the WNC 5G NR sub-6 router and 7% for the Siemens Scalance M800. Testing was not possible for the other three devices on this network, two of them due to limitations of the device and one due to problems with the network itself. Beyond network technology, the strength of the signal proved to be the second most impactful factor. Tests with worse than average RSRP were the most power intensive ones in all devices when compared to the other scenarios in the same network. In general, an increase in the RSRP resulted in lower power consumption, even though the case with the lowest power consumption was not the one with the higher RSRP for all the devices. Regarding the sending frequency, it is the third most impactful factor, since each transmission has an associated energy cost. Conversely, long periods of inactivity also allow for power saving modes to activate, further reducing the power consumption. In two of the transceivers, the lowest power consumption happens in the “30 s 256 bytes” scenario. The least influential aspect is the packet size, as starting the transmission is more costly than the actual transmission of the packet.

Focusing on the devices, their testing was successful, with all six devices on the SA network and three of them on the NSA network having been tested. The device with the highest power consumption was the Siemens Scalance M800, with  $(5.42 \pm 0.17)$  W consumed on the average case in the SA network and  $(5.82 \pm 0.16)$  W on the average case in the NSA network. On the other hand, the most energy efficient transceiver proved to be the Quectel RG255C a reduced capacity Quectel device, currently still in engineering sample status. This device has a power consumption between  $(0.44 \pm 0.02)$  W and  $(0.61 \pm 0.05)$  W, making it the best choice for applications where energy is limited. However, this device also has only 20% of the data rate of a full capability device of the same type. If the amount of data to be transferred continues to increase as forecasted for Industry 4.0, more efficient solutions must be developed. A possible solution is to shape the communication in order to reduce the energy used if compatible

with the application requirements. This may be done by holding onto the data and sending it all at once, with idle periods above one second between communications. The reason behind this is that all tests revealed that higher frequencies of communication have much higher energy costs than payload sizes. However, this may not be possible for cases that require constant communication with very little delays. Another solution is to ensure that the link is of the highest quality possible. This may even be done without energy usage by installing reflectors or similar passive boosting apparatus on or around the transceiver.

From the point of view of the energy harvesters, the comparisons proved that at least for the kinetic electromagnetic variety it was viable to power the transceivers, although this required multiple units of the same type of harvesters. By using four units of the Revibe 00204, it would already be possible to power even the worst case scenario of RG255C requiring  $(0.61 \pm 0.05)$  W with more than 0.120 W remaining to cover for losses during rectification or to power sensors and other components.

In case an installation has little to no kinetic energy available there are other harvesting techniques such as photovoltaic and thermoelectric, however their generation is not enough to achieve energy autonomy. This is due to the low energy density of these technologies, requiring large areas with large amounts of energy available in order to have an impact. Photovoltaic cells underperform in indoor conditions, making them good supporters for other technologies, but hardly capable of powering devices on their own. For comparison, it would require  $(4.83 \pm 0.68)$  m<sup>2</sup> of the best performing cell to power the RG255C alone in its average case. Thermoelectric harvesters have a similar problem, having poor energy density and the need to be placed in the heat sink of devices, which may compromise their cooling and reduce their efficiency. Their generation is not enough to justify the extra thermal wear in the installation, and while this technology can be useful, it still has much to improve in order to provide energy autonomy for 5G transceiver units. The more energy intensive devices are another point of concern, as there is no realistic setup that could achieve energy autonomy for them. While there is no doubt that any generation will likely increase the battery life, the setup might not be worth the cost.

As of now, for energy autonomy to be possible, the use case requirements must be satisfied by the RedCap device and enough kinetic energy must be present for harvesting. In projects where the use case requires more throughput, faster communication, or simply do not have a network capable of supporting RedCap devices, a full capability Quectel model can be used. However, a large amount of kinetic energy would be required to supply the  $(1.33 \pm 0.17)$  W required by the transceiver on the worst scenario in the SA network. Even so, the setup from the theoretical use case would be able to supply around half of the power needed, extending the battery life by at least 50% assuming there are no significant idle times when the battery could charge

and improve this figure. If the Quectel device cannot satisfy the requirements, the other routers may be considered. However, as discussed in Section 6.1, numerous harvesters coupled with a large amount of energy may be required to achieve energy autonomy, or at least significantly offset the power consumption, depending on the transceiver and consumption of the other components.

## 7.1 FUTURE WORKS

Some future works can be drawn from the results collected in this work.

The crux of this project was the mismatch between the energy consumption of the 5G transceivers and the energy harvester generation. An in-depth study into more powerful energy harvesters, as well as other energy harvesting techniques, may be in order. Another possible study is a similar study to this one focusing only on RedCap devices, as the one measured in this project is still an engineering sample and other brands or versions may also present better results or improved capabilities.

Another venue of research that has proven to be necessary for the use of multiple energy harvester technologies is the development of a multi-source energy harvester energy admin platform. This can be a continuation of the project used as a basis or a novel solution. In any way, this technology is critical for the advancement of multi-source energy harvesting.

Yet another project of interest would be the study of energy efficient protocols using these same 5G transceivers in order to evaluate their impact. As not only the data here collected presents a baseline that could be used for comparison, but many of the devices here sorely need a reduction in power consumption to be useful in scenarios with limited energy availability.

A final possible project would be an implementation of the theoretical use case presented in Section 6.2.1. The theoretical study already provides the components that would be required, leaving the assembly and coding of the microcontroller to be developed. It would be even better if it is paired with a project that involves developing or just testing a multi-source energy admin board, as the theoretical case presented used a work-around due to the lack of this technology.

## REFERENCES

3GPP. **Introducing 3GPP**. [S.l.: s.n.], 2024. Accessed: 2024-05-12. Available from: <https://www.3gpp.org/about-us/introducing-3gpp>.

3RD GENERATION PARTNERSHIP PROJECT. **3GPP TR 21.915 V15.0.0 (2019-09) Technical Report**. [S.l.], Sept. 2019.

3RD GENERATION PARTNERSHIP PROJECT. **3GPP TR 21.916 V16.2.0 (2022-06) Technical Report**. [S.l.], June 2022.

5G ALLIANCE FOR CONNECTED INDUSTRIES AND AUTOMATION (5G-ACIA). **5G for Automation in Industry: Primary Use Cases, Functions and Service Requirements**. Frankfurt am Main, Germany: [s.n.], July 2019. White Paper. Accessed: 2024-05-28. Available from: <https://www.5g-acia.org>.

AFROZ, Farhana; SUBRAMANIAN, Ramprasad; HEIDARY, Roshanak; SANDRASEGARAN, Kumbesan; AHMED, Solaiman. SINR, RSRP, RSSI and RSRQ measurements in long term evolution networks. **International Journal of Wireless & Mobile Networks**, Academy and Industry Research Collaboration Center (AIRCC), 2015.

AIJAZ, Adnan. Private 5G: The Future of Industrial Wireless. **IEEE Industrial Electronics Magazine**, v. 14, n. 4, p. 136–145, 2020. DOI: 10.1109/MIE.2020.3004975.

ATTARAN, Mohsen. The impact of 5G on the evolution of intelligent automation and industry digitization. **Journal of ambient intelligence and humanized computing**, Springer, v. 14, n. 5, p. 5977–5993, 2023.

BAGHERI, Hamidreza; NOOR-A-RAHIM, Md; LIU, Zilong; LEE, Haeyoung; PESCH, Dirk; MOESSNER, Klaus; XIAO, Pei. 5G NR-V2X: Toward Connected and Cooperative Autonomous Driving. **IEEE Communications Standards Magazine**, v. 5, n. 1, p. 48–54, 2021. DOI: 10.1109/MCOMSTD.001.2000069.

BARB, Gordana; OTESTEANU, Marius. 4G/5G: A Comparative Study and Overview on What to Expect from 5G. In: 2020 43rd International Conference on Telecommunications and Signal Processing (TSP). [S.l.: s.n.], 2020. P. 37–40. DOI: 10.1109/TSP49548.2020.9163402.

BELFKIH, Abderrahmen; DUVALLET, Claude; SADEG, Bruno. A survey on wireless sensor network databases. **Wireless Networks**, v. 25, n. 8, p. 4921–4946, 2019. ISSN 1572-8196. DOI: 10.1007/s11276-019-02070-y. Available from: <https://doi.org/10.1007/s11276-019-02070-y>.

CHEN, Xiaojing; NI, Wei; WANG, Xin; SUN, Yichuang. Provisioning quality-of-service to energy harvesting wireless communications. **IEEE Communications Magazine**, v. 53, n. 4, p. 102–109, 2015. DOI: 10.1109/MCOM.2015.7081082.

CHUNG, Tien-Kan et al. An Attachable Electromagnetic Energy Harvester Driven Wireless Sensing System Demonstrating Milling-Processes and Cutter-Wear/Breakage-Condition Monitoring. **Sensors**, v. 16, n. 3, 2016. ISSN 1424-8220. DOI: 10.3390/s16030269. Available from: <https://www.mdpi.com/1424-8220/16/3/269>.

DENG, Fang; YUE, Xianghu; FAN, Xinyu; GUAN, Shengpan; XU, Yue; CHEN, Jie. Multisource Energy Harvesting System for a Wireless Sensor Network Node in the Field Environment. **IEEE Internet of Things Journal**, v. 6, n. 1, p. 918–927, 2019. DOI: 10.1109/JIOT.2018.2865431.

DEVICES, Analog. **ADP5091/ADP5092 Ultralow Power Energy Harvester PMUs with MPPT and Charge Management**. [S.l.], May 2022a. Rev. A. Available from: <https://www.analog.com/media/en/technical-documentation/data-sheets/ADP5091-5092.pdf>.

DEVICES, Analog. **ADXL345: 3-Axis,  $\pm 2$  g/ $\pm 4$  g/ $\pm 8$  g/ $\pm 16$  g Digital Accelerometer**. [S.l.], May 2022b. Rev. G. Available from: <https://www.analog.com/media/en/technical-documentation/data-sheets/ADXL345.pdf>.

DIAKHATE, Ismaila; NIANG, Boudal; KORA, Ahmed Dooguy; FAYE, Roger Marcelin. Optimizing the Energy Consumption of a Sensor Node. In: 2020 6th Information Technology International Seminar (ITIS). [S.l.: s.n.], 2020. P. 46–50. DOI: 10.1109/ITIS50118.2020.9321059.

ELECTRONICS, Matt's. **MINI-360 RC Power Supply Step-down Module**. [S.l.], 2016. Datasheet - production data. Available from: <https://www.matts-electronics.com/MINI-360-RC-Power-Supply-step-down-Module.pdf>.

ETSI. **TS 138 331 - V15.3.0 - 5G; NR; Radio Resource Control (RRC); Protocol specification (3GPP TS 38.331 version 15.3.0 Release 15)**. [S.l.], Oct. 2018.

Reference RTS/TSGR-0238331vf30. Available from:

<https://portal.etsi.org/TB/ETSIDeliverableStatus.aspx>.

FAN, Xueming et al. Triboelectric-electromagnetic hybrid nanogenerator driven by wind for self-powered wireless transmission in Internet of Things and self-powered wind speed sensor. **Nano Energy**, v. 68, p. 104319, 2020. ISSN 2211-2855. DOI:

<https://doi.org/10.1016/j.nanoen.2019.104319>. Available from:

<https://www.sciencedirect.com/science/article/pii/S2211285519310262>.

FRAUNHOFER. **Joseph von Fraunhofer**. 2022. Available from:

<https://www.fraunhofer.de/en/about-fraunhofer/profile-structure/chronicles/joseph-von-fraunhofer.html#1>. Visited on: 8 Apr. 2024.

FRAUNHOFER. **Profile / structure**. 2023. Available from:

<https://www.fraunhofer.de/en/about-fraunhofer/profile-structure.html>.

Visited on: 8 Apr. 2024.

FRENGER, Pal; TANO, Richard. More Capacity and Less Power: How 5G NR Can Reduce Network Energy Consumption. In: 2019 IEEE 89th Vehicular Technology Conference (VTC2019-Spring). [S.l.: s.n.], 2019. P. 1–5. DOI:

10.1109/VTCSpring.2019.8746600.

GANGAKHEDKAR, Sandip; CAO, Hanwen; ALI, Ali Ramadan; GANESAN, Karthikeyan; GHARBA, Mohamed; EICHINGER, Josef. Use Cases, Requirements and Challenges of 5G Communication for Industrial Automation. In: 2018 IEEE International Conference on Communications Workshops (ICC Workshops). [S.l.: s.n.], 2018. P. 1–6. DOI: 10.1109/ICCW.2018.8403588.

HARB, Adnan. Energy harvesting: State-of-the-art. **Renewable Energy**, v. 36, n. 10, p. 2641–2654, 2011. Renewable Energy: Generation & Application. ISSN 0960-1481.

DOI: <https://doi.org/10.1016/j.renene.2010.06.014>. Available from:

<https://www.sciencedirect.com/science/article/pii/S0960148110002703>.

HUAWEI TECHNOLOGIES CO., LTD. **Comparison of maximum power use by base stations between generations**. [S.l.: s.n.], 2023. online image. Viewed in: 14/04/2024.

Available from: <https://www.huawei.com/en/huaweitech/publication/89/5g-power-green-grid-slashes-costs-emissions-energy-use>.

IPT. **Fraunhofer IPT**. 2023a. Available from:

<https://www.ipt.fraunhofer.de/de/profil.html>. Visited on: 8 Apr. 2024.

IPT. **Fraunhofer IPT**. 2023b. Available from: <https://www.ipt.fraunhofer.de/en/Profile/departments/production-metrology.html>.

Visited on: 28 Apr. 2024.

JARVISMS. **Python code for UM24C USB meter interface**. [S.l.: s.n.], 2023.

Accessed: 13/04/2023. Available from:

<https://github.com/jarvisms/PythonUM24C/blob/master/um24c.py>.

KIM, Younsun et al. New radio (NR) and its evolution toward 5G-advanced. **IEEE Wireless Communications**, IEEE, v. 26, n. 3, p. 2–7, 2019.

KONGARA, Phanindra Chowdary. **Development of Multi-Source Energy Harvesting for the Power Supply of IoT Sensors**. Jan. 2023. Master Thesis – Bremen University of Applied Sciences.

LAUSCHER, Felix. **Evaluation of Different Energy Harvesters for the Planned Energy Supply of 5G Sensor Technology**. May 2022. Bachelor's thesis – Hochschule Bonn-Rhein-Sieg, Sankt Augustin.

LEE, Ju-Hyuck; KIM, Jeonghun; KIM, Tae Yun; AL HOSSAIN, Md Shahriar; KIM, Sang-Woo; KIM, Jung Ho. All-in-one energy harvesting and storage devices. **Journal of Materials Chemistry A**, Royal Society of Chemistry, v. 4, n. 21, p. 7983–7999, 2016.

LIU, Guangyi; HUANG, Yuhong; CHEN, Zhuo; LIU, Liang; WANG, Qixing; LI, Na. 5G Deployment: Standalone vs. Non-Standalone from the Operator Perspective. **IEEE Communications Magazine**, v. 58, n. 11, p. 83–89, 2020. DOI: 10.1109/MCOM.001.2000230.

MARUTSU. **2W Solar Panel 80X180 313070003 SeedStudio**. [S.l.: s.n.], 2024.

Accessed: 2024-07-12. Available from: <https://www.marutsu.co.jp/pc/i/829574/>.

MIT. **Propagation of Uncertainty**. [S.l.: s.n.], 2024. Accessed: 2024-06-28. Available from: [https://web.mit.edu/fluids-modules/www/exper\\_techniques/2.Propagation\\_of\\_Uncertainty.pdf](https://web.mit.edu/fluids-modules/www/exper_techniques/2.Propagation_of_Uncertainty.pdf).

MOHAMED, Ramy; ZEMOURI, Sofiane; VERIKOUKIS, Christos. Performance Evaluation and Comparison between SA and NSA 5G Networks in Indoor Environment. In: 2021 IEEE International Mediterranean Conference on Communications and Networking (MeditCom). [S.l.: s.n.], 2021. P. 112–116. DOI: 10.1109/MeditCom49071.2021.9647621.

PERALTA, Elena; LEVANEN, Toni; IHALAINEN, T.; NIELSEN, Sari; NG, M.; RENFORS, M.; VALKAMA, M. 5G New Radio Base-Station Sensitivity and Performance. **2018 15th International Symposium on Wireless Communication Systems (ISWCS)**, p. 1–6, 2018. DOI: 10.1109/ISWCS.2018.8491061.

PITCH TECHNOLOGIES. **Quel module Peltier laird pour quelle température.** [S.l.: s.n.], 2024. Accessed: 2024-07-12. Available from: <https://pitch-technologies.fr/produits/modules-thermoelectriques/quel-module-peltier-laird-pour-quelle-temperature/>.

PRAMONO, Subuh; ALVIONITA, Lia; DANANG, Mustofa; SULISTYO, Meiyanto Eko. Optimization of 4G LTE (Long Term Evolution) Network Coverage Area in Sub Urban. **AIP Conference Proceedings**, v. 2217, p. 30193 1–9, Apr. 2020. DOI: 10.1063/5.0000732.

QUECTEL WIRELESS SOLUTIONS CO., LTD. **Quectel RM520N Series 5G Specification V1.3.** English. [S.l.], 2022. Available: <https://www.quectel.com/product/5g-rm520n-series>. Available from: <https://www.quectel.com/product/5g-rm520n-series>.

RAHMAN, Imadur; RAZAVI, Sara Modarres; LIBERG, Olof; HOYMANN, Christian; WIEMANN, Henning; TIDESTAV, Claes; SCHLIWA-BERTLING, Paul; PERSSON, Patrik; GERSTENBERGER, Dirk. 5G Evolution Toward 5G Advanced: An overview of 3GPP releases 17 and 18. **Ericsson Technology Review**, v. 2021, n. 14, p. 2–12, 2021. DOI: 10.23919/ETR.2021.9904665.

RAKUTEN MOBILE. **Rakuten Mobile Launches Full Commercial Service.** [S.l.: s.n.], 2021. Accessed on: 2024-05-03. Available from: [https://corp.mobile.rakuten.co.jp/english/news/press/2021/0712\\_01/](https://corp.mobile.rakuten.co.jp/english/news/press/2021/0712_01/).

RAO, Sriganesh K.; PRASAD, Ramjee. Impact of 5G Technologies on Industry 4.0. **Wireless Personal Communications**, v. 100, n. 1, p. 145–159, 2018.



SANIN-VILLA, Daniel. Recent Developments in Thermoelectric Generation: A Review. **Sustainability**, v. 14, n. 24, 2022. ISSN 2071-1050. DOI: 10.3390/su142416821.

Available from: <https://www.mdpi.com/2071-1050/14/24/16821>.

SHARMA, Pankaj. Evolution of mobile wireless communication networks-1G to 5G as well as future prospective of next generation communication network. **International Journal of Computer Science and Mobile Computing**, Citeseer, v. 2, n. 8, p. 47–53, 2013.

SHAW, Joseph A. Radiometry and the Friis transmission equation. **American Journal of Physics**, American Association of Physics Teachers, v. 81, n. 1, p. 33–37, 2013.

DOI: 10.1119/1.4755780. Available from: <http://dx.doi.org/10.1119/1.4755780>.

SHURDI, Olimpjon; RUCI, Luan; BIBERAJ, Aleksander; MESI, Genci. 5G energy efficiency overview. **Eur. Sci. J. ESJ**, v. 17, n. 03, p. 315–327, 2021.

SIEMENS AG. **Industrial Remote Communication - Remote Networks SCALANCE MUM856-1 Operating instructions**. [S.l.], 2023.

Available:[https://cache.industry.siemens.com/dl/files/734/109814734/att\\_1142161/v1/BA\\_SCALANCE-MUM856\\_76.pdf](https://cache.industry.siemens.com/dl/files/734/109814734/att_1142161/v1/BA_SCALANCE-MUM856_76.pdf). Available from:

[https://cache.industry.siemens.com/dl/files/734/109814734/att\\_1142161/v1/BA\\_SCALANCE-MUM856\\_76.pdf](https://cache.industry.siemens.com/dl/files/734/109814734/att_1142161/v1/BA_SCALANCE-MUM856_76.pdf).

SOLUTIONS, Quectel Wireless. **5G RM520N Series**. [S.l.: s.n.], 2024.

<https://www.quectel.com/product/5g-rm520n-series/>. Accessed: 2024-05-23.

SOLYMAN, Ahmed Amin Ahmed; YAHYA, Khalid. Evolution of wireless communication networks: from 1G to 6G and future perspective. **International journal of electrical and computer engineering**, IAES Institute of Advanced Engineering and Science, v. 12, n. 4, p. 3943, 2022.

STMICROELECTRONICS. **STM32L051x6 STM32L051x8 Access line ultra-low-power 32-bit MCU Arm®-based Cortex®-M0+, up to 64 KB Flash, 8 KB SRAM, 2 KB EEPROM, ADC**. [S.l.], Oct. 2019. Datasheet - production data, DS10184 Rev 10. Available from:

<https://www.st.com/resource/en/datasheet/stm32l051r6.pdf>.

STMICROELECTRONICS. **STPS10L25 Low Drop Power Schottky Rectifier Datasheet**. Version Rev 5. [S.l.], Oct. 2016. Product in full production. Available from: <https://www.st.com>.

SUDEVALAYAM, Sujesha; KULKARNI, Purushottam. Energy Harvesting Sensor Nodes: Survey and Implications. **IEEE Communications Surveys & Tutorials**, v. 13, p. 443–461, 2011. DOI: 10.1109/SURV.2011.060710.00094.

TELTONIKA NETWORKS. **Teltonika RUTX50 Industrial 5G Router User Manual**. [S.l.], 2022. Available: [https://wiki.teltonika-networks.com/view/RUTX50\\_Manual](https://wiki.teltonika-networks.com/view/RUTX50_Manual). Available from: [https://wiki.teltonika-networks.com/view/RUTX50\\_Manual](https://wiki.teltonika-networks.com/view/RUTX50_Manual).

TEXAS INSTRUMENTS. **INA219 High-Side Measurement, Bi-Directional Current/Power Monitor**. [S.l.], 2020. Available: <https://www.ti.com/product/INA219>. Available from: <https://www.ti.com/product/INA219>.

VEEDU, Sandeep Narayanan Kadan; MOZAFFARI, Mohammad; HÖGLUND, Andreas; YAVUZ, Emre A.; TIRRONEN, Tuomas; BERGMAN, Johan; WANG, Y.-P. Eric. Toward Smaller and Lower-Cost 5G Devices with Longer Battery Life: An Overview of 3GPP Release 17 RedCap. **IEEE Communications Standards Magazine**, v. 6, n. 3, p. 84–90, 2022. DOI: 10.1109/MCOMSTD.0001.2200029.

WEDDELL, Alex S.; MAGNO, Michele; MERRETT, Geoff V.; BRUNELLI, Davide; AL-HASHIMI, Bashir M.; BENINI, Luca. A survey of multi-source energy harvesting systems. In: 2013 Design, Automation & Test in Europe Conference & Exhibition (DATE). [S.l.: s.n.], 2013. P. 905–908. DOI: 10.7873/DATE.2013.190.

YOON, Eun-Jung; PARK, Jong-Tae; YU, Chong-Gun. Thermal energy harvesting circuit with maximum power point tracking control for self-powered sensor node applications. **Frontiers of Information Technology & Electronic Engineering**, v. 19, n. 2, p. 285–296, 2018. ISSN 2095-9230. DOI: 10.1631/FITEE.1601181. Available from: <https://doi.org/10.1631/FITEE.1601181>.

ZAPPONE, Alessio; SANGUINETTI, Luca; BACCI, Giacomo; JORSWIECK, Eduard; DEBBAH, Mérouane. Energy-Efficient Power Control: A Look at 5G Wireless Technologies. **IEEE Transactions on Signal Processing**, v. 64, n. 7, p. 1668–1683, 2016. DOI: 10.1109/TSP.2015.2500200.

ZHAO, Fuyuan; DENG, Wei; JIA, Haikun; YE, Wenjing; WAN, Ruichen; CHI, Baoyong. A Band-Shifting Millimeter-Wave T/R Front-End with Enhanced Imaging and Interference Rejection Covering 5G NR FR2 n257/n258/n259/n260/n261 Bands. In: 2023 IEEE Radio Frequency Integrated Circuits Symposium (RFIC). [S.l.: s.n.], 2023. P. 29–32. DOI: 10.1109/RFIC54547.2023.10186166.

ZHOU, Wenting; WANG, Xin; HU, Changyue; LI, Qing; LI, Chunlong; DU, Lin; YU, Huizong. Research on Multi-source Environmental Micro Energy Harvesting and Utilization. In: IEEE. 2021 6th Asia Conference on Power and Electrical Engineering (ACPEE). [S.l.]: IEEE, 2021. P. 1072–1076. DOI: 10.1109/ACPEE51499.2021.9437121. Available from: <https://www.ieee.org>.

## APPENDIX A – PYTHON SCRIPT: FAST PING ON WINDOWS PLUS PUTTY SINCRONIZATION

```
import time
import pygetwindow as gw
delay = (0.01)
test_duration = 65
times = range(int(150/delay))
measuring = False
print("Waiting for measurement start")

while not measuring:
    try:
        win = gw.getWindowsWithTitle('COM6 - PuTTY')[0]
        measuring=True
    except:
        time.sleep(1)
        start=time.time()

'''
start=time.time()
while True:
    now=time.time()
    progress = now - start
    if(progress > test_duration):
        break

response = os.system("ping -n 1 -l 256 8.8.8.8 -f")
time.sleep(delay)
'''

for x in times:
    now=time.time()
    progress = now - start
    if(progress > test_duration):
        break

    #Command goes directly to cmd prompt. Test in one before to avoid errors
    response = os.system("ping -n 1 -l 256 127.0.0.1 -f")
    #print(x)
```

```
time.sleep(delay)
```

```
win = gw.getWindowsWithTitle('COM6 - PuTTY')[0]
```

```
win.close() #Close PuTTY window to save log
```

## APPENDIX B – PYTHON SCRIPT: COMMUNICATION WITH UM34C MEASUREMENT DEVICE

```
import time
import serial
from um24c import UM24C
meter = UM24C("COM8",False)
times=range(1100);
log=1
#time.sleep(15)
if log:
try:
with open('D:/tiago/ipt/test results raw data/REDCAP/256bytes.txt', 'w') as f:
print("Energy measurement in progress, DO NOT TURN OFF")
for x in times:
result=meter.get_reads()
f.write(str(result.V)+"\n")
f.write(str(result.A)+"\n")
f.write(str(result.W)+"\n")

except FileNotFoundError:
print("The 'docs' directory does not exist")
else:
for x in times:
result=meter.get_reads()
print(str(result.V))
print(str(result.A))
print(str(result.W))
time.sleep(0.05)
```

## APPENDIX C – PYTHON SCRIPT: RAW TEXT OUTPUT FROM UM34C TO EXCEL FORMATTER

```
import os
import pandas as pd

def process_file(file_path):
    with open(file_path, 'r') as file:
        lines = file.read().splitlines()

    voltage = [float(lines[i]) for i in range(0, len(lines), 3)]
    current = [float(lines[i]) for i in range(1, len(lines), 3)]
    power = [float(lines[i]) for i in range(2, len(lines), 3)]

    data = {'Voltage (V)': voltage, 'Current (A)': current, 'Power (W)': power}

    return pd.DataFrame(data)

def save_to_excel(dataframe, output_path):
    dataframe.to_excel(output_path, index=False)

def main(directory):
    for filename in os.listdir(directory):
        if filename.endswith(".txt"):
            file_path = os.path.join(directory, filename)
            df = process_file(file_path)
            output_path = os.path.join("D:raw data/Quectel rm520/NSA final",
            f"{os.path.splitext(filename)[0]}.xlsx") #Excel to be created
            save_to_excel(df, output_path)
            print(f"Processed {filename}")

if __name__ == "__main__":
    directory = 'D:raw data/Quectel rm520/NSA final' # Endereço original
    main(directory)
```

## APPENDIX D – PYTHON SCRIPT: RSRP EXTRACTOR FROM QCOM LOGS OF SA MEASUREMENTS

```

import csv
import os

def extract_values_from_file(file_path):
    values = []
    with open(file_path, 'r') as file:
        for line in file:
            if "NOCONN" in line: #Line containing results
                parts = line.strip().split(',') #
                value = parts[len(parts)-5] # Get the RSRP value
                values.append(value)
    return values

def process_files_in_directory(directory_path, output_csv_path):

    # Gather data from all files
    all_data = []
    filenames = []
    for filename in os.listdir(directory_path):
        if filename.endswith(".txt"):
            file_path = os.path.join(directory_path, filename)
            extracted_values = extract_values_from_file(file_path)
            if extracted_values: # Only add if there are any values extracted
                all_data.append(extracted_values)
                filenames.append(filename)

    max_length = max(len(lst) for lst in all_data)
    for data_list in all_data:
        data_list.extend([''] * (max_length - len(data_list))) #Padding

    # Write the consolidated data to CSV
    with open(output_csv_path, 'w', newline='') as csvfile:
        writer = csv.writer(csvfile)
        writer.writerow(filenames) #Writing filenames as header
        for values in zip(*all_data): #Writing data transposed

```



```
writer.writerow(values)
```

```
process_files_in_directory('D:/ raw data/LAST REDCAP, 'Quectelrc2.csv')
```

## APPENDIX E – PYTHON SCRIPT: RSRP EXTRACTOR FROM QCOM LOGS OF NSA MEASUREMENTS

```

import csv
import os

def extract_values_from_file(file_path):

    values = []
    with open(file_path, 'r') as file:
        for line in file:
            if "NR5G-NSA" in line:
                parts = line.strip().split(',') #
                value = parts[len(parts)-6] # Get the RSRP value
                values.append(value)
    return values

def process_files_in_directory(directory_path, output_csv_path):

    # Gather data from all files
    all_data = []
    filenames = []
    for filename in os.listdir(directory_path):
        if filename.endswith(".txt"):
            file_path = os.path.join(directory_path, filename)
            extracted_values = extract_values_from_file(file_path)
            if extracted_values: # Only add if there are any values extracted
                all_data.append(extracted_values)
                filenames.append(filename)

    max_length = max(len(lst) for lst in all_data)
    for data_list in all_data:
        data_list.extend([''] * (max_length - len(data_list))) #Padding

    # Write the consolidated data to CSV
    with open(output_csv_path, 'w', newline='') as csvfile:
        writer = csv.writer(csvfile)
        writer.writerow(filenames) #Writing filenames as header

```

```
for values in zip(*all_data): #Writing data transposed
    writer.writerow(values)
```

```
process_files_in_directory('D:raw data/Quectel rm520/Quectel logs/NSA',
'Result_NSA_with good.csv')
```

## APPENDIX F – PYTHON SCRIPT: INA219 LOG TO EXCEL FILE CONVERTER

```

import os
import pandas as pd

def process_file(file_path):
    with open(file_path, 'r') as file:
        lines = file.readlines()

    data = []
    temp_dict = {}

    for line in lines[1:]: # Skip time data
        if line.strip(): # Check if there is data on the file
            if ':' in line: #Data starts after :
                try:
                    key, value = line.split(':')
                    value, unit = value.strip().split()
                except:
                    print(line)

                temp_dict[key.strip()] = float(value.replace('m', 'e-3'))
                # Convert mV and mA appropriately
            else:
                if temp_dict:
                    data.append(temp_dict)
                    temp_dict = {}
        if temp_dict:
            data.append(temp_dict)

    return pd.DataFrame(data)

def save_to_excel(dataframe, output_path):
    dataframe.to_excel(output_path, index=False)

def main(directory):
    for filename in os.listdir(directory):
        if filename.endswith('.log'):
            print(f"Processing {filename}")

```

```
file_path = os.path.join(directory, filename)
df = process_file(file_path)
#Remember to update the path to not overwrite the previous file
output_path = os.path.join('D:/raw data/siemens/excels',
f"{filename.split('.')[0]}.xlsx")
save_to_excel(df, output_path)
print(f"Processed {filename}")

if __name__ == "__main__":
    directory = 'D:/raw data/siemens'
    main(directory)
```